In Sweden and India– on green chemistry business

I have been privileged to be involved in two significant green chemistry activities in the first two months of 2001. In February, the interviews were held for a new full Professorship in Green Chemistry at Chalmers University in Gothenburg in Sweden. This new Chair, which is possibly the first of its kind, is part of the Chalmers Environmental Initiative. The Initiative involves an investment of $11M in the area of environmental systems analysis with a total of seven new Professorships including others in Sustainable Energy Systems, Environmental Systems Technology and Management for Sustainability. Most of the new professors have now been appointed. They will greatly enhance the Chalmers Environment Network, which is closely linked to Swedish industry and the University of Gothenburg. It is especially appropriate that this should take place during the term of Sweden in the EU Presidency. We look forward to hearing of progress with this initiative and we hope that the new Professor of Green Chemistry will play a prominent role on the European and international stages.

Earlier in the year in Delhi the First IUPAC International Symposium on Green Chemistry took place with over 220 delegates, including about 40 from outside India. It was very significant, given the increase in chemical manufacturing in the country to see how importantly the Indians regard this area. The inauguration ceremony was graced with the presence of the Chief Minister Mrs Sheila Dixit (requiring a huge security operation), who gave a speech to the conference on the positive and negative aspects of new technology. She concluded with a most appropriate quotation from the Father of her country, Mahatma Gandhi "There is enough for everybody's need in this world, but not enough for everybody's greed". Among the other speeches that of the Vice-Chancellor of the University of Delhi, Professor Deepak Nayyar, was also memorable. He concluded that it is the interface of science and technology which needs to be developed for the world to become a greener place. There were many excellent presentations during the conference some of which illustrated the interdisciplinary nature of green chemistry especially at the chemistry–chemical engineering and biology–chemistry boundaries. However, I have to admit that it was not the high quality of the science or my first impressions of one of the world's busiest cities that is likely to last longest in my memory—it was the interest of the ordinary staff in my hotel who quizzed me about the conference and the meaning of green chemistry. Readers will be pleased to hear that a complementary copy of this great journal now resides in the staff common room of one of India's leading hotels!

Platform party at the IUPAC International Symposium on Green Chemistry in Delhi. Professor James Clark is in the centre, with Chief Minister Sheila Dixit on his right and Professor Pietro Tundo (University of Venice) on his left.

James Clark
York, March 2001

DOI: 10.1039/b102397g

Highlights

Duncan Macquarrie reviews the latest research in green chemistry

Oxidations

A team led by Craig Hill, from Emory University, Atlanta, has succeeded in using a diversity-based approach to develop a new highly efficient and selective oxidation catalyst for the oxidation of sulfides to sulfoxides (*J. Am. Chem. Soc.*, 2001, **123**, 1625). They combined various redox-active cations with a range of (mostly polyoxometallate) anions, and came up with a catalyst derived from the reaction of a gold and a silver species. The product of this reaction was found to oxidize sulfides to the corresponding sulfoxide with excellent efficiency under very mild conditions, being more active than any other known catalyst for this transformation. The oxidation used oxygen as primary oxidant, and turnover numbers reached 200.

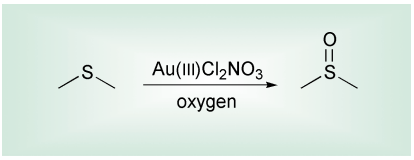

A further oxygen-based oxidation has been reported by B. M. Choudhary of the Indian Institute of Chemical Technology in Hyderabad (*Angew. Chem., Int. Ed.*, 2001, **40**, 763). They used a nickel–aluminium hydrotalcite as a catalyst for the aerobic oxidation of alcohols to aldehydes and ketones. In particular, they found that the system was excellent for the oxidation of α-ketols to α-diketones, as well as for vicinal diols to the corresponding diketones. Yields were high in the optimum solvents (hydrocarbons such as cyclohexane or toluene) after 6 h at temperatures below 100 °C. Reuse was also demonstrated.

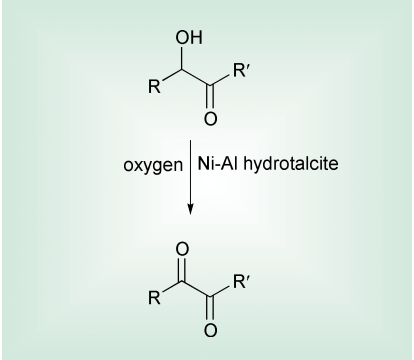

Diols from osmium tetroxide

The formation of diols from osmium tetroxide remains a thorny challenge. The reagent gives unparalleled activity, but is both highly toxic and volatile, making it unsuitable for use. Attempts to immobilise it, for example, on polyvinylpyridine have failed, since the coordinative link to the backbone must be broken for the reaction to proceed. The group led by Pierre Jacobs of the Catholic Univerity of Leuven, Heverlee, Belgium, have now provided an elegant method for the immobilisation of osmium tetroxide, leading to a stable, immobilised reagent (*Angew. Chem., Int. Ed.*, 2001, **40**, 586). Their approach relies on the ability of osmium tetroxide to form a stable osmate ester by coordination with a silica-supported tetrasubstituted double bond. This material can then form an osmate with a second molecule of alkene. This di-alkene complex then undergoes selective hydrolysis to form the product diol and regenerate the starting complex. Leaching studies indicated that no dihydroxylation occurred after removal of the solid catalyst, unlike that observed with polyvinylpyridine complexes.

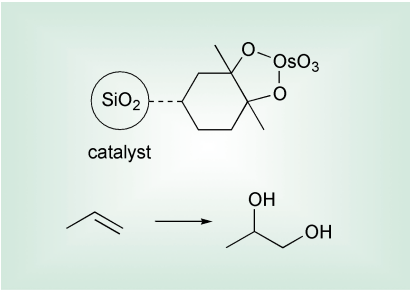

Epoxidation

Thomas Maschmeyer's group at the University of Delft, The Netherlands, have published details of a rapid screening study aimed at the preparation of titanium silsesquioxane catalysts for epoxidation (*Angew. Chem., Int. Ed.*, 2001, **40**, 740). They investigated methods to speed up and simplify the synthesis of these interesting materials, and found several improvements to the conventional method, making synthesis faster and cheaper. Catalytic activity was also found to be dependent on the conditions of synthesis. While the best catalytic activities were not better than those previously reported, the improvements in the synthetic methodology should allow access to these catalysts in a cleaner manner.

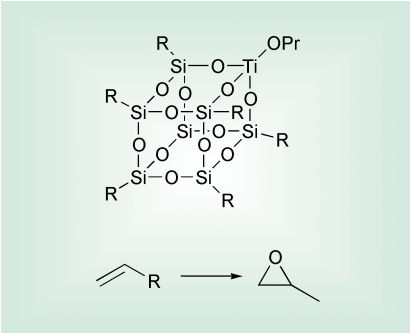

Spinning disk reactors

Alternative reactor design is one method which can have an enormous impact on a process, both from the point of view of optimising the performance of the reaction and from simpler isolation. Norman Lewis and his collaborators at SmithKline Beecham and Newcastle University, UK, have published details of an evaluation of a spinning disc reactor in the synthesis of a pharmaceutical intermediate and in the crystallisation of an active pharmaceutical (*Org. Proc. R+D*, 2001, **5**, 65). They found that the phase transfer-catalysed Darzens reaction proceeded very well in such a reactor, giving high yields and throughput, with significantly reduced impurity levels. Throughput for a 15-cm disc was estimated to be 8 tonnes p.a. In a second application, crystallisation of a salt was shown to be successful too with good control over particle size.

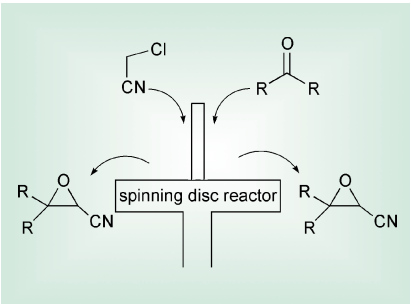

DOI: 10.1039/b102398p

Formamides

The synthesis of formamides can be cleanly carried out by the direct carbonylation of amines with CO. The group led by Youquan Deng from the Chinese Academy of Sciences in Langzhou has developed a novel catalyst system based on gold, rather than the usual palladium (*Chem Commun.*, 2001, 345). They looked at the formation of diamides from diamines, and found that, in the presence of small amounts of oxygen, the selectivity towards product was well above 90% at 100% conversion levels. This compared favourably with the *ca.* 80% selectivity achieved with the conventional Pd complex catalyst tried.

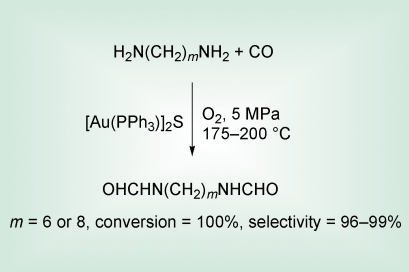

Ionic liquids

Ionic liquids have been attracting a lot of interest as alternative solvents for a range of reaction types. Andrei Fadeev and Michael Meagher of the University of Nebraska, USA, have now applied these materials to the extraction of butanol from fermentation broths (*Chem. Commun.*, 2001, 295). The production of chemicals from biomass fermentation is an attractive route to certain feedstocks, but the isolation of some components can be difficult from the aqueous mixtures produced. Butanol is particularly difficult to separate cleanly and energy efficiently. The workers from Nebraska have shown that butanol can be efficiently extracted into some ionic liquids. Pervaporation of the extracted butanol was then used to isolate the butanol from the ionic liquid.

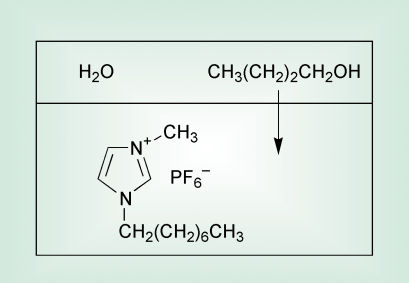

Enantioselective catalysis

The drive towards enantioselective catalysis has provided some excellent ligand systems, and highly selective synthetic methodologies. However, the preparation of some of these systems is complex and generates considerable waste. A mini-review by Harald Gröger and Jörg Wilken of SKW Trostberg and SBE Pharma (*Angew. Chem., Int. Ed.*, 2001, **40**, 529) highlights the opportunities which very simple enantioselective catalysts or ligands provide. Particularly striking is the excellent selectivities obtained in the aldol condensation using L-proline as catalyst. Not only are yield and enantioselectivity both > 96%, but the proline-catalysed process does not require the formation of silyl enol ethers, obviating the need for protection/deprotection. Mannich reactions are also possible with this simple catalyst.

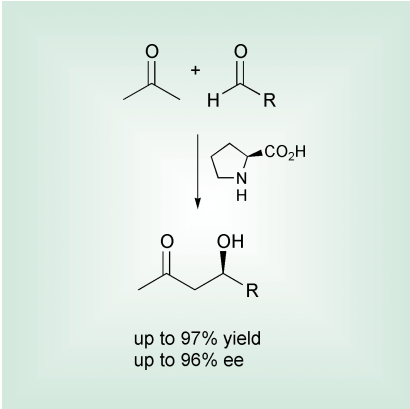

The use of microorganisms is another potential route to achieve enantioselective catalysis, in a potentially clean manner. Sonia Rodriguez, Margaret Kayser and Jon Stewart of the Universities of Florida, USA, and New Brunswick, Canada, have collaborated on the development of such a stereoselective reduction process using genetically engineered bakers yeast (*J. Am. Chem. Soc.*, 2001, **123**, 1547). The reduction of β-keto esters can be achieved by bakers yeast, but mixtures of stereoisomers are usually formed. This is due to there being a range of different genes in the yeast, all of which can effect the reduction, with varying degrees of selectivity. The groups in Florida and New Brunswick have shown that it is possible to genetically modify the yeast to either eliminate or over-express each of the key genes, and have used the information gained from this to design a highly stereoselective strain of yeast. Using this, they showed that reductions can proceed with > 98% enantioselectivity for a series of β-keto esters, compared to 70–95% ee obtained without modification.

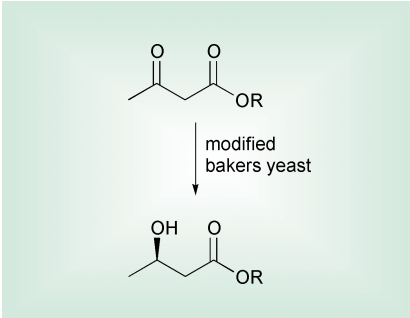

Suzuki coupling

The coupling of aryl groups to form biaryls *via* the Suzuki coupling is the most general and cleanest method available for the synthesis of these important intermediates. The groups led by Henri Doucet and Maurice Santelli of the CNRS in Marseille (*Chem. Commun.*, 2001, 325) have now published details of a new phosphine ligand system, which allows exceptionally high turnover numbers (up to 28 million) to be achieved. The tetradentate ligand system is thought to have the correct balance of steric and electronic factors, thus stabilising the catalyst over an enormous number of cycles.

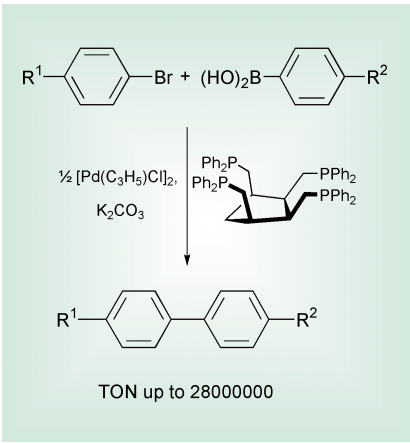

Supercritical fluids

The use of supercritical fluids as reaction media is an important theme, and recent results have demonstrated that the properties of the fluid can be tuned by changing the pressure and density of the fluid, making it a tunable solvent. Thus, regioselectivity and enantioselectivity can be altered by changing the pressure in the reactor. One common reaction type studied is hydroformylation, which may

give either branched or linear aldehyde products. Bin Lin and Aydin Akgerman have demonstrated that these differences may be related to differences in transition-state volume of the two possible reaction pathways in hydroformylation (*Ind. Eng. Chem. Res.*, 2001, **40**, 1113). They have correlated both rate and selectivity data with changes in product molar volume, on the assumption that the relative molar volumes of the products are closely related to the relative molar volumes of the two transition states. This approach was successful in explaining the trends in regioselectivity seen, and their hope is that this technique could be used to predict similar behaviour in other conditions, making finding the right conditions (and the likelihood of finding pressure-sensitive reactions) simpler.

A review article by Sharon Wells and Joe DeSimone describes another application of supercritical CO_2—its use as a solvent for polymer processing (*Angew. Chem., Int. Ed.*, 2001, **40**, 518). The review focuses on the use of CO_2 as an environmentally acceptable solvent for

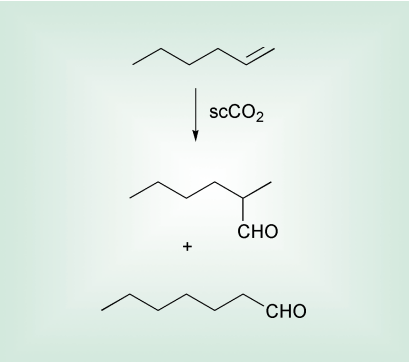

polymer synthesis and processing and coating technologies, and describes the advances in fluorinated surfactant technologies which allow the extension of the technique to many systems otherwise unsuited to CO_2 as solvent.

Fluorous biphasic systems

Perfluorinated compounds are useful not only as components in systems for $scCO_2$ processing, but also as ligands/catalysts for use in fluorous biphasic systems. The synthesis of such ligands is a key step in realising the potential of fluorous biphase catalysis. Jean-Pierre Genet's group from the CNRS in Paris (ENSC Paris) have succeeded in forming perfluoroalkyl aryl bromides using the Heck reaction of diazonium salts with perfluoroalkenes. Subsequent transformation leads to perfluoroalkyl phosphines, which can be used in a range of catalysts. Yields and purities of the products were excellent.

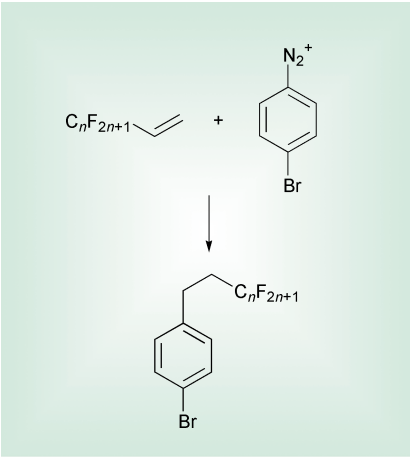

Focus On... green chemistry in Germany

Wolfgang Hoelderich from the University of Technology RWTH, Aachen, looks at the increasing importance of green chemical technology in Germany and some of the excellent examples coming from the German chemical industry

In 1998, the German journal *Der Spiegel* carried out a survey of public opinion in Germany on the subject "What are the important challenges for modern industrial society in the next Millennium?" The answers of the Germans were:

1. Protection and creation of jobs
2. Protection of living standards
3. Protection of our environment[1]

Addressing these challenges presents some significant difficulties.

- *Jobs versus Environment:* at the present time about 800M automobiles are driven worldwide. Every fifth job in Germany depends on automobile manufacture. According to the opinion of experts, the number of cars will be doubled to 1.6B by the year 2030.[2] With respect to global warming, how can the exhaust of each car be significantly reduced and thereby environmentally maintain the mobility of each person?
- *Living Standard versus Environment*: in populated rich countries, and in particular in the Far East, a rapidly increasing market for chemical products is expected in order to satisfy the basic needs of the people. The legitimate desire for the raising of living standards to the western level is strongly related to a constant increase in chemical production. How can the expansion of the capacities in the chemical industry be managed without harmful side-effects on the environment?
- *More and more, ecological and economical considerations should be combined*: based on increasing costs for energy and resources, processes of the chemical industry include high basic costs, *e.g.* for heating, and their economic and environmental viability is questionable. How can the utilisation of resources be drastically improved through new synthesis routes and intelligent process design?

One area of chemical technology which can help to solve these problems is catalysis. This has been developed into an economically and ecologically extremely important field in the chemical and refinery industries. The application of catalysis, however, is not limited to these industrial branches. To the general public,

catalysis has become associated with environmental protection, in particular because one connects the word 'catalyst' with the decontamination of environmentally harmful exhaust gases of automobiles using 3-way catalysts, or with the denitrification of the flue gases of electrical power plants. But these are only two examples of the widespread applications of catalysts, in 'end-of-pipe' technology. These secondary approaches have become synonymous with environmental proctection over the past 25 years. Processes which generate waste have to meet more and more stringent governmental regulations by means of consecutive separation devices or of catalysed chemical transformations. These procedures are often very expensive due to the complex nature of environmentally harmful compounds.

The function of catalysts in the future should not be to eliminate and destroy harmful substances in an expensive way at the end of the process, but rather to avoid the formation of such harmful substances in the process by means of primary approaches. With regard to this so-called *production or reactor integrated environmental protection*, catalysts are used as modern tools for the selective transformations of chemical compounds. They should help us to synthesize products in the oil and chemical industries in a resource-protective way, without any formation of by-products and waste, as well as being economically competitive. Thus catalysts are the key for sustainable developments in the chemical and refinery industries as was proposed on the occasion of the environment summit conference held in Rio de Janeiro. The German chemical industry supported this request with its commitment to *responsible care*.

The economic importance of catalysts is mirrored in the world market for catalysts and, in particular, in the sale of chemicals produced in catalysed processes. The value of the worldwide catalyst market is about 6 billion $US. In the USA, the largest chemical market, catalysts worth about 1.5 billion $US were used in the annual production of chemicals and petrochemical products in the 1990s. The added value of the catalytically manufactured products was about 900 billion $US. That represents about 20% of the gross national product in the USA.[3] These figures demonstrate the great significance of catalysis, not only to the chemical industry but to the world economy. In fact, at least one catalytic step is involved in the production of about 90% of all chemical products.

Catalyst research and industrial catalyst development will face new challenges in the future. Thus, environmentally friendly, optically pure chemicals for the pharmaceutical and agrochemical as well as fragrance industry must be produced by means of catalysts. Furthermore, highly selective and resources-protecting synthesis routes have to be developed without the formation of by-products and waste. Increasingly chemicals have to be produced from renewable feedstocks. A broad utilisation of alternative energy sources must be achieved in various areas of technology and in our daily lives as, for example, in transportation.

In the field of production integrated environmental protection, heterogeneous catalysts will play an important role. Already, today, there are a reasonable number of examples.[4,5] For instance, the direct synthesis of *tert*-butylamine, a valuable intermediate for the tire and pharmaceutical industry, is being manufactured starting from isobutene and ammonia.[4–6] BASF researchers have developed a catalyst for this process showing a catalytic performance of more than 99% selectivity with an industrially feasible process time. In comparison to the conventional process based on the Ritter route, which starts from isobutene but uses highly toxic HCN and corrosive H_2SO_4, the new BASF process does not involve such toxic compounds. The 3-step Ritter process starts with 4.5 tons of starting material and produces 1 ton of *tert*-butylamine and about 3 tons of waste. In the one-step BASF process, 1 ton of feedstock is converted to 1 ton *tert*-butylamine in an environmentally benign procedure without the formation of dangerous intermediates.

The replacement of chlorine as a traditional oxidant by the more environmentally friendly H_2O_2 or O_2 is a major goal of chemists in industrial and academic laboratories. In this connection, there is a remarkable BASF process for the production of citral from isobutene and formaldehyde.[3,4] Citral is a valuable intermediate in the preparation of the violet aroma used in perfumes and household cleaners. Furthermore it is used as a building block for the synthesis of carotinoids and vitamin A. Production by extraction from fruits makes no commercial sense due to the high demand for citral. In the traditional route this important intermediate is synthesized in a 5-step procedure starting from β-pinene extracted from pine trees. The drawbacks to this conventional process are low yields, chlorine containing by-products and a multistep synthesis route. The ecologically and economically more favoured BASF process starts with cheaply available isobutene and formaldehyde. The most important stage in this 3-step procedure is the partial oxidation of isoprenol to isoprenal in the presence of pure oxygen. A silver catalyst in a special shortfixed bed reactor allows the adjustment of the residence time by 1000th of a second. A 95% overall yield

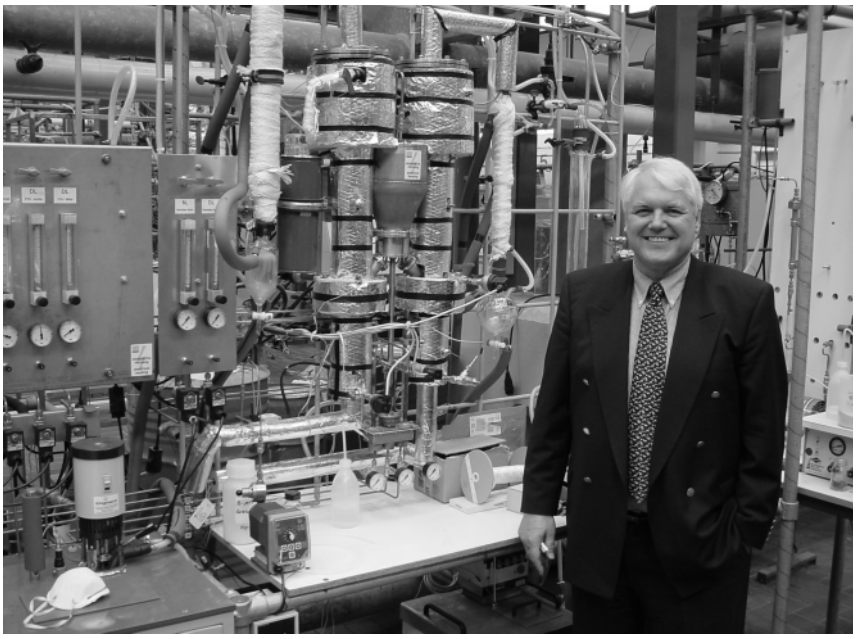

Wolfgang Hoelderich in the Chemical Technology and Heterogeneous Catalysis Laboratory at the University of Technology RWTH, Aachen, Germany.

of citral can be achieved. The advantages of the BASF technology are less synthesis steps, no production of chlorinated side-products and more favourable starting materials.

In order to evaluate the exploitation of the starting materials and the environmental compatibility of chemical processes, the so called E-factor[7] and atom utilisation[8] can be considered. The above mentioned examples make it evident that the E-factor (ratio of by-products to desired compound) can be drastically reduced by the use of heterogeneous catalysts. Future chemical processes will have to be measured in comparison to such examples of green chemical technology.

References

1 Div., Serie: Projekt Deutschland 2000. In: *Der Spiegel*, 1998, **40**.

2 Jacques Leslie, Down of the Hydrogen Age. In: *Wired*, October 1997, pp. 138–148

3 W. F. Hoelderich. New Reactions in Various Fields and Production of Speciality Chemicals. *Stud. Surf. Sci. Catal.*, 1993, **75**, 127–163.

4 A. Chauvel, B. Delmon, W. F. Hoelderich. New Catalytic Processes Developed in Europe During The 1980s. *Appl. Catal. A: General*, 1994, **115**, 17.

5 K. Tanabe and W. F. Hoelderich. Industrial application of solid acid-base catalysts. *Appl. Catal. A: General*, 1999, **181**, 399–434.

6 W. F. Hoelderich and G. Heitmann. Synthesis of intermediate and fine chemicals on heterogeneous catalysts with respect to environmental protection. *Catal. Today*, 1997, **38**, 227–233.

7 R. A. Sheldon. Catalysis and Polution Prevention. *Chem. Ind.*, January 1997, 12–15.

8 B. M. Trost, *Angew. Chem., Int. Ed. Engl*, 1995, **34**, 259.

Greening the chemistry curriculum at the University of Scranton

Michael Cann from the Chemistry Department at the University of Scranton in the USA reports on progress in introducing green chemistry into the curriculum since 1996

In the USA, green chemistry can trace its major roots back to the Pollution Prevention Act of 1990 and the subsequent formal focus on green chemistry by the EPA beginning in 1991. By 1990, in the USA over 130 environmental laws had been passed but they all dealt with the remediation or capture of pollutants after they were formed, or they offered the so-called 'end-of-the-pipe' solution. The Pollution Prevention Act of 1990 was the first act in the US to foster the notion of preventing pollution at the source. This act is in part responsible for the subsequent formal focus on green chemistry by the EPA in 1991. Since the early nineties significant strides have been made in the areas of research, development and application of green chemistry/technology. A small but growing number of industrial and academic chemists, across the globe, have recognized the significant environmental, social and economic benefits that green chemistry has to offer. Each year a growing number of national and international conferences focus in part, or solely, on green chemistry. Of course, 1999 saw this *journal* make its debut focusing only on green chemistry. National awards recognizing outstanding achievements in green chemistry are now given in the USA,[1] the UK,[2] Australia,[3] Italy,[4] Germany[5] and a European Green Chemistry Award has been proposed.[6] Although a small and growing number of research chemists are focusing on green chemistry, in order to broaden this base we must bring green chemistry into the classroom. We must teach our students of today/our chemists of tomorrow to view all chemistry with pollution prevention in mind. It is time to turn a significant amount of our energies toward the greening of the chemistry curriculum.

At the University of Scranton we began to green our curriculum in 1996. This started on a small scale with our environmental chemistry course. The summer of 1996 saw the first awards made for the Presidential Green Chemistry Challenge. We thought that the topics of these awards might make excellent discussion themes in this course. Teams of students were assigned to each of the awards with an objective of presenting these awards as both poster and oral presentations.[7,8] The staff at the EPA graciously supplied us with copies of the winning Presidential Green Chemistry Challenge proposals. Each team, armed with a proposal, was to assemble further information on the topic. Gathering information on the topic was accomplished *via* direct contact with the proposal authors, searching the literature using STN, and searching the web. The content of the poster presentation consists of an abstract, a discussion of the prior art in the field (the problem/brown chemistry), a discussion of the green chemistry/technology and a bibliography. This experience is valuable to students for several reasons, which include:

- It exposes them to state of the art, award winning, applied and novel green chemistry.
- By contacting the authors of the proposals they are exposed to real-live chemists. This compels them to realize that people make discoveries, something they seem to lose track of when reading most textbooks.
- This is often the first time that have the opportunity to do a poster presentation and an oral presentation on a technical topic.

- Although working in teams in many other disciplines is encouraged, seldom do they have to function as a team in a traditional chemistry lecture course. Functioning as a team perhaps is more like what they will find in the real world.

We continue to provide this project each year within the course.

Although this was a start at greening our curriculum, this course only 'plays' to about 10–15 students per year. Only our environmental science majors are required to take environmental chemistry, while our chemistry and biochemistry students may take it as an option. In order to reach a much wider audience of both majors and non-majors, it is necessary to insert green chemistry into the mainstream chemistry courses starting with general chemistry and organic chemistry, all the way through our senior level courses. Although the Presidential Green Chemistry Challenge proposals provide an excellent source of outstanding green chemistry, they were never intended for a student audience. Recognizing the need to bring green chemistry into the curriculum, in 1998, the ACS (American Chemical Society) and the EPA partnered to form the Green Chemistry Educational Materials Development Project. Goals of this project are to develop:

- an annotated bibliography
- real-world cases in green chemistry
- laboratory modules
- short courses on green chemistry

We were fortunate to be able to participate in this project by authoring *Real-World Cases in Green Chemistry*.[9] This book attempts to take examples of outstanding green chemistry that were nominated for the Presidential Green Chemistry Challenge program, and present them in a form that is suitable for an undergraduate student audience, and discussion in the classroom. It is our hope and intent that the content and layout of these cases will allow their use by instructors in a wide variety of university chemistry courses to green the chemistry curriculum. Each of the cases is cast in the same format, which consists of the following sections:

- The *Overview* briefly describes the environmental concerns of the current industrial processes (the 'Problem' or the 'brown' chemistry) and how the green chemistry (the 'Solution'), which has been developed, alleviates many of these environmental problems. This section gives a snapshot of the case.
- The *Background* describes the chemistry that is needed to understand the case, and provides a more detailed discussion of current industrial practices and the environmental dilemmas associated with these practices.
- The *Green Chemistry* section explains the environmentally benign chemistry that was developed to replace the current industrial practices. This section also elucidates how the new technology will reduce or eliminate the environmental problems associated with the current industrial processes.
- The *Green Chemistry in Action* section illustrates how green chemistry has been implemented by industry. This section demonstrates how green chemistry can actually reduce pollution at the source.

In addition to the ten examples of green chemistry, there is also an *Introduction* to green chemistry. This provides a definition of green chemistry, the Twelve Principles of Green Chemistry, and discussions of the Presidential Green Chemistry Challenge Awards, the need for, and industrial interest in green chemistry, and the ACS/EPA Green Chemistry Educational Materials Development Project. A *Notes to Instructors* section suggests ways these real-world examples might be used to infuse the chemistry curriculum with green chemistry and what courses (and topics in a course) a particular case is best suited for. We have used this publication extensively in our environmental chemistry course. One may also find these real-world examples a valuable resource in teaching a course in green chemistry.

The examples of green chemistry in *Real-World Cases in Green Chemistry* were written to provide general information, in a broad sense so that they might be applicable to many different courses. In 2000 we were awarded a Camille and Henry Dreyfus Foundation grant[10] to develop green chemistry teaching modules for use in specific courses. The objective of this project was to take the general information provided by a particular case in *Real-World Cases in Green Chemistry*, supplement this with more (course specific) detailed information so that the module specifically addressed a topic(s) in a particular course. The module is then to be used for insertion of green chemistry into a course under a particular topic already covered in such a course. Thus we have attempted to green a typical course topic without adding a great deal of new material to an already overcrowded course. Each of the modules was written by an instructor who is, adept at and experienced in, teaching the target course. Six members of the University of Scranton Chemistry Department (T. Dickneider, T. Foley, D. Marx, D. Narsavage-Heald, J. Wasilewski and M. Cann) participated in writing modules for the following nine courses.

- General chemistry
- Organic chemistry
- Inorganic chemistry
- Biochemistry
- Environmental chemistry
- Polymer chemistry
- Advanced organic chemistry
- Chemical toxicology
- Industrial chemistry

These modules have been placed on the web along with an introduction to green chemistry.[11] The modules are now being used at Scranton to *green our chemistry curriculum*. As our students progress from freshman to senior year they will be exposed to green chemistry across our curriculum with the intent to inculcate green chemistry into their psyche, so they 'think green' in all the chemistry they encounter as practicing scientists.

For each of the modules there is an accompanying PowerPoint presentation, which may be viewed online or simply downloaded. In addition there are *Notes to Instructors*, which suggest what topics the module can be related to (in the target course) and additional courses that the module might be applicable to. We hope that by developing and placing the *Module*, PowerPoint, and *Notes to Instructors* on the web, that we have 'lowered the energy of activation' for instructors at other institutions to insert green chemistry into their courses. We encourage others to use the modules in whole or in part, intact or modified, to green their curriculum.

We have also begun to work on greening our chemistry laboratory courses and our non-science major chemistry classes at Scranton. In addition attempts are underway to infuse green chemistry/technology into our business curriculum.

A partial listing of other efforts at greening the chemistry curriculum and developing green chemistry educational

materials can be found in the following references and web sites:

- Dennis L. Hjeresen, David L. Schutt and Janet M. Boese. Green Chemistry and Education, *J. Chem. Educ*., 2000, **77**, 1543.
- Scott M. Reed and James E. Hutchison. Green Chemistry in the Organic Teaching Laboratory: An Environmentally Benign Synthesis of Adipic Acid, *J. Chem. Educ*., 2000, **77**, 1627.
- Mono M. Singh, Zvi Szafran and Ronald M. Pike. Microscale Chemistry and Green Chemistry: Complementary Pedagogies. *J. Chem. Educ*., 1999**, 76**, 1684.
- Terrence J. Collins. Introducing Green Chemistry in Teaching and Research. *J. Chem. Educ.*, 1995, **72**, 965.
- http://www.chemsoc.org/networks/gcn/educate.htm
- http://www.chemsoc.org/networks/gcn/links4.htm. See the links on this page.
- http://www.acs.org/education/greenchem/
- http://www.epa.gov/opptintr/greenchemistry/ educat.htm
- http://www.scs.uiuc.edu/ISTP/
- http://www.elmhurst.edu/~chm/onlcourse/chm212/semgreentalk.html
- http://www.uoregon.edu/~hutchlab/greenchem/

References

1 Presidential Green Chemistry Challenge Awards, http://www.epa.gov/opptintr/greenchemistry/presgcc.htm
2 UK Green Chemistry Awards, http://www.chemsoc.org/networks/gcn/awards.htm
3 The Royal Australian Chemical Institute Inc. Green Chemistry Challenge Awards, www.raci.org.au/RACI/awards.html
4 NCA Recognition Program, http://helios.unive.it/inca
5 Haltermann Innovation Prize, http://www.haltermann.com/product/news/default.htm
6 http://www.fbr.dk/chemaware/newslet/issue13/article8.html
7 For further information on this project see: M. C. Cann, "Bringing State of the Art, Applied, Novel, Green Chemistry to the Classroom, by Employing the Presidential
8 Green Chemistry Challenge Awards," *J. Chem. Educ*., 1999, **76**, 1639; the syllabus for this course can be viewed at: http://academic.scranton.edu/faculty/CANNM1/CH340SYL00.html
9 M. C. Cann and M. E. Connelly, Real-World Cases in Green Chemistry, American Chemical Society, Washington, D.C., 2000.

10 Additional support for this project from the ACS/EPA Green Chemistry Educational Materials Development Project, the University of Scranton Faculty Development Fund and the University of Scranton Chemistry Department is also gratefully acknowledged.

11 http://academic.scranton.edu/faculty/CANNM1/dreyfusmodules.html

Novel recyclable catalysts for atom economic aromatic nitration

Chris Braddock of the Department of Chemistry at Imperial College, London, presents the work for which he was awarded the Jerwood Salters' Environment Award, 2000

Introduction

Nitration of aromatic compounds is an immensely important industrial process.[1] The nitroaromatic compounds so produced are themselves widely utilized and act as chemical feedstocks for a wide range of useful materials such as dyes, pharmaceuticals, perfumes and plastics. Unfortunately nitrations typically require the use of potent mixtures of concentrated or fuming nitric acid with sulfuric acid leading to excessive acid waste streams and added expense. Alternatively, nitric acid may be used in conjunction with strong Lewis acids such as boron trifluoride.[2] The Lewis acid is used at or above stoichiometric quantities and is destroyed in the aqueous quench liberating large amounts of strongly acidic by-products. With chemists under increasing pressure to perform atom economic processes,[3] creating minimal or no environmentally hazardous by-products, development of novel catalyst systems that facilitate aromatic nitrations in this manner should be of great importance.[4]

Lanthanides have found increasing use as mild and selective reagents in organic synthesis.[5] In particular, lanthanide(III) triflates[6] have been used to good effect as Lewis acids in Diels–Alder,[7] Friedel–Crafts,[8] Mukaiyama aldol[9] and other reactions.[10] For the Mukaiyama reaction the optimum solvent system was found to be aqueous THF; the catalyst was recycled *via* aqueous work up and used repeatedly with little detriment to rate or yield. The compatibility of lanthanide(III) triflate salts with water and other protic solvents and yet their apparent ability to function as strong Lewis acids is somewhat paradoxical. We sought to harness this water tolerant Lewis acidity and have instigated a program in the area of clean technology using lanthanide(III) triflates for atom economic transformations.[11] Herein we report on the use of catalytic quantities of lanthanide(III)[12] and group IV metal[13] triflates [$Ln(OTf)_3$, Ln = La–Lu; $M(OTf)_4$, M = Hf, Zr] and tris(trifluoromethanesulfonyl)methides ('triflides') [$M(CTf_3)_3$; M = Yb, Sc] for the nitration of a range of simple and electron deficient aromatic compounds in good to excellent yield using a stoichiometric amount of 69% nitric acid wherein the only by-product is water. Furthermore the catalysts are readily recycled and re-used by a simple evaporative process.

Results and discussion

Ytterbium(III) triflate as a recyclable catalyst for the nitration of arenes with nitric acid. Our investigations began with the commercially available hydrated ytterbium(III) triflate.[14] A range of simple aromatic compounds, both electron rich (quantified by a negative Hammett coefficient, σ_p^+) and electron poor (positive coefficient), were treated with 1 equiv. of 69% nitric acid in refluxing 1,2-dichloroethane in the presence of 10 mol% ytterbium(III) triflate (Scheme 1).[15] Initial work utilized anisole (Hammett coefficient $\sigma_p^+ = -0.78$), however this led to extensive polymerisation with the formation of intractable organic tars even at room temperature. Alkyl bearing aromatic compounds (Table 1, entries 2, 6 and 8) and naphthalene (Table 1, entry 9) were nitrated smoothly and efficiently in refluxing 1,2-dichloroethane and this represents the effective upper limit in reactivity for the arenes (toluene $\sigma_p^+ = -0.31$). The lower reactivity limit was next explored. Biphenyl (entry 3, $\sigma_p^+ = -0.18$), and bromobenzene (entry 4, $\sigma_p^+ = +0.15$) were nitrated successfully (Table 1) but little success was achieved with benzoic acid ($\sigma_p^+ = +0.42$), acetophenone ($\sigma_p^+ = +0.47$), ethyl benzoate ($\sigma_p^+ = +0.48$) or benzonitrile ($\sigma_p^+ = +0.70$). No dinitrated products were observed in any case and in accord with this the system failed to nitrate nitrobenzene (Table 1, entry 5, $\sigma_p^+ = +0.79$) and the lower reactivity limit is set at approximate Hammett values of $\sigma_p^+ = +0.3$. In the control experiments with no catalyst, only slow reaction occurred and no more than 10% of nitrated products were observed under these conditions.

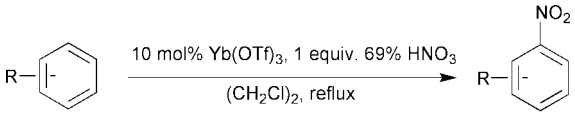

Scheme 1 Nitration of simple arenes with Yb(OTf)$_3$.

Table 1 Nitration of aromatics with catalytic quantities of $Yb(OTf)_3$[a]

Entry	Arene	Conversion (%)[b,c]	Product distribution[c] *ortho*	*meta*	*para*
1	Benzene	> 95 (95)	n/a		
2	Toluene	> 95 (95)	52	7	41
3	Biphenyl	89	38	trace	62
4	Bromobenzene	92	44	trace	56
5	Nitrobenzene	0	—	—	—
6	*p*-Xylene	> 95	n/a		
7	*p*-Dibromobenzene	8	n/a		
8	*m*-Xylene	> 95	$4\text{-}NO_2$:85	$2\text{-}NO_2$:15	
9	Naphthalene	> 95	$1\text{-}NO_2$:91	$2\text{-}NO_2$:9[d]	

[a] All reactions carried out on a 3 mmol scale with 10 mol% ytterbium(III) triflate and 1.0 equiv. of 69% nitric acid in refluxing 1,2-dichloroethane (5 ml) for 12 h. [b] Isolated yields in parentheses. [c] Determined by GC and/or ^{1}H NMR analysis. [d] Care: nitronaphthalenes are potent human carcinogens.

DOI: 10.1039/b102113n

It is important to note that the only side product from these nitrations is water. With the additional benefit that the catalyst can be recycled, this simple methodology represents an efficient and environmentally friendly process.

Kobayashi has demonstrated the feasibility of recycling lanthanide(III) triflates for a range of reactions.[6b,16] Consequently, ytterbium(III) triflate could be recovered from the reaction mixture at the completion of any particular nitration run *via* simple partition work-up and isolated by evaporation of the aqueous phase.[15] [evaporation of the organic phase gives the nitroaromatic]. The resulting free-flowing white solid was found to have an identical IR spectrum to that of the commercially available material and could be re-used as the catalyst for further nitration runs with no loss in rate or yield or change in isomer distributions. The results for four successive nitrations of *m*-xylene with recycled ytterbium(III) triflate are shown above (Table 2).

Table 2 Recycled ytterbium(III) triflate for the nitration of *m*-xylene[a]

Run	Conversion(%)[b]	Mass of catalyst/mg[c]
1	89	190 (>100)
2	81	152 (82)
3	90	127 (68)
4	88	115 (62)

[a] All runs performed with 3 mmol *m*-xylene, 10 mol% ytterbium triflate (run 1) and 1 equiv. of 69% nitric acid in refluxing 1,2-dichloroethane (5 ml) for 5 h. [b] Determined by GC analysis. The isomeric ratio of 4- and 2-nitroxylene was unchanged throughout (85:15 respectively). [c] Mass of ytterbium(III) triflate recovered from each run. The figures in parentheses indicate the percentage recovery which were not optimised.

Screening the lanthanide(III) triflates

With a view towards rate optimisation a range of lanthanide(III) triflates were examined as potential catalysts. All were found to exhibit catalytic competence but marked differences were apparent (Table 3).

Inspection of the data reveals a clear inverse correlation (with the exception of a few scattered data points) between the ionic radii of the various tripositive lanthanide ions and the extent of nitration whereby the heavier congeners are the most effective. Thus lanthanum(III) ($Z = 57$) triflate gave a 64% conversion of naphthalene to mononitronaphthalenes over 1 h, whereas the ytterbium(III) ($Z = 70$) triflate catalysed reaction gave a >95% conversion over the same time period.

Table 3 Effect of various $Ln(OTf)_3$ for the nitration of naphthalene

$Ln(OTf)_3$[a,b]	Ionic radius/Å[c]	Charge/size (Z/r)	Conversion(%)[d]
Control	n/a	n/a	38
La (57)	1.172	2.56	64
Ce (58)	1.15	2.61	—
Pr (59)	1.13	2.65	73
Nd (60)	1.123	2.67	39
Pm (61)	(1.11)	(2.70)	Radioactive
Sm (62)	1.098	2.73	67
Eu (63)	1.087	2.76	>95
Gd (64)	1.078	2.78	82
Tb (65)	1.063	2.82	93
Dy (66)	1.052	2.85	64
Ho (67)	1.041	2.88	93
Er (68)	1.033	2.90	95
Tm (69)	1.020	2.94	—
Yb (70)	1.008	2.98	>95
Lu (71)	1.001	3.00	>95

[a] All reactions performed on a 3 mmol scale in 5 ml refluxing 1,2-dichloroethane with 1.05 equiv. of 69% nitric acid and 10 mol% catalyst. [b] The atomic number is shown in parentheses. [c] Taken from *Lanthanides in Organic Synthesis*, ed. T. Imamoto, Academic Press, New York, London, 1994, p. 4. [d] Determined by GCMS: 1-nitro:2-nitro-naphthalene were obtained in a 9:1 ratio.

Postulated mechanism and structural analysis

The isomer distributions from the nitrations of various arenes (Table 1) are consistent with direct electrophilic attack by nitronium ion or, more probably, a nitronium 'carrier' of some description (**1**). The inverse correlation of ionic radii (which should more properly be expressed as charge-to-size ratio, Z/r) and catalytic competence (Table 3) is indicative of interplay between the lanthanide ion and nitric acid where evidently an increasing electrostatic interaction leads to greater reactivity. On this basis a working mechanism can tentatively be proposed. Firstly, nitric acid binds to the lanthanide metal *via* displacement of water from its inner co-ordination sphere (the reactions are performed with 69% nitric acid and the catalyst resides predominately in the aqueous phase as judged by solubility studies). The triflate counterions are outer sphere and effectively spectator ions [Scheme 2, eqn (1)]. The resulting strong polarisation due to the metal results in proton liberation affording a lanthanide bound nitrate species **1** [Scheme 2, eqn (2)] and the proton goes on to liberate NO_2^+ in the classical manner [Scheme 2, eqn (3)]. Thus, the experimentally observed correlation between increasing charge-to-size ratios (*i.e.* decreasing ionic radii) and extent of conversion is rationalised by noting that the release of the 'catalytic proton' is more facile as the metal becomes more polarising.

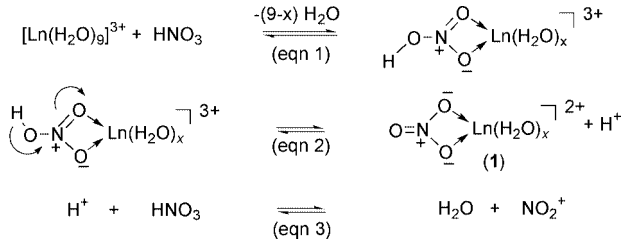

Scheme 2 Proposed mode of action.

It becomes clear that the lanthanide salt is acting as a 'sink' for nitrate ions, displacing the classical equilibrium process (Scheme 3) invoked for the autoionisation of nitric acid to the right hand side; the stronger the binding, the greater the equilibrium concentration of nitronium ion and hence the increased rate of nitration.

Inspection of the proposed nitration mechanism (Scheme 2) reveals that the mononitrate dipositive lanthanide species $[Ln(H_2O)_x(NO_3)](OTf)_2$ **1** is the key intermediate. An independent preparation and characterisation of such a species enables possible identification of **1** directly *in situ* in the reaction mixture. Additionally, spectroscopic examination of these salts may provide some evidence for our working model. We have developed a novel preparation of these mixed salts by simple metathesis of lanthanide chlorides with the requisite quantities of silver nitrate and silver triflate in water (Scheme

The lanthanide salt 'captures' nitrate ions increasing the equilibrium concentration of the *de facto* nitrating agent: NO_2^+

Scheme 3 Effect of lanthanide on classical nitronium ion equilibrium.

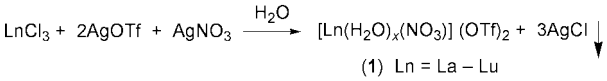

Scheme 4 Preparation of putative intermediate 1.

4).[17] The resulting hydrated salts were white or lightly coloured (pink, green or yellow) solids which were found to be stable indefinitely at room temperature in the solid state.

Characterisation was accomplished by IR spectroscopy. These materials exhibited the six stretches in the IR spectrum indicative of a symmetrically bound (*i.e.* inner sphere) bidentate nitrate species[18] as well as the requisite (outer sphere) triflate stretches. For example, ytterbium(III) based analogue displayed characteristic nitrate absorptions at 1492, 1384, 1326, 814, 769 and 751 cm^{-1}. The stretch at 1492 cm^{-1}, assigned as the A_1 symmetrical stretch, is known to be critically dependent on the polarising power of the metal centre where increased polarisation of the nitrate leads to the observation of stretches at increased wavenumbers.[18]

The A_1 stretching frequencies were found to increase steadily in magnitude across the lanthanide period for the $[Ln(H_2O)_x(NO_3)](OTf)_2$ salts starting at 1450 cm^{-1} for lanthanum (r^{3+} = 1.172 Å, Z/r = 2.56) and ending at a value of 1497 cm^{-1} for lutetium (r^{3+} = 1.00, Z/r = 3.00) (Table 4). This structural data correlates extremely well with the observed reactivity of the respective lanthanide(III) triflates for nitration and can be taken as strong evidence for the proposed mode of action.

A plot of the A_1 IR stretching frequencies *versus* the charge-to-size ratio of tripositive lanthanide ions reveals two straight lines with an intersection point located around atomic number Z = 60 (Fig. 1). This can be interpreted as a change in coordination number where the hydration sphere is somewhat more compact for the heavier (and thus smaller) lanthanide ions in line with literature precedent.[19]

Table 4 Characterisation of $[Ln(H_2O)_x(NO_3)](OTf)_2$ by IR spectroscopy

Ln	Ionic radius (+3)/Å	Charge-to-size ratio (Z/r)	IR stretch[a]/cm^{-1}
La	1.172	2.56	1450
Ce	1.15	2.61	1461
Pr	1.13	2.65	1469
Nd	1.123	2.67	1477
Pm	(1.11)	(2.70)	(Radioactive)
Sm	1.098	2.73	1478
Eu	1.087	2.76	1482
Gd	1.078	2.78	1484
Tb	1.063	2.82	1480
Dy	1.052	2.85	1490
Ho	1.041	2.88	1489
Er	1.033	2.90	1492
Tm	1.020	2.94	1496
Yb	1.008	2.98	1492
Lu	1.001	3.00	1497

[a] The bands for these stretches were fairly broad and at times split into two poorly resolved signals—the corresponding error due to peak picking is estimated to be *ca.* 5 cm^{-1}.

Group IV metal triflates as superior nitration catalysts

From the above structural analysis it becomes clear that metal triflates with charge-to-size ratios greater than '3' (*i.e.* greater than that of the smallest lanthanide: lutetium) should be more effective nitration catalysts. We considered that the group IV metals hafnium (r^{4+} = 0.78 Å, Z/r = 5.13) and zirconium (r^{4+} = 0.79 Å, Z/r = 5.06) might be suitable for such a purpose. In line with this reasoning we noted that hafnium(IV) triflate has been shown to be an effective catalyst for Friedel–Crafts acylations and alkylations where the corresponding lanthanide salts were less active.[20]

Extrapolation of the plot shown in Fig. 1 indicates that a metal cation with a charge-to-size ratio of approximately '5.1' might be expected to show an A_1 nitrate stretching frequency in its IR spectrum for salts of the type $[M(H_2O)_x(NO_3)](OTf)_3$ in the vicinity of 1650 cm^{-1} (Fig. 2) suggestive of a very tightly bound nitrate and hence a very active nitration catalyst [for $M(OTf)_4$].

Hafnium and zirconium mononitrate tris(triflate), $[M(H_2O)_x(NO_3)](OTf)_3$, were prepared from their tetrachlorides in analogous fashion to the lanthanide salts. Much to our delight these (deliquescent) salts displayed A_1 nitrate stretching frequencies in their IR spectra at 1651 and 1650 cm^{-1} respectively. Armed with this pleasing information and with a specific programme aim of nitrating *o*-nitrotoluene (ONT) to dinitrotoluenes (DNTs) with these catalyst types (catalytic quantities of ytterbium(III) triflate were essentially ineffective for this transformation), hafnium(IV) and zirconium(IV) triflate were prepared as their hydrated salts *via* metathesis of their tetrachlorides with silver triflate in water.

The freshly prepared hafnium salt was employed at a 10 mol% loading for the nitration of ONT with nitric acid in

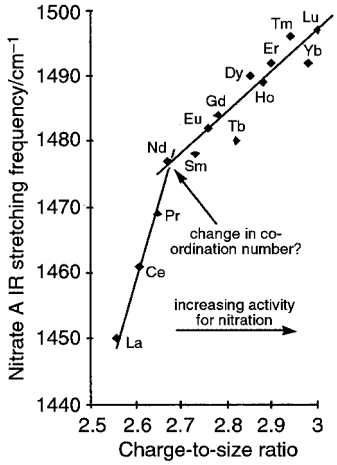

Fig. 1 Plot of A_1 IR nitrate stretches for the $Ln(H_2O)_x(NO_3)(OTf)_2$ complexes.

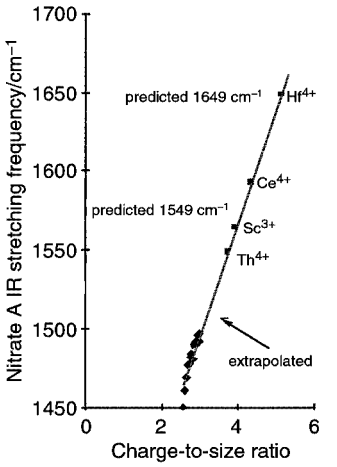

Fig. 2 Extrapolation of A_1 stretching frequencies for metals with increased charge-to-size ratios.

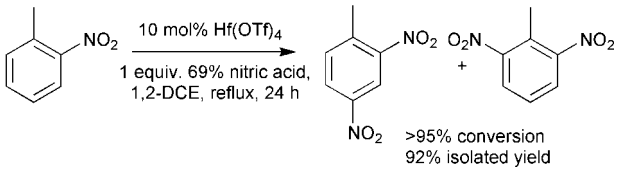

Scheme 5 Nitration of o*-nitrotoluene with Hf(OTf)$_4$*

refluxing 1,2-dichloroethane (Scheme 5). After 24 h no ONT remained and 2,4- and 2,6-DNT were isolated in 92% yield as a 65:35 mixture after aqueous work-up. Similarly, zirconium(IV) triflate (10 mol%) was found to have comparable catalytic activity for the nitration of ONT; essentially complete conversion was obtained after 24 h, and 2,4- and 2,6-DNT were isolated in 87% yield in a 66:34 ratio. The catalyst could be recovered by the usual aqueous work-up regime. This recovered material had an identical IR spectrum to that of the freshly prepared catalyst with additional minor signals for (presumably) nitro containing compounds and was utilized for

Table 5 Recycled zirconium(IV) triflate for the nitration of *o*-nitrotoluene

Run[a]	*t*/h	Conversion (%)[b]	Mass recovery/mg[c]
1	24	> 95 (87)	173 (86)
2	27	> 95 (80)	134 (67)
3	23	88 (76)	121 (61)

[a] All runs performed with 3 mmol *o*-nitrotoulene, 10 mol% zirconium(IV) triflate (200 mg) (run 1) and 1 equiv. of 69% nitric acid in refluxing 1,2-dichloroethane (2 ml). [b] Determined by GC analysis. The isomeric ratio of 2,4- and 2,6-DNT was unchanged throughout (65:35, respectively). The isolated yields are shown in parenthesis. [c] Mass of zirconium(IV) triflate recovered from each run. The figures in parentheses indicate the percentage recovery which was not optimised.

a further two nitration runs (Table 5). These results demonstrate that our model based on charge-to-size ratios successfully predicted the activities of various metal triflates for nitrations.

Solvent and counterion effects

The two phase nature of the reaction mixture (aqueous nitric acid/lanthanide salt and solvent/substrate) poses a number of questions. Foremost amongst these is the following: in which phase does the actual nitration occur? Comparison of the nitration rates using 1,2-dichloroethane (bp 83 °C) *versus* cyclohexane (bp 80 °C) as the solvents (both reactions performed at reflux) allows speculation on this matter. For the nitration of naphthalene with 10 mol% ytterbium(III) triflate a 78% conversion of naphthalene to mononitronaphthalenes occurred over 0.5 h in 1,2-dichloroethane whereas for cyclohexane only a 24% conversion was observed. Based on this result it seems reasonable to conclude that the electrophilic substitution process transpires in the organic phase.

We have previously surmised that the nitrating agent in this system is the nitronium ion. Evidently the nitronium ion diffuses into the organic phase from the aqueous layer where it has been generated. Moreover, it becomes apparent that in order to maintain overall charge neutrality, the nitronium ion must be accompanied by an anionic counterion (*i.e.* triflate). Thus, the triflate conterion fulfills two roles; it is the conjugate base of a sufficiently strong acid such that nitric acid is preferentially protonated, producing the nitronium ion and acts as a 'shuttle' for the transportation of the nitronium ion into the

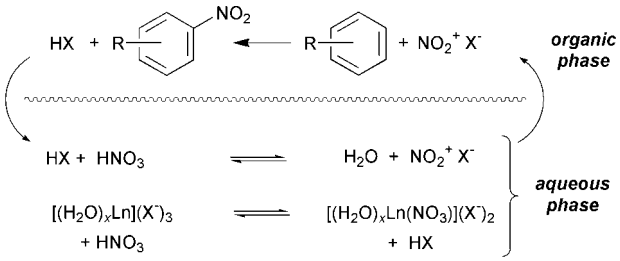

Scheme 6 The dual rôle of the counterion

organic phase where nitration occurs (Scheme 6) and where it is thought that the solubility of the nitronium salt (NO_2^+ OTf^-) is a key factor.[21]

Evidence to support this 'counterion modified' model comes from the investigation of hydrated $Ln(NO_3)Cl_2$ prepared in the usual way in water ($LnCl_3$, $AgNO_3$). The lanthanide(III) chlorides themselves show little or no catalytic activity for nitrations. A possible rationale for this is obtained by noting that HCl is a poor activator of nitric acid in nitration chemistry since it is not sufficiently acidic to protonate nitric acid. However, the IR spectra of the $Ln(NO_3)Cl_2$ salts are essentially identical to those of $Ln(NO_3)(OTf)_2$ indicating that the chloride ions are outer sphere in these complexes. Additionally the nitrate bands show the same trend as demonstrated for the triflate series [*e.g.*, for $La(NO_3)Cl_2$ the characteristic nitrate stretch is observed at 1459 cm^{-1} and for $Yb(NO_3)Cl_2$ the band appears at 1497 cm^{-1}]. This indicates that the lanthanide chlorides are capable of activating nitric acid (*via* metal–nitrate interactions) but critically, the counterion (*i.e.* chloride) is incapable of fulfilling its role (in whatever capacity that may be) and hence no nitration occurs.

We considered various other counterions for the lanthanide salts with a view to producing more active nitration catalysts. The use of trifluoroacetate and pentafluorobenzene sulfonate were ineffective presumably on acidity grounds. The use of the classical conjugate bases of strong acids (BF_4^-, PF_6^-, SbF_6^-) was precluded by their known tendency to undergo fluoride abstraction by strong electrophiles and their penchant for hydrolysis.[22]

Yamamoto *et al*. have demonstrated the use of scandium triflamide, $Sc(NTf_2)_3$, for acetylation and acetalisation chemistry where this material is more active than scandium triflate.[23,24] We recognised that Tf_2NH is itself a very strong acid (gas phase acidity measurements have shown it to be a stronger acid than triflic acid[25] and as such the triflamide anion may well be successful as a counterion for nitrations. Additionally it was hoped that the proposed *in situ* nitrating agent Tf_2N^- NO_2^+ would have enhanced solubility over nitronium triflate thus leading to an additional rate acceleration. Interestingly, Tf_2N^- NO_2^+ is known,[26] as is TfO^- NO_2^+,[27] but does not appear to have been utilized for nitrations. Indeed, experiments have shown that catalytic quantities of $Yb(NTf_2)_3$[28] and $Sc(NTf_2)_3$[29] are 2–3 times more effective than $Yb(OTf)_3$ and $Sc(OTf)_3$ for the nitration of toluene respectively. However at this stage it is not clear whether this rate enhancement is due to the triflamides increased inherent acidity or due to a solubility effect or both.

A logical progression along the series TfO^-, Tf_2N^- leads us to Tf_3C^- ('triflide'). Tf_3CH is a known compound.[30] Remarkably, this material has been shown to be an even stronger acid than either HOTf or $HNTf_2$ (in the gas phase)[25] and has been employed as an electrolyte in non-aqueous high

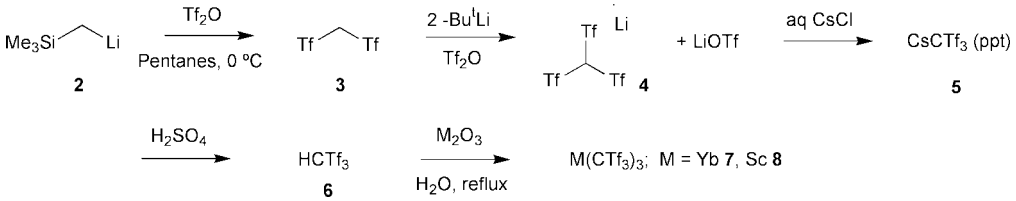

Scheme 7 Preparation of triflidic acid and ytterbium(III) and scandium(III) triflide.

voltage batteries,[31] displaying high anodic stability.[32] The Tf_3C^- counterion would seem to be an attractive target on two counts for lanthanide catalysed nitrations: an inherent acidity increase would lead to faster rates and it seems probable that Tf_3C^- NO_2^+ would have increased solubility in organic phases compared to the triflate and triflamide salts.

The literature preparation of the triflide anion is non-trivial involving handling of gases and non-commercial materials. Accordingly, we have recently developed a novel and convenient synthesis of the triflide anion from readily available triflic anhydride and trimethylsilylmethyllithium (Scheme 7).[33]

Slow addition of triflic anhydride to a stirred solution of trimethylsilylmethyllithium **2** in pentanes at 0 °C resulted in smooth reaction as evidenced by the gradual precipitation of lithium triflate with only a slight increase in the internal temperature (max. *ca.* 10 °C). Basic aqueous quench, extraction with dichloromethane and strong acidification (conc. HCl) of the remaining aqueous phase followed by extraction with dichloromethane led to the isolation of methyleneditriflone **3** as a yellow oil which was essentially pure by ^{1}H NMR but could be obtained as a low-melting white solid after vacuum sublimation. The acidic nature of **3**, which has been estimated[34] to have a pK_a of −1 allows for easy purification *via* acid–base extraction as above and this procedure allows gram quantities to be prepared in a reproducible 50–55% yield.

Triflylation of **3** with triflic anhydride was carried out by double deprotonation with *tert*-butyllithium followed by the addition of triflic anhydride. The expected reaction product, **4**, would, by the precondition of employing triflic anhydride, be contaminated with at least stoichiometric quantities of lithium triflate and a suitable separation regime was required. After quenching with aqueous base, acidification and extraction with dichloromethane to remove all neutral organic side products, lithium triflide and triflate could be extracted effectively from the aqueous phase with diethyl ether. The triflide anion was completely freed from any triflate anion by selective precipitation with cesium chloride in water to give **5**. Purification was effected by vacuum sublimation of the cesium salt from concentrated sulfuric acid (generating the free acid **6**) and re-precipitation with caesium chloride followed by recrystallization giving **5** as an analytically pure white solid. The caesium salt **5** is a convenient way to store the triflide anion and does not decompose or color on standing at room temperature. Simple vacuum sublimation from sulfuric acid using a modification of Seppelt's procedure[30] generates the free acid **5** which is best handled as an aqueous solution.

Ytterbium(III) and scandium(III) triflides [$Yb(CTf_3)_3$ **7** and $Sc(CTf_3)_3$ **8**] were obtained by an analogous protocol employed for the triflate series *viz.* the metal oxides were heated to reflux with the free acid in water. Thus, heating at reflux Yb_2O_3 or Sc_2O_3 in an aqueous solution of $HCTf_3$ **6** provided the both the metal triflides and in essentially quantitative yields as white powders after drying for 24 h. Recrystallization furnished single crystals of the aqua complexes of both $Yb(CTf_3)_3$ and $Sc(CTf_3)_3$ suitable for X-ray crystallography.

Whilst $Yb(OTf)_3$ was essentially ineffective for the nitration of *o*-nitrotoluene (ONT) to dinitrotoluenes (DNT's) giving 8% conversion under our standard conditions (*i.e.* 10 mol% catalyst, 1 equiv. 69% HNO_3, 1,2-DCE, reflux, 24 h), 10 mol% $Yb(CTf_3)_3$ was found to mediate the nitration of ONT to 93% conversion in 24 h. The use of 10 mol% $Sc(OTf)_3$ gave a 50% conversion to DNT's in 24 h although the reaction mixture was found to darken considerably. In contrast, $Sc(CTf_3)_3$ was found to give a 91% conversion within the same time period and no darkening was observed. In all cases, the ratio of 2,4-:2,6-DNT's was found to be 65:35.

Conclusions

We have developed an environmentally acceptable nitration procedure with our initial investigations commencing with the commercially available lanthanide(III) triflates. As a result of an in-depth mechanistic study we have delineated the role both of the metal centre and the counterion. We have used this understanding to design superior catalysts by changing the metal centre or the counterion. In all cases the nitration systems use a single equivalent of nitric acid, the only side-product is water and the catalysts may be recycled and reused. We believe this to be a significant step forward in the area of clean technology for aromatic nitration. This programme of research has in addition had many spin-off discoveries and developments of significance to green chemistry. We have reported a scandium(III) catalysed acetylation of 1°, 2° and 3° alcohols using acetic acid as the acetyl source.[35] We have also shown that the lanthanide(III) triflates are effective catalysts for the oxidation of benzyl alcohols to benzaldehydes where the stoichiometric oxidant is nitric acid.[36] In both these systems the only side-product is water and the catalysts may be recycled and reused. The highly active triflide catalysts have been used to nitrate a series of fluoroaromatics.[37] Industrially, mixed-acid systems (*i.e.* HNO_3/H_2SO_4) present a serious problem in this series of compounds since HF liberation occurs. In our system, HF liberation does not occur. Furthermore we have now extended our 'triflide' technology to the preparation of long chain perfluorinated homologues as funded by the Institute of Applied Catalysis (iAc). We have thereby recently demonstrated the first fluorous phase acylation of arenes[38] with catalyst recycle and re-use, and, accordingly we have applied for patent protection.[39]

Acknowledgements

The Imperial College group thank Air Products and Chemicals Inc. for the support of our research under the auspices of the Joint Strategic Alliance, and the EPSRC.

Notes and references

1 (*a*) G. A. Olah, R. Malhotra and S. C. Narang, *Nitration: Methods and Mechanisms*, VCH, New York, 1989; (*b*) C. K. Ingold, *Structure and Mechanism in Organic Chemistry*, Cornell University Press, Ithaca, New York, 1969, 2nd edn. (*c*) G. A. Olah and S. J. Kuhn, in *Friedel–Crafts and Related Reactions*,

ed. G. A. Olah, Wiley-Interscience, New York, 1964, vol. 2; (*d*) K. Schofield, *Aromatic Nitrations*, Cambridge University Press, London, 1980.

2 (*a*) R. J. Thomas, W. F. Anzilotti and G. F. Hennion, *Ind. Eng. Chem.*, 1940, **32**, 408; (*b*) G. F. Hennion, *US Pat.*, 1943, **2**, 314, 212.

3 B. M. Trost, *Angew. Chem., Int. Ed. Engl.*, 1995, **34**, 259.

4 For a recent nitration using clean methodology see: K. Smith, A. Musson and G. A. DeBoos, *J. Chem. Soc., Chem. Commun.*, 1996, 469. However this method suffers from the disadvantage of stoichiometric quantities of acidic by-products. For the use of clays and other such solid supported acid sources see reference 1*a*.

5 T. Imamaoto, in *Lanthanides in Organic Synthesis*, Academic Press, London, 1994.

6 Reviews: (*a*) R. W. Marshmann, *Aldrichim. Acta*, 1995, **28**, 77; (*b*) S. Kobayashi, *Synlett*, 1994, 689; (*c*) J. B. N. F. Engberts, B. L. Feringa, E. Keller and S. Otto, *Recl. Trav. Chim. Pays Bas*, 1996, **115**, 457.

7 (*a*) H. Ishitani and S. Kobayashi, *Tetrahedron Lett.*, 1996, **37**, 7357; (*b*) S. Kobayshi, H. Ishitani, I. Hachiya and M. Araki, *Tetrahedron*, 1994, **50**, 11 623; (*c*) I. E. Marko and G. R. T. Evans, *Tetrahedron Lett.*, 1994, **35**, 2771; (*d*) T. Saito, M. Kawamura and J.-I. Nishimura, *Tetrahedron Lett.*, 1997, **38**, 3231.

8 (*a*) A. Kawada, S. Mitamura and S. Kobayashi, *Chem. Commun.*, 1996, 183; (*b*) A. Kawada, S. Mitamura and S. Kobayashi, *J. Chem. Soc., Chem. Commun.*, 1993, 1157.

9 (*a*) S. Kobayashi and S. Nagayama, *J. Org. Chem.*, 1997, **62**, 232l; (*b*) S. Kobayashi and I. Hachiya, *J. Org. Chem.*, 1994, **59**, 3590 and references cited therein.

10 (*a*) S. Kobayashi, H. Ishitani and M. Ueno, *Synlett*, 1997, 115; (*b*) S. Kobayshi, H. Ishitani, S. Komiyama, D. C. Oniciu and A. R. Katritzky, *Tetrahedron Lett.*, 1996, **37**, 3731; (*c*) J. H. Forsberg, V. T. Spaziano, T. M. Balasubramanian, G. K. Liu, S. A. Kinsley, C. A. Duckworth, J. J. Poteruca, P. S. Brown and J. L. Miller, *J. Org. Chem.*, 1987, **52**, 1017; (*d*) M. Meguro and Y. Yamamoto, *Heterocycles*, 1996, **43**, 2473; (*e*) S.-C. Diana, K.-Y. Sim and T.-P. Loh, *Synlett*, 1996, 263; (*f*) M. Meguro, N. Asao and Y. Yamamoto, *J. Chem. Soc., Perkin Trans. 1*, 1994, 2579; (*g*) R. Annunziata, M. Cinquini, F. Cozzi, V. Molteni and O. Schupp, *J. Org. Chem.*, 1996, **61**, 8293; (*h*) P. E. Harrington and M. A. Kerr, *Synlett*, 1996, 1047; (*i*) Y. Makioka, T. Shindo, Y. Taniguchi, K. Takaki and Y. Fujiwara, *Synthesis*, 1995, 801; (*j*) S.-I. Fukuzawa, T. Tsuchimoto and T. Kanai, *Bull. Chem. Soc. Jpn.*, 1994, **67**, 2227; (*k*) S. Hosono, W.-S. Kim, H. Sasai and M. Shibasaki, *J. Org. Chem.*, 1995, **60**, 4; (*l*) M. Chini, P. Crotti, L. Favero, F. Macchia and M. Pineschi, *Tetrahedron Lett.*, 1994, **35**, 433; (*m*) H. C. Aspinall, A. F. Browning, N. Greeves and P. Ravenscroft, *Tetrahedron Lett.*, 1994, **35**, 4639; (*n*) S. Matsubara, M. Yoshioka and K. Utimoto, *Chem. Lett.*, 1994, 827; (*o*) P. G. Cozzi, B. Di Simone and A. Umani-Ronchi, *Tetrahedron Lett.*, 1996, **37**, 1691; (*p*) G. Jenner, *Tetrahedron Lett.*, 1996, **37**, 3691; (*q*) T. Hanamoto, Y. Sugimoto, Y. Yokoyama and J. Inanaga, *J. Org. Chem.*, 1996, **61**, 4491; (*r*) E. Keller and B. L. Feringa, *Synlett*, 1997, 842.

11 For the atom economic acylation of alcohols using acetic acid as the acetyl source where the only side product is water and the catalyst is readily recyclable see: A. G. M. Barrett and D. C. Braddock, *Chem. Commun.*, 1997, 351.

12 F. J. Waller, A. G. M. Barrett, D. C. Braddock and D. Ramprasad, *Chem. Commun.*, 1997, 613. For an interesting report utilizing $La(NO_3)_3$/HCl/$NaNO_3$ for the nitration of phenols (but not applicable to any less electron rich aromatics) see: M. Ouertani, P. Girard and H. B. Kagan, *Tetrahedron Lett.*, 1982, **23**, 4315.

13 F. J. Waller, A. G. M. Barrett, D. C. Braddock and D. Ramprasad, *Tetrahedron Lett.*, 1998, **39**, 1641.

14 All the lanthanide(III) triflates are commercially available from the Aldrich Chemical Co. bar promethium (radioactive) and cerium (available in its +4 oxidation state).

15 The following procedure is representative: nitric acid (69%; 192 μl, 3.0 mmol) was added to a stirred suspension of ytterbium(III) triflate (186 mg, 0.30 mmol) in 1,2-dichloroethane (5 ml). The suspension dissolved to give a two phase system in which the aqueous phase was the more dense. Toluene (240 μl, 3.0 mmol) was added and the stirred mixture was heated at reflux for 12 h. During the reaction a white solid precipitated and the organic phase became yellow, and after 12 h no phase boundary was apparent. The solution was allowed to cool and diluted with water. The yellow organic phase was dried ($MgSO_4$) and evaporated to give nitrotoluene (390 mg, 95%). The colourless aqueous phase was evaporated to give ytterbium(III) triflate as a white free-flowing solid (183 mg, 98%).

16 (*a*) S. Kobayshi, I. Hachiya and Y. Yamanoi, *Bull. Chem. Soc. Jpn.*, 1994, **67**, 2342; (*b*) S. Kobayashi, I. Hachiya and T. Takahori, *Synthesis*, 1993, 371; (*c*) S. Kobayashi, I. Hachiya, T. Takahori, M. Araki and H. Ishitani, *Tetrahedron Lett.*, 1992, **33**, 6815.

17 The following procedure is representative: ytterbium(III) chloride (775 mg, 2 mmol) as a solution in water was added to a solution of silver nitrate (340 mg, 2 mmol) and silver triflate (1.03 g, 4 mmol) in water. A white precipitate (AgCl) was formed immediately which was filtered at the pump giving a colourless solution. The solution was evaporated under reduced pressure to give a white solid (1.36 g, 99%).

18 C. C. Addison, N. Logan and S. C. Wallwork, *Quart. Rev.*, 1971, **25**, 289.

19 (*a*) A. Chatterjee, E. N. Maslen and K. J. Watson, *Acta Crystallogr., Sect. B*, 1988, **44**, 381; (*b*) T. Lu, L. Ji, M. Tan, Y. Liu and K. Yu, *Polyhedron*, 1997, **16**, 1149; (*c*) L. I. Semenova, B. W. Skelton and A. H. White, *Aust. J. Chem.*, 1996, **49**, 997; (*d*) D. L. Faithfull, J. M. Harrowfield, M. I. Ogden, B. W. Skelton, K. Third and A. H. White, *Aust. J. Chem.*, 1992, **45**, 583; (*e*) J. M. Harrowfield, W. M. Lu, B. W. Skelton and A. H. White, *Aust. J. Chem.*, 1994, **47**, 321.

20 I. Hachiya, M. Moriwaki and S. Kobayshi, *Bull. Chem. Soc. Jpn.*, 1995, **68**, 2053.

21 Nitronium triflate is approximately 150-fold more reactive than the 'more-ordered' nitronium tetrafluoroborate and hexafluorophosphate salts in chlorinated solvents and this is attributed to increased solubility conferred to the nitronium ion by the triflate counterion.[27a]

22 S. H. Strauss, *Chem. Rev.*, 1993, **93**, 927.

23 (*a*) K. Ishihara, M. Kubota and H. Yamamoto, *Synlett*, 1996, 265; (*b*) K. Ishihara, Y. Karumi, M. Kubota and H. Yamamoto, *Synlett*, 1996, 839.

24 For the use of bis(trifluorosulfonylmethane)imide as a alternative counterion in conjunction with lanthanides, see: (*a*) H. Kobayashi, J. Nie and T. Sonada, *Chem. Lett.*, 1995, 307; (*b*) K. Mikami, O. Kotera, Y. Motoyama, H. Sakaguchi and M. Maruta, *Synlett*, 1996, 171. For the use of perfluorooctanesulfonate see: (*c*) T. Hanamoto, Y. Sugimoto, Y. Z. Jin and J. Inanaga, *Bull. Chem. Soc. Jpn.*, 1997, **70**, 1421. For the use of a sulfonated resin as a 'counterion' see: (*d*) L. Yu, D. Chen, J. Li and P. G. Wang, *J. Org. Chem.*, 1997, **62**, 3575.

25 I. A. Koppel, R. W. Taft, F. Anvia, S.-Z. Zhu, L.-Q. Hu, K. S. Sung, D. D. DesMarteau, L. M. Yagupolskii, Y. L. Yagupolskii, N. V. Ignatév, N. V. Kondratenko, A. Y. Volkonskii, V. M. Vlasov, R. Notario and P.-C. Maria, *J. Am. Chem. Soc.*, 1994, **116**, 3047.

26 J. Foropoulos, Jr., and D. D. DesMarteau, *Inorg. Chem.*, 1984, **23**, 3720.

27 (*a*) C. L. Coon, W. G. Blucher and M. E. Hill, *J. Org. Chem.*, 1973, **38**, 4243; (*b*) L. M. Yagulpol'skii, I. I. Maletina and V. V. Orda, *Zh. Org. Khim.*, 1974, **10**, 2226; (*c*) F. Effenberger and J. Geke, *Synthesis*, 1975, 40.

28 The ytterbium salt was prepared from commercially available lithium triflamide (3M chemical company). A representative procedure is given in ref. 29.

29 $Sc(NTf_2)_3 \cdot 8H_2O$ was prepared as follows: a column (2 cm diameter and 21 cm in length) was loaded with an aqueous slurry of Amberlyst A-26 in the chloride form. Lithium triflamide (48.8 g, 0.166 mol) dissolved in 1100 mL of water was eluted through the column. A halide test was negative in the last collected fractions. The column was washed with 500 mL water followed by 200 mL methanol. Scandium triflate (0.9 g, 1.82 mmol) was dissolved in 100 ml methanol and eluted through the column. The column was washed with 100 mL methanol and all washings were collected and evaporated in air to yield an oil. Under vacuum, the oil became a light tan solid (1.5 g). A ^{13}C NMR in D_2O showed a characteristic quartet. A ^{19}F NMR spectrum showed a singlet at 79.29 ppm. The solid contained 15% water by Karl-Fischer analysis. The best fit from all the data is $Sc[N(SO_2CF_3)_2]_3 \cdot 8H_2O$ with a theoretical Sc of 4.37% (found 4.97%).

30 L. Turowsky and K. Seppelt, Inorg. Chem., 1988, **27**, 2135.
31 (*a*) L. A.Dominey, *US Pat*, 5,273,840, 993; (*b*) L. A. Dominey, V. R. Koch and T. J. Blakley, *Electrochim. Acta*, 1992, **37**, 1551; D. Benrabah, D. Baril, J. Y. Sanchez, M. Armand and G. G. Gard, *J. Chem. Soc., Faraday Trans.*, 1993, **89**, 355; (*c*) V. R. Koch, C. Nanjundiah, G. Appetecchi, G. Battista and B. Scrosati, *J. Electrochem. Soc.*, 1995, **142**, L116; (*d*) D. Aurbach, O. Chusid, I. Weissman and P. Dan, *Electrochem. Acta*, 1996, **41**, 747.
32 (*a*) V. R. Koch, L. A. Dominey, C. Nanjundiah and M. J. Ondrechen, *J. Electrochem. Soc.*, 1996, **143**, 798; (*b*) C. W. Walker, Jr., J. D. Cox and M. Salomon, *J. Electrochem. Soc.*, 1996, **143**, L80.
33 F. J. Waller, A. G. M. Barrett, D. C. Braddock, D. Ramprasad, R. M. McKinnell, J. P. White, D. J. Williams and R. Ducray, *J. Org. Chem.*, 1999, **64**, 2910.
34 R. J. Koshar and R. A. Mitsch, *J. Org. Chem.*, 1973, **38**, 3358.
35 A. G. M. Barrett and D. C. Braddock, *Chem. Commun.*, 1997, 351.
36 A. G. M. Barrett and D. C. Braddock, R. M. McKinnell and F. J. Waller, *Synlett*, 1999, 1489.
37 A. G. M. Barrett and D. C. Braddock, R. Ducray, R. M. McKinnell and F. J. Waller, *Synlett*, 2000, 57.
38 A. G. M. Barrett and D. C. Braddock, D. Catterick, D. Chadwick, J. P. Henschke and R. M. McKinnell, *Synlett*, 2000, in press.
39 *Catalytic Compounds and Processes*, UK Pat. Appl. No 9919583.6.

Perspective

Diversion from landfill: mechanical recycling of plastics from materials recovery facilities and from shredder residue

Richard Hooper,* Anthony K. N. Potter and M. Margaret Singh

Waste & Energy Research Group, University of Brighton, School of the Environment, Cockcroft Building, Lewes Road, Brighton, UK BN2 4GJ.
E-mail: www.brighton.ac.uk/environment/WERG/intro.htm

Received 1st November 2000
First published as an Advance Article on the web 6th February 2001

Diversion from landfill of post-consumer and shredder residue plastics can occur through some simple mechanical recycling techniques. Mechanically recycled post-consumer high-density polyethylene (HDPE) has been remoulded into bottle shapes. Both the chemical and mechanical properties of this polymer have been analysed and found to behave as well as the virgin material. Polyolefin plastic, separated from a complex mixture of shredder residue, has been remoulded into test samples and also compares favourably to a sample of the virgin polymer.

Introduction

For the first time recycling targets have been set by the Government, through the publication of their Waste Strategy 2000.[1] In order to meet these targets we, as a nation, will have to change the way in which we view our waste streams and possibly alter our habits regarding recycling. Currently we only recycle 9% of our Municipal Solid Waste (MSW)† which is 16% short of the Government target of 25% by 2005.[2] Many mechanisms exist by which we can potentially reach this target of 25%,[3] and individual local authorities will have to decide which method best suits their needs.

Research within the Waste & Energy Research Group (WERG) is currently examining the waste streams in Brighton & Hove and East Sussex region to provide data on the composition and volume of MSW, also analysing its potential for recovery and recycling. Other areas of research include the recycling of mixed plastic waste from Materials Recovery Facilities (MRFs) and the recycling of plastics from Automotive Shredder Residue (ASR). All three projects are inherently linked together, since all three are attempting to reduce the amount of plastic waste entering landfill sites. Plastic waste is problematic owing to the high volume/weight ratio; as such it is not an attractive material for collection and recycling.

This paper will focus on the results of the latter two projects, which are tied together through the End of Life Vehicle (ELV) Directive[4] and a voluntary agreement by car manufacturers to incorporate a minimum of 25% recycled plastic back into cars.[5] Our first thought was to utilise some post-consumer plastic waste and recycle this material into a product to be reused in an automobile. Our target was a blow moulded windscreen washer solution reservoir, and to prepare a sample of this we required post-consumer‡ high-density polyethylene (HDPE)—as used in plastic milk bottles. Samples of this plastic were received from Viridor Waste Management (Ipswich) through their Materials Recovery Facility. We will show that post-consumer recycled plastic has excellent processing properties and can therefore be used in high-quality products rather than being discarded to landfill, or used for low-grade purposes.

A second problem exists with shredder residue (SR) that also contains a high plastic content, which is currently being disposed of through landfill. As shown in Table 1, after separation of the ferrous and non-ferrous metals from a shredded scrap metal feedstock (using a system of over-band magnets and eddy currents), the single largest remaining material is plastic.[6] As such, colleagues within WERG are analysing the best methods available to separate the plastic components from a highly mixed material, Table 2, which is typically known as 'fluff' within the shredding industry.[7]

The recycling rate for ELVs, which make up, on average, half of the shredded material is actually quite high at 75%, where approximately 95% of the ferrous and non-ferrous material can readily be recycled.[8] Therefore, the non-metallic component of shredder residue is being targeted as the way forward to reach the goals set by the Directive, Table 3. There can be up to 27 different plastic resins currently used in cars (CARE 1999),[9] with the vast majority of components made from either polypropylene (PP), nylon or acrylonitrile–butadiene–styrene

Green Context

The fate of chemical products when they enter the environment will become a very important issue in the 21st century. Generally speaking, increasing the useful lifetime of a chemical product will decrease the environmental impact and this can be achieved by developing effective methods of recovery and reuse. This paper illustrates that it is possible and easy to recover polyolefin plastics from different mixed wastes. Research on recycled plastics has focussed on chemical or thermal degradation of the recovered material to provide a second use *via* feedstocks or fuel, but this requires chemical (*e.g.* acid) or energy input, reducing the overall environmental benefit. The authors of this paper have used analytical methods and fabrication to show that reasonably separated polyolefin plastics are largely unchanged from the virgin materials and can be reused without consumption of new chemicals or substantial energy input. ***JHC***

† All waste under the control of local authorities or agents on their behalf. It includes all household waste, street litter, waste delivered to council recycling points, municipal parks and garden waste, council office waste, civic amenity waste, and some commercial waste from shops and smaller trading estates where local authority collection agreements are in place.
‡ Post-consumer is considered as materials that have been recovered from residential and commercial consumers, such as newspapers, plastic and glass bottles, and aluminium and steel cans.

Table 1 Material breakdown of an average car (1998)

Material breakdown	Average all cars (%)		Average weight (kg per car)	
	1997	1998	1997	1998
Ferrous metal	68.6	68.3	773	780
Light non-ferrous	6.1	6.3	68	72
Heavy non-ferrous	1.8	1.5	20	17
Electrical/electronics	0.7	0.7	8	8
Fluids	2.1	2.1	23	24
Plastics	8.5	9.1	96	104
Carpet/NVH	0.6	0.4	6	4
Process polymers	1.2	1.1	14	12
Tyres	3.5	3.5	40	40
Rubber	1.7	1.6	19	18
Glass	2.9	2.9	33	33
Battery	1.1	1.1	13	13
Other	1.2	1.5	13	17

Table 2 Summary of approximate gross identifiable material type composition of shredder 'fluff' fraction waste at five sites (% by mass)

	Plastic	Foam	Metal	Wire	Rubber (ex. tyres)	Wood, paper, card	Misc. & fines
Site 1	13.1	5.8	3.2	3.3	4.0	4.7	68.7
Site 2	15.1	2.6	9.8	1.8	2.8	2.8	61.6
Site 3	16.8	3.1	1.7	0.6	0.8	3.1	73.9
Site 4	15.1	3.1	1.8	2.7	4.8	5.5	67.1
Site 5	9.4	3.5	13.2	6.3	5.3	3.2	59.3

Table 3 ELV Directive targets (%)

	ELV Directive	
Year	Recovery	Recycling
2006	85	80
2015	95	85

(ABS). The amount of plastic occurring in shredder residue is expected to grow over the next decade (and longer), reflecting the increasing amount of plastics integrated into modern day cars, for 'light-weighting' purposes. Our first target was to look at reclaiming polyolefins from SR as a viable, easily separated, source for recycling. Part of this work is presented here and a more detailed discussion will be provided in the near future.

Results

1. HDPE

Legislation will not allow recycled plastics to come into contact with food or drink, unless they are coated with a layer of virgin material. Technology exists that will allow materials of this kind to be produced, but is expensive and limits its usefulness.[10] Thus our options for recycling the different types of domestic waste plastics, Table 4, precludes their use in a closed loop manner. In order to produce a 'high-quality' product from post-consumer HDPE plastic waste we must be able to show what the chemical and mechanical properties of this recycled material are. Before we can analyse these properties we have to prepare samples for testing, which is achieved in the following manner.

First, the post-consumer material is granulated into small pieces (< 10 mm), followed by washing in warm (60 °C) water with constant agitation for 2 h. The material was allowed to settle and the float fraction (HDPE, $d = 0.95$ g cm^{-3}) removed, and then subsequently dried in an oven (80 °C) for 6 h. This left a clean polymer fraction that was completely dried and devoid of contaminants such as paper and putrescibles. The polymer sample was then moulded into tensile stress samples and analysed by mechanical and chemical analyses.

Table 4 Household waste plastics (1996)

Polymer	%
PET	8
HDPE	17
PVC	11
LDPE	23
PP	19
PS	12
Other	10

Table 5 Characteristics of recycled post-consumer HDPE

HDPE tests			
		Tensile strength at yield	
	Mp/°C	MPa	%
Specification	134	22	5.6
Injection moulded	135	30.2	15.6
Blow moulded	131	37.7	12.6

Both the infrared (IR) analysis and differential scanning calorimetry (DSC) thermograms of this sample were readily interpreted as HDPE. IR spectroscopy showed that no oxidative degradation of the polymer had occurred, whilst the melting point of the material was equivalent to that known for virgin resin (135 °C) and the glass transition temperature (T_g) was determined to be −130 °C.

Tensile stress analysis of these samples was performed using a Shimadzu test instrument. Tensile stress at yield was found to be 30.2 MPa, with an elongation at yield of 15.6%. Comparison with an engineering specification for a wash bottle showed that both of these tests exceeded the specifications (22 MPa and 5.6%, respectively).

With these results to hand it was determined that the material should be blow-moulded into bottle shapes to verify that the use of this process did not adversely affect that polymer resin. The samples were moulded into small bottle shapes at the University of North London and the results of the tests are shown in Table 5, which shows that they are as good as (if not better) than the virgin material for which the specifications were designed.

2. Shredder residue

Plastic from shredder residue was analysed in a similar manner. In this example several kilograms of large plastic fragments were hand-picked from a pile of shredder fluff. The IR spectrum of each piece was recorded and the plastic separated into polyolefin (mainly polypropylene) and non-polyolefin fractions. The polyolefin fraction was subjected to a quick sink/float test in water, at which point almost 50% of the material sank; this is likely to be caused by fillers within the polyolefins. The float fraction was granulated and again tested through a sink/float experiment—this time all the material floated—indicative of polyolefins. Finally the sample was treated as for the HDPE material—washing with warm water, dried in an oven and tensile stress samples moulded.

As with the HDPE samples, these strips were subjected to chemical and mechanical tests. Again IR spectroscopy could not identify any oxidised material and the DSC showed melting points of 129 and 164 °C, Table 6, which are indicative of

Table 6 Characteristics of recycled shredder residue PP

PP tests				
			Tensile strength at yield	
	Mp/°C		MPa	%
Specification	130	165	22–25	5–10
SR Brighton	129	164	22.7	17.7
PP sample Belgium	130	164	24.1	12.5

mixtures of polypropylenes (isotactic and syndiotactic). The results of the tensile stress measurements showed a stress at yield of 22.7 MPa and an elongation at yield of 17.7%. The former value falls into the range required by another specification (for recycled polypropylene)[11] whilst the latter elongation value is much higher than anticipated.

We were also asked to analyse a sample of polypropylene pellets that had been separated by a Belgian Shredding Company using a heavy media process.[12] This sample was moulded in the same way as our own separated SR thermoplastic olefin (TPO) specimen, but one major difference was the presence of a very odorous acidic smell—we are still investigating reasons why this odour is present. Again IR and DSC spectroscopy show analogous results to our own sample, Table 6.

Discussion

With both post-consumer plastic recycling and shredder residue recycling some interesting, yet not surprising, results were obtained. It is often stated that the properties of recycled plastics are not as good as the virgin material—the results shown in this paper are where part of this myth ends. Although we realise that more tests (impact, melt-flow index) are required on these samples, the initial results show promise for further investigation.

Mechanical recycling of post-consumer HDPE for use in a high-quality product, one that has very precise specifications, shows that there is more value in collecting and recycling this polymer resin in the future. Whilst we realise that this plastic is already targeted for mechanical recycling, the end use is usually one of very low value—such as rubbish bins. Previously, tests have been carried out on 100% post-industrial[13] HDPE recycling for incorporation into such a high-end application; these samples usually failed in one or more tests and had to be mixed with a large proportion of virgin polymer to pass.

Whilst we are convinced that we can meet the vast majority of the materials specifications, it is debatable that we will pass them all. Therefore, it is important that we establish a polymer resin of good all-round quality and use these 'good' qualities to sell the material, regardless if it becomes a car washer reservoir or not. By advising the 'purchaser' what the mechanical properties of the 100% post-consumer resin are, a product can be made according to its attributes. Such data, we believe, could be used to persuade manufacturers to use 100% post-consumer plastic and thus divert this material away from landfill.

The results from the shredder residue tests were especially pleasing. By using a very simple sink/float technique we have been able to separate the vast majority of polyolefin plastics from this highly complicated mixture of materials. On average a typical car has about 9% plastic by weight,[6] and the average thermoplastic content is about 45% polyolefin (40% PP, 4–6% PE), Table 7,[14] this resin appears ideal for reclamation and would also help to reach the recycling target set through the ELV Directive.

Table 7 Thermoplastic content of car plastics (1998)

Plastic resin	% by mass of TP
PP	41
PE	6
ABS	17.5
PMMA	2
PVC	12
PA	7
Acetal	2
PC	3.5
PPO	2
PC+PBT	1
Others (inc. polyesters)	6

Mechanical recycling of the plastic recovered, through both our own research and that acquired from colleagues, show the material to be polypropylene. Between the two, differently isolated materials (water float *vs.* heavy media), there is little difference in either their chemical or mechanical properties. This implies that, for isolation of polyolefins only, a simple water sink/float separation is the only step necessary. We are currently analysing the effect of using a heavy media separation on the sink fraction of these plastics, which contain filled polyolefins and other resins, Table 7, and will report these results in due course.

Conclusions

The results presented here show that mechanical recycling of a plastic resin (HDPE), from a MRF, could potentially be used as a 'high-quality' product in an automotive application. Currently, we are looking towards a trial of this post-consumer HDPE recyclate into windscreen washer bottles for a car manufacturer, with the aim of potentially introducing these reservoirs into cars in the near future.

The simple separation of polyolefin plastics from shredder residue has been attempted, and samples prepared for materials testing. These results show that the isolated plastic is of a sufficient quality to potentially become another 'high-end' product, possibly into another automotive part. Further research into the separation of other polymer resins, by the use of heavy media, is in progress.

Unless local authorities are specifically targeting household plastics for collection, or other collection schemes are in place,[15] these post-consumer plastics eventually arrive at landfill sites. Plastics that arrive at reprocessors are typically sold on for remoulding, but usually as a low-quality product. These results show that this need not be the route to take with post-consumer plastics, rather that they could potentially be reused in some non-household application, such as a car windscreen washer reservoir.

Diversion from landfill of some plastics found in shredder residue can be achieved by a simple water sink/float of some hand-picked plastics; analysis of methods for a more automated separation are being researched. This approach diverts some 45% of polyolefin material away from landfill and shows promise for mechanical recycling into a high-quality product. Further diversion from landfill, to attain the 80% recycling rate of ELVs, could be achieved through more complex separation processes using heavy media floatation methods.

Experimental

IR spectra were recorded using a Perkin-Elmer 1600 FT-IR machine. Analysis of the spectrum revealed that the material

absorbs energy at wavenumbers characteristic for polyethylene: 2914, 2846, 1471, 1462, 1262, 1030, 801, 729, 718 cm^{-1}.

Differential scanning calorimetry (DSC) thermograms were recorded on a Polymer Laboratories Differential Scanning Calorimeter using DSC Gold (Version 5.41) software. The thermograms were recorded from −160 to 300 °C and were repeated for each sample to ensure reproducibility with the moulding technique. During each run for HDPE, a glass transition temperature (T_g) was observed at −130 °C and melting points were recorded at 135 °C (injection moulded) and 131 °C (blow moulded). For the polypropylene samples melting points of 129 and 164 °C (Brighton SR sample), and 130 and 164 °C (German PP sample) were recorded; no T_g could be detected for either sample.

Injection moulding was performed on a TP1 mini-moulder air operated machine, using a quick action vice. HDPE samples were moulded at 230 °C whilst the polypropylene samples were moulded at 260 °C.

Mechanical testing was performed on Shimadzu tensile testing machine, and standard tensile stress measurements were made at 50 mm min^{-1}.

Acknowledgements

This research is supported by Viridor Waste Management (formerly Haul Waste) through the Greenbank Trust. The third party donation is provided by the automotive industry *via* its co-operative recycling initiative, the Consortium for Automotive Recycling (CARE).

References

1 DETR (2000): *Waste Strategy 2000 for England and Wales*, Parts 1 and 2.
2 Reference 1, p. 104: the recycling rate of plastics is currently 8%.
3 For example, increased collection of plastics through either kerbside collection or bring banks.
4 EU ELV Directive (2000/53/EC).
5 *Mater. Recycling Weekly*, 2000, Feb 25, 3.
6 ACORD from http://www.smmt.co.uk/downloads/acord/acordreport99.doc
7 Unpublished results, University of Brighton, 2000.
8 C. A. Ambrose, *I.W.M. Sci. Technical Rev.*, 2000, submitted.
9 CARE 1999, unpublished results.
10 Plysu Containers, Woburn Sands, Milton Keynes: www.plysu-.co.uk
11 CARE at http://www.caregroup.org.uk/ppspec.pdf
12 A Belgian company (Galloo) claims to have separated polypropylene from a mixture of shredder residue plastics using heavy media (density differences).
13 Post-industrial recyclate is considered as a resin that comes from off-cuts during the manufacture of goods from virgin plastic—it has never been 'used'.
14 CARE: Phase 1 Report, Summer 1995–1998.
15 Examples include kerbside collection schemes run by independent companies, such as Magpie Recycling in Brighton.

Salt-free esterification of α-amino acids catalysed by zeolite H-USY

M. A. Wegman, J. M. Elzinga, E. Neeleman, F. van Rantwijk and R. A. Sheldon*

Laboratory of Organic Chemistry and Catalysis, Delft University of Technology, Julianalaan 136, 2628 BL Delft, The Netherlands. E-mail: R.A.Sheldon@tnw.tudelft.nl

Received 6th November 2000
First published as an Advance Article on the web 31st January 2001

A truly catalytic procedure is described for the esterification of α-amino acids, thereby circumventing the formation of stoichiometric quantities of salts associated with conventional procedures. The acid form of ultrastable zeolite Y (H-USY), a naphtha cracking catalyst, acted as a solid acid catalyst in the reaction of several α-amino acids with methanol at 100–130 °C (15–20 bar). For example, L-phenylalanine afforded the methyl ester in 83% yield after 20 h at 100 °C. Based on the (unlikely) participation of all the Al atoms of the zeolite this corresponded to a turnover number of 180. The ester product was partially racemised (52% ee). Phenylglycine, *p*-hydroxyphenylglycine and homophenylalanine were similarly converted to their methyl esters. The H-USY catalyst could be recycled albeit with decreased activity after each cycle owing to the adsorption of water (formed in the reaction). Its activity was completely restored, however, after calcination.

Introduction

Amino acid esters are key raw materials in the manufacture of, *inter alia*, pharmaceuticals and flavours.[1] For example, the methyl ester of racemic phenylalanine is used in the enzymatic synthesis (DSM–Tosoh process) of the artificial sweetener aspartame.[2] Esters of D-phenylglycine (D-PG) and D-*p*-hydroxyphenylglycine (D-HPG) are key intermediates in enzymatic routes to semi-synthetic penicillins and cephalosporins.[3]

Amino acids exist as zwitterions and in order to generate a free carboxyl group, for esterification, a stoichiometric amount of mineral acid, *e.g.* HCl or H_2SO_4, is required (Scheme 1). Consequently the product ester is formed as the corresponding salt and generation of the free amino acid ester necessitates neutralisation with a base and concomitant generation of at least one equivalent of salt, *e.g.* NaCl or H_2SO_4. For example, the synthesis of phenylglycine methyl ester (PG-OMe) involves the production of at least 0.35 kg of NaCl or 0.43 kg Na_2SO_4 per kg of product. In practice substantially larger amounts are produced owing to the use of a large excess of mineral acid.[4]

We surmised that esterification over a solid acid catalyst could, in principle, yield the ester as the free base in a salt-free, non-corrosive process. This was based on the notion that desorption of the ester from the solid catalyst into the bulk solution would enable the adsorption of new amino acid. In this way a situation is created where an acid-catalysed reaction is occurring in the pores of the solid acid even though the bulk solution, containing the amino acid ester, is basic.

Yadav and Krishnan reported that the esterification of anthranilic acid is catalysed by ion-exchange resins.[5] However, the difference in pK_a values of the carboxyl and amino groups in anthranilic acid[6] (ΔpK_a = 2.4) is much smaller than that in α-amino acids[7] (ΔpK_a = 7). Hence, the catalytic esterification of α-amino acids over solid acids would be expected to be much more difficult. Herein we report the successful catalytic salt-free esterification of several α-amino acids over ultrastable zeolite Y (H-USY) which is used industrially on a very large scale as a naphtha cracking catalyst.[8]

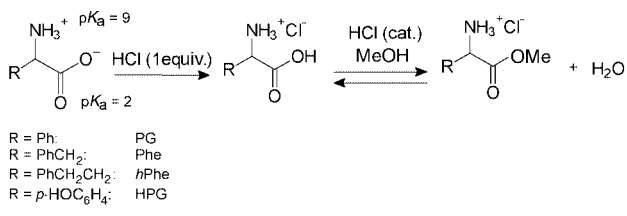

Scheme 1 Conventional esterification of an α-amino acid using >1 equiv. of mineral acid.

Results and discussion

Screening of several heterogeneous catalysts

For our initial screening of solid acid catalysts we studied the esterification of D-PG with methanol. Different solid acids (*e.g.* acid-treated clays, zeolites, ion-exchange resins and heteropolyacids) were tested in a standard esterification reaction under reflux conditions. Only zeolite H-Y and H-USY catalysed the esterification of PG to the corresponding methyl ester. A plausible explanation is that H-Y and H-USY are highly hydrophilic, which facilitates the adsorption of D-PG. Moreover, these zeolites consist of a three-dimensional large pore system (7.4 Å) with supercages (12 Å) which allows an efficient

Green Context

Esterification is one of the key transformations in many areas of chemicals. It is especially tricky in the field of amino acid chemistry, where acid catalysis typically leads to salt formation. Such a situation means that catalyst is deactivated, and additional steps need to be taken to liberate the free amino ester, resulting in neutralisation and loss of catalyst. This paper describes a novel approach involving the use of a zeolite as an acid catalyst, which catalyses esterification to give the complexed ester, which is then competitively removed by fresh substrate, leaving the product as a free base in a non-acidic environment. Such a process is significantly simpler than using homogeneous acids. ***DJM***

migration of the substrate into—and product out of—the channel system.[9] Owing to restricted accessibility of the acidic sites an acid catalysed reaction can be performed even though the bulk solution is basic owing to the accumulation of the free amino acid ester. Because of the superior results, H-USY was used in all further experiments.

Effect of the amount of H-USY

The effect of the amount of the catalyst on the reaction rate was investigated. The amount of H-USY was varied between 0.25 and 2 g and in all cases equilibrium was reached at 30 mM product concentration (35% yield). The initial rate, however, increased as more H-USY was used, as would be expected (Table 1).

Table 1 Initial rate of H-USY catalyzed esterification of D-PG

USY/g	Initial rate/ mM h^{-1}
0.25	1.3
0.5	3.6
1	5.3
2	9.4

Reaction conditions: H-USY was added to a suspension of D-PG (1 g, 6.6 mmol) in 80 ml methanol. The reaction mixture was refluxed over KA molecular sieves.

Stability of the product

The ester always racemised during the reaction, regardless of the amount of H-USY. A blank experiment showed that racemisation occurred in the absence of the catalyst. It is known that amino acid esters undergo thermal racemisation.[10]

Free amino esters are also known to be susceptible to self-condensation to diketopiperazines and polycondensation products.[11] Therefore, the stability of D-PG-OMe in methanol (50 mM) under reflux conditions, in the absence of the catalyst was monitored for 30 h. No degradation of PG-OMe was observed, but the product was completely racemised.

Reusability of the catalyst

H-USY was used in a recycle experiment; after each cycle the catalyst was filtered off and reused in the next cycle without any post-treatment. The activity of the catalyst slowly decreased after each cycle as shown in Fig. 1. However, H-USY completely recovered its activity upon calcination. The Si/Al ratio of H-USY was found to be unchanged after three consecutive esterifications consistent with no leaching of Al having occurred during the reaction.

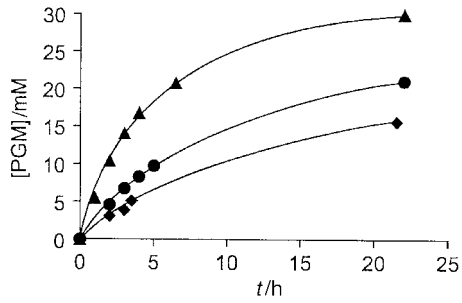

Fig. 1 H-USY-catalysed esterification of D-phenylglycine: (▲) first cycle, (●) second cycle, (◆) third cycle.

Inhibition effects

Because hydrophilic zeolites selectively adsorb water,[12] the possible inhibition of H-USY by this side-product was investigated. The addition of an equimolar amount of water to the reaction mixture resulted in approximately 50% reduction of the initial rate as well as the equilibrium conversion. Refluxing the reaction mixture over KA molecular sieves only partially restored the rate, indicating that water accumulation in the highly hydrophilic H-USY could not be prevented completely (Fig. 2). Dimethylcarbonate, which reacts with water to methanol and CO_2, was also not effective as a water scavenger (data not shown).

Since the product ester is rather hydrophilic, we also studied product ester inhibition of H-USY by adding 2 mmol PG-OMe to the reaction mixture. The initial rate decreased considerably in the presence of PG-OMe and the additional amount of PG-OMe formed was less than in the standard reaction (Fig. 2).

Furthermore, we observed that 0.5 mmol of the added ester was directly adsorbed on the catalyst (1 g), which gives an estimate of the amount of accessible catalytic sites *i.e.* 0.5 mmol/g H-USY.

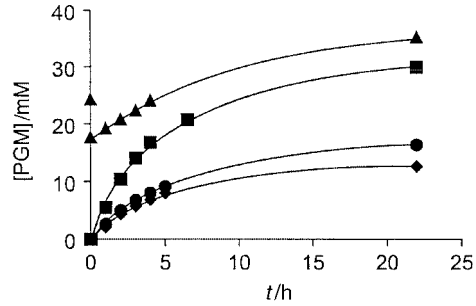

Fig. 2 Inhibition effect on H-USY: (■) standard reaction, (▲) in the presence of 2 mmol PG-OMe, (●) in the presence of 1 equiv. H_2O and 2 g KA molecular sieves, (◆) in the presence of 1 equiv. H_2O, no molecular sieves.

Effect of temperature

A drawback of the H-USY-catalysed esterification under reflux conditions (64 °C) is that equilibrium is reached at only 30 mM PG-OMe. The reaction was performed at increased temperature[5,13] in an autoclave at 100 °C and 15 bar (N_2) in order to shift the equilibrium towards product formation. The reaction rate was enhanced 10-fold and after 2 h equilibrium was reached at 60 mM PG-OMe (73% yield) according to HPLC. An isolated yield of 73% PG-OMe was obtained after working up. To enhance the conversion even further, the temperature was increased to 130 °C. The equilibrium conversion increased with temperature, but the racemisation rate of PG-OMe also increased at elevated temperatures. At 130 °C equilibrium was reached at 70 mM PG-OMe (86% yield). We note, however, that the yield corresponded to the amount of amino ester present in the bulk solution and, as mentioned above, 0.5 mmol of the ester is adsorbed on the catalyst. In practice the adsorbed ester will be recovered when the catalyst is recycled and used in a new batch. Hence, the maximum yield of ester, observable in solution, from 6.6 mmol of substrate with 1 g catalyst is 92% (Table 2).

Scope of the reaction

In order to investigate the scope of the salt-free esterification, several amino acids were subjected to H-USY-catalysed esterification at 130 °C (20 bar N_2). Phenylglycine (PG) was

Table 2 Effect of temperature on the H-USY-catalysed esterification of D-PG

T/°C	*p*/bar	*t*/h	Conversion[a](%)	ee[a](%)
65	1	20	36	4
100	15	2.0	73	29
130	20	0.5	86	51

Reaction conditions: 1 g H-USY was added under stirring to a suspension of D-PG (1 g, 6.6 mmol) in 80 ml methanol. [a] Analysed by HPLC.

compared with phenylalanine (Phe) and homophenylalanine (*h*Phe) as they comprise a series of three amino acids in which the phenyl group is progressively further separated from the stereogenic centre by a methylene group (Scheme 1).

As the chain-length increased, the equilibrium conversion declined (Fig. 3). This is possibly due to the increasingly hydrophobic character of the amino acid with increasing chain length. Alternatively it could be due to increasing bulk of the substrate hindering access to the active site. L-Phe-OMe was found to be more stable than D-PG-OMe towards racemisation (Table 3). This is consistent with the higher reactivity of the benzylic C–H bond at the stereogenic centre in the latter.

Because racemic Phe-OMe is a key intermediate in the industrial synthesis of the artificial sweetener Aspartame,[2] a more detailed study was carried out. Since equilibrium is reached regardless of the amount of the catalyst, the loading of H-USY was gradually decreased. As little as 10 mg H-USY sufficed to convert 2 g L-Phe at 100 °C into Phe-OMe in 83% yield after 20 h. This corresponds to a minimum turnover number (TON) of 180 (mol product/mol Al), based on the unlikely participation of all the aluminium atoms present in the zeolite (5.6 mmol Al/g H-USY). As noted above, 1 g of H-USY adsorbed 0.5 mmol of amino ester suggesting that $< 10\%$ of the available 5.6 mmol of Al atoms are catalytically active, *i.e.* the actual catalytic turnover is > 1800.

We subsequently studied the salt-free esterification of D-*p*-hydroxyphenylglycine (D-HPG). The corresponding ester is a key intermediate in the synthesis of semi-synthetic antibiotics.[3] At 130 °C (20 bar N_2) HPG-OMe decomposed into several unidentified products. Therefore, the reaction was carried out at 100 °C (15 bar N_2). After 2.5 h a moderate conversion equilibrium was reached of 23 mM HPG-OMe (31% yield).

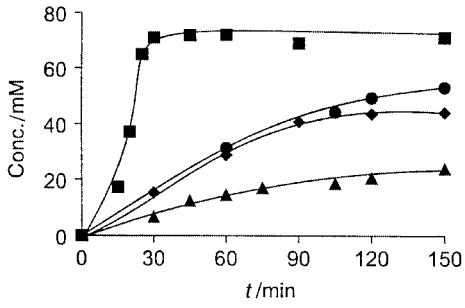

Fig. 3 H-USY catalysed esterification of (■) PG, (●) Phe, (◆) *h*Phe at 130 °C, (▲) HPG at 100 °C.

Table 3 H-USY catalysed esterification of several amino acids

Substrate	*t*/h	Conversion[a](%)	Yield[b](%)	ee[a](%)
D-PG	0.5	87	86	51
L-Phe	2.0	84	77	52
D,L-*h*Phe	2.0	70	68	—
D-HPG[c]	2.5	32	14	35

Reaction conditions: a suspension of 1 g H-USY and 1 g of amino acid in 80 ml methanol was stirred at 130 °C and 15 bar (N_2). [a] Analysed by HPLC. [b] Isolated yield. [c] Reaction temperature was 100 °C

We also attempted the esterification of L-proline, which differs from the other amino acids in that it contains a secondary rather than a primary amino group. However, its esterification over H-USY failed. Similarly, esterification of anthranilic acid was unsuccessful over H-USY, possibly owing to its higher hydrophobicity. Yadav and Krishnan[5] similarly found that ZSM-5 was ineffective in the esterification of anthranilic acid.

Conclusions

Zeolite H-USY efficiently catalysed the esterification of aromatic α-amino acids at 130 °C. The rate and equilibrium conversion declined with increasing chain-length of the amino acid. The TON for Phe was 180 based on (the unlikely) participation of all Al atoms in H-USY. Currently we are improving the salt-free esterification in order to avoid racemisation of the product.

Experimental

Chemicals and catalyst

Zeolite H-Y (Si/Al 2.5) and H-USY (Si/Al 2.5) were kindly donated by AKZO-Nobel Chemicals (Amsterdam, The Netherlands). Enantiomerically pure D-phenylglycine (D-PG), D-*p*-hydroxyphenylglycine (D-HPG), D-PG-OMe and D-*p*-hydroxyphenylglycine methyl ester (D-HPG-OMe) were a gift from DSM (Geleen, The Netherlands). Racemic PG, racemic phenylalanine (Phe), L-Phe, L-proline (L-Pro), L-proline methyl ester (L-Pro-OMe) and anthranilic acid were obtained from Acros. Racemic homophenylalanine (*h*Phe) was obtained from Sigma. Molecular sieves KA—activated at 400 °C for 24 h before use—were purchased from Aldrich. Racemic PG-OMe, racemic phenylalanine methyl ester (Phe-OMe) and racemic homophenylalanine methyl ester (*h*Phe-OMe) were chemically synthesised from the corresponding α-amino acids according to the literature.[14]

Activation of H-Y and H-USY was performed in a stationary oven. The catalyst was heated from room temperature to the final activation temperature (550 °C) at 1 °C min^{-1} and held at this temperature for 7 h. The catalyst was cooled down to 200 °C and transferred to a vacuum desiccator where it was allowed to cool to room temperature.

Esterification under reflux conditions

H-Y or H-USY (1 g, unless stated otherwise), pre-activated, was added to a suspension of 1 g α-amino acid in 80 ml methanol. The reaction mixture was refluxed over molecular sieves KA. Samples were withdrawn periodically, the catalyst was removed by centrifugation and the supernatant was analysed by HPLC. The experiments were performed in duplicate and were reproducible within the margin of error. The markers in Figs. 1 and 2 indicate the margin of error.

Esterification at elevated temperatures

H-USY (1 g, unless otherwise stated), pre-activated, was added to a suspension of 1 g α-amino acid in 80 ml methanol. The reaction was performed in a 200 ml Parr stainless steel autoclave at the selected temperature under an inert atmosphere (15 bar N_2, $p_0 = 10$ bar). Samples were withdrawn periodically, the catalyst was removed by centrifugation and supernatant was analysed by HPLC. The experiments were performed in

duplicate and were reproducible within the margin of error. The markers in Fig. 3 indicate the margin of error.

Isolation of α-amino acid methyl ester

The catalyst and the excess α-amino acid were filtered off. Methanol was evaporated and the residue was resuspended in ether in which only the ester dissolved. The precipitate was filtered off, ether was evaporated and the ester was obtained as a yellowish oil.

Analysis and equipment

Inductively coupled plasma atomic emission spectroscopy (ICP-AES) was used to determine Si/Al ratios before and after reactions. ICP-AES measurements were conducted on a Perkin-Elmer plasma 2000.

The reaction mixtures were analysed by chiral HPLC on a Daicel Chemical Industries Ltd. 4.6 × 150 mm 5 μ Crownpak CR (+) column using a Waters 625 LC pump and a Waters 486 UV detector. The eluent was aqueous $HClO_4$, pH 1.0 at a flow of 0.6 ml min^{-1}. The column temperature was set to 24 °C for PG and anthranilic acid, to 30 °C for Phe and to 32 °C for HPG. For *h*Phe the eluent was adjusted to pH 2.0 and the column temperature was 48 °C. Esterification of Pro was monitored by ^1H NMR ($CDCl_3$) using a 400 MHz Varian-VXR 400S spectrometer.

Acknowledgements

Generous donations of H-Y and H-USY by AKZO-Nobel Chemicals (Amsterdam, The Netherlands) are gratefully acknowledged. The authors thank DSM Life-Sciences for a gift of D-phenylglycine and D-*p*-hydroxyphenylglycine. The ICP-AES measurements were carried out by Mr J. Padmos of Delft ChemTech, to whom the authors express their thanks. We thank Dr M. J. Verhoef (Delft University of Technology, The Netherlands) for his helpful discussions. The authors wish to thank Professor Dr A. Bruggink of DSM Life Sciences Products (Geleen, The Netherlands) for his encouragement. This work was financially supported by the Netherlands Ministry of Economic Affairs and coordinated by DSM Life Sciences (Geleen, The Netherlands).

References

1 R. A. Sheldon, *Chirotechnology: Industrial synthesis of optically active compounds*, Marcel Dekker, New York, 1993.
2 S. Hanzawa, *Encyclopedia of Bioprocess Technology: Fermentation, Biocatalysis and Bioseperation*, Wiley, New York, 1999.
3 A. Bruggink, E. C. Roos and E. de Vroom, *Org. Process Res. Dev.*, 1998, **2**, 128.
4 W. H. J. Boesten, *Eur. Pat. Appl.*, EP 2297, 1979, (*Chem. Abstr.*, 1980, **92**, 22083f).
5 G. D. Yadav and M. S. Krishnam, *Org. Process Res. Dev.*, 1998, **2**, 86.
6 M. S. K. Niazi and J. Mollin, *J. Bull. Chem. Soc. Jpn.*, 1987, **60**, 2605.
7 J. P. Greenstein and M. Winitz, *Chemistry of the Amino Acids*, Wiley, New York, 1961, vol. 1.
8 I. E. Maxwell, *Catal. Today*, 1987, **1**, 385.
9 R. Szostak, *Stud. Surf. Sci. Catal.*, 1991, **58**, 153.
10 E. J. Ebbers, G. J. A. Ariaans, J. P. M. Hobiers, A. Bruggink and B. Zwanenburg, *Tetrahedron*, 1997, **53**, 9417.
11 J. P. Greenstein and M. Winitz, *Chemistry of Amino Acids*, Wiley, New York, 1961, vol. 2.
12 W. F. Hölderich and H. van Bekkum, *Stud. Surf. Sci. Catal.*, 1991, **58**, 642.
13 G. D. Yadav and P. H. Metha, *Ind. Eng. Chem. Res.*, 1994, **33**, 2198.
14 St. Guttman, *Helv. Chim. Acta*, 1961, **85**, 733.

A novel single step synthesis of 2-methyl-6-phenylpyridine from non-heterocyclic compounds over molecular sieve catalysts†

D. Venu Gopal, N. Srinivas, B. Srinivas, S. J. Kulkarni and M. Subrahmanyam*

Catalysis Division, Indian Institute of Chemical Technology, Hyderabad-500 007, India.
E-mail: subrahmanyam@iict.ap.nic.in

Received 7th November 2000
First published as an Advance Article on the web 14th February 2001

The industrially important 2-methyl-6-phenylpyridine is synthesized for the first time in a single step by reacting acetophenone, acetone, formaldehyde and ammonia in the vapor phase over microporous and mesoporous molecular sieve catalysts.

Introduction

Conventional homogeneous acid catalysts such as H_2SO_4, HF, $AlCl_3$, $FeCl_3$ *etc.*, show several disadvantages such as high corrosiveness, tedious work-up, requirement of stoichiometric quantities, the presence of several undesirable side products, and non-recycling of catalyst, and thus are highly non-ecofriendly. The major goals of 'Green chemistry' are to increase process selectivity, maximize the use of starting materials, and to replace hazardous and stoichiometric reagents with eco-friendly catalysts in order to facilitate easy separation of the final reaction mixture, including recovery of the catalyst. Microporous aluminosilicate molecular sieves have been studied extensively in the area of acid catalysis and cyclization reactions, and these materials have contributed greatly to hydrocarbon processing and the chemical industry.[1] Mesoporous MCM-41 materials have well defined pore sizes of 15–100 Å, *i.e.* larger than the pore size constraint of 15 Å) characteristic of microporous zeolites. The large pore size (relative to that of microporous zeolites) reduces diffusional restriction of reactants and products and so enables reactions involving bulky molecules to occur.[2–4] Although extensive research efforts have been undertaken to explore the catalytic applications of modified MCM-41 materials in the field of catalytic oxidations,[5,6] acid catalysis[7] and alkylation reactions[8] applications in a variety of fields of organic chemistry still remain limited.

Among heterocyclic compounds, alkyl substituted phenylpyridines are extensively used as intermediates in the synthesis of drugs, pharmaceuticals, herbicides and agrochemicals.[9] A substituted phenylpyridine 2-(4-carboxyphenyl)pyridine is a starting material for BMS-232632, a potent azapeptide HIV protease inhibitor which has shown high anti-HIV activity.[10] Among various synthetic routes for pyridine and its derivatives, aldehyde/ketone and ammonia condensation is a commercially proven success.

The synthesis of 2-methyl-6-phenylpyridine over molecular sieve catalysts has not been reported. 2-Phenylpyridine and substituted 2-phenylpyridines are generally synthesized from the reaction of aryllithium with pyridine and picolines in homogenous conditions.[11] Regioselective alkylation of 2-phenylpyridine with olefins in the presence of Rh(I) as a catalyst gave 3-methyl-2-phenylpyridine[12] and 2-(4-methylphenyl)pyridine,[13] but not 2-methyl-6-phenylpyridine. It was reported that 2-methyl-6-phenylpyridine can be synthesized by a homogeneous photocatalytic reaction from benzonitrile and ethylene using a Co(I) complex as a photocatalyst.[14] A Japanese patent[9] reported that acetophenones catalytically react with symmetric ketones, formaldehyde and ammonia using a metal-modified amorphous silica-alumina catalyst in the vapor phase at 350–550 °C, however, the amorphous silica-alumina catalyst is prone to deactivation with time on stream.

Here, we report for the first time, the synthesis of 2-methyl-6-phenylpyridine over a novel mesoporous MCM-41 catalyst in a continuous fixed bed using simple and inexpensive raw materials, *i.e.* acetophenone, acetone, formaldehyde and ammonia.

Results and discussion

The heterocyclization reaction of acetophenone, acetone, formaldehyde and ammonia for the synthesis of 2-methyl-6-phenylpyridine was carried out over HZSM-5, HM, Hβ, HY and MCM-41 catalysts and the results are shown in Table 1 and in Fig. 1. The order of catalytic activity for 2-methyl-6-phenylpyridine was found to be MCM-41 > HY > Hβ > HM ⩾ HZSM-5. It is assumed that the small pore size (5.4 Å) of the HZSM-5 zeolites imposes diffusion control through which the bulky product 2-methyl-6-phenylpyridine can not diffuse out, with the formation of the small amount of the product probably through a surface reaction. The intermediate activity of HY zeolite (pore size 7.4 Å) indicates that diffusion control is reduced compared to HZSM-5 for the large size product 2-methyl-6-phenylpyridine. The lowerer catalytic activity of Hβ relative to HY may be due to its geometry of two

Green Context

The ability to carry out clean synthetic transformations over solid catalysts has been transformed by the advent of MCM type materials. While initial attempts to use the larger pores showed that the acidity of the materials is much lower than that of most zeolites of similar composition, this can often be advantageous. Here, for example, a multicomponent condensation is carried out using the large pore dimensions and mild acidity of these materials. It is shown that yields of this gas phase (no-solvent) reaction are much better than found with a range of zeolites. ***DJM***

† IICT Communication No. 4649.

types of pores (pore sizes: 5.4 and 7.6 Å) in the intersecting channel system. It is observed that mesoporous Al-MCM-41 (pore size 30 Å) shows high catalytic activity for 2-methyl-6-phenylpyridine formation with no diffusional constraint. It is evident from the data shown in Fig. 1 that the pore size of the catalyst plays a major role during the synthesis of 2-methyl-6-phenylpyridine, a large molecule. Fig. 1 summarizes the important relation between pore size and molecular size of the reactant/product. The pore size of the catalyst must be accessible to reactant and product molecules in order to take part in the reaction.

A plausible reaction mechanism based on the product distribution is given in Scheme 1, which involves a multi-reactant system leading to several competitive and parallel reactions. Acetophenone and acetone upon reacting with ammonia form the corresponding imines. Thus, the two molecules of imine which form react with formaldehyde and subsequently undergo cyclization and dehydrogenation reactions leading to the formation of 2-methyl-6-phenylpyridine. Similarly, cyclization between two imine molecules of acetone and formaldehyde resulted the formation of 2,6-lutidine as a major side product. In similar manner, the reaction between two molecules of imine deriving from acetophenone and formal-

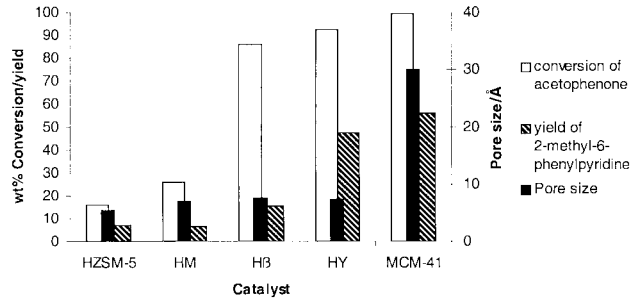

Fig. 1 Effect of pore size on the synthesis of 2-methyl-6-phenylpyridine.

Table 1 Synthesis of 2-methyl-6-phenylpyridine over molecular sieve catalysts

Catalyst	SiO_2/Al_2O_3	TOS/h	Conversion of acetophenone (wt%)	Yield of 2-methyl-6-phenylpyridine (wt%)[a]	Pore size/Å
HZSM-5	30	1	50.6	15.7	5.4
		4	16.0	7.2	
HM		4	25.9	6.3	7.1
Hβ	20	1	83.0	28.0	7.6, 5.4
		4	86.2	15.6	
HY	2.9	1	99.1	48.0	7.4
		4	92.3	47.5	
MCM-41	25	3	99.4	58.6	30
		4	99.3	56.0	
SiO_2-Al_2O_3	4	4	86.1	21.5	—
		4	86.1	21.5	—

Feed = acetophenone : acetone : formaldehyde : ammonia = 1 : 1.5 : 1 : 5 (molar ratio); reaction temperature = 400 °C; weight hour space velocity (WHSV) = 0.5 h^{-1}. [a] The yields are calculated based on the acetophenone conversion.

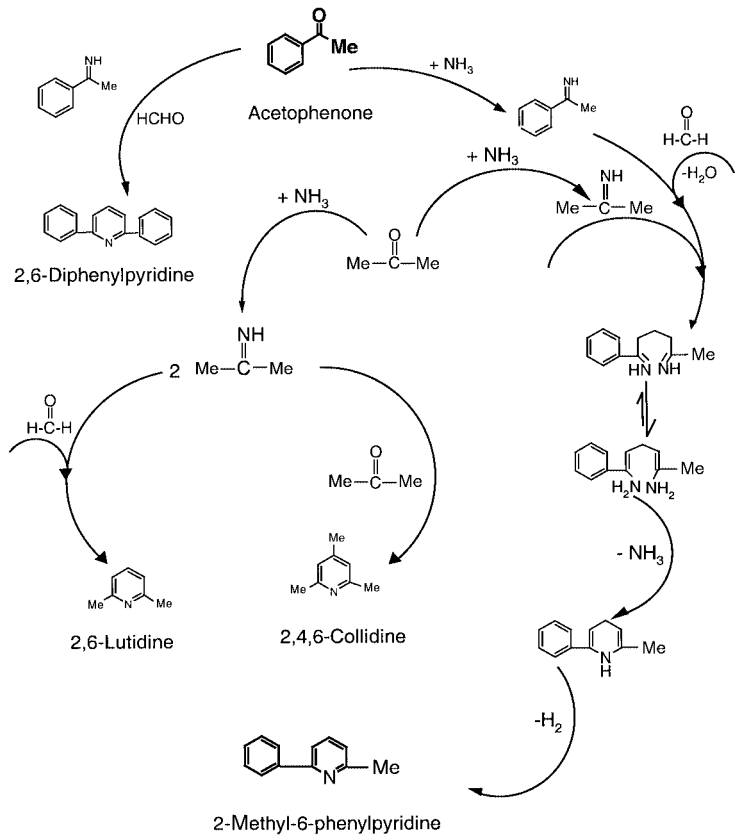

Scheme 1 A plausible reaction mechanism for the formation of various products during the synthesis of 2-methyl-6-phenylpyridine.

dehyde lead to the formation of 2,6-diphenylpyridine. Furthermore, 2- and 4-picolines were observed as minor products. The isomers of alkylated and mono- and di-methyl- phenylpyridines result from the cyclization of acetone with acetophenone in different mol ratios in the presence of formaldehyde and ammonia. Aldol condensation products of acetophenone and acetone are also observed in trace amounts. Ethylbenzene, trace amounts of styrene, α-methylstyrene and cumene were also observed. The internal acidity of the zeolites is responsible for the various transformations. It is clear that the acidic strength of the sites depends on the chemical composition of the zeolite and is related to the framework topology. It was observed that medium strength acid sites are favored for the required specific heterocyclization product.

Conclusion

In conclusion, this work shows that mesoporous molecular sieves such as MCM-41 are active catalysts for heterocyclization reactions, especially in the present case, for the synthesis of 2-methyl-6-phenylpyridine. It is also shown that the large pore mesoporous MCM-41 catalyst is more active than microporous aluminosilicates like HZSM-5, HM, Hβ and HY zeolites for the synthesis of 2-methyl-6-phenylpyridine which is a large molecule. The data also substantiate the phenomenon of diffusion control of reactants, products and shape selectivity with respect to pore size of the catalysts.

Experimental

Al-MCM-41 was prepared as reported by Ortlam *et al.*[15] and calcined at 500 °C in air for 12 h. The BET surface area was determined by N_2 adsorption at 77 K and also characterized by XRD, IR and MAS-NMR spectroscopic techniques. The HZSM-5 zeolite was obtained from Conteka (Sweden), Hβ was obtained from Sud-chemie (India) and HM, HY zeolites were obtained from PQ Corporation (USA).

The cyclization reaction was carried out in a continuous fixed-bed down-flow Pyrex glass reactor of internal diameter 18 mm, using 4 g of the sized catalyst (18–30 mesh) in the middle of the reactor, with an electrically heated furnace. The reaction was carried out at 400 °C. The feed (acetophenone : acetone : formaldehyde: ammonia = 1 : 1.5 : 1 : 5 mol ratio) was fed from the top of the reactor using a B. Braun (Germany) syringe pump. The products were collected through an ice-cold water trap and analyzed by GC (10% SE-30, 20 % Carbowax in 1.8 meter S.S. packed columns) and identified by GC–MS and ^{1}H NMR spectroscopy.

References

1 S. J. Kulkarni, *Stud. Surf. Sci. Catal.*, 1998, **113**, 151.
2 C. T. Kresge, M. E. leonowicz, W. J. Roth, J. C. Vartuli and J. S. Beck, *Nature*, 1992, **359**, 710.
3 J. S. Beck, J. C. Vartuli, W. J. Roth, M. E. Leonowicz, C. T. Kresge and K. D. Schmitt, C. T. W. Chu, D. H. Oslam, E. E. Sheppard, S. B. Mc Cullen, J. B. Higgins and J. L. Schlenker, *J. Am. Chem. Soc.*, 1992, **114**, 10 834.
4 J. Y. Ying, C. P. Mehnert and M. S. Wong, *Angew. Chem., Int. Ed.*, 1999, **38**, 56.
5 A. Corma, M. T. Navarro and J. P. Pariente, *J. Chem. Soc., Chem. Commun.*, 1994, 147.
6 P. T. Tanev, M. Chibwe and T. J. Pinnavaia, *Nature*, 1994, **368**, 321.
7 A. Corma, A. Matinez, V. Martinez-Soria and J. B. Monton, *J. Catal.*, 1995, **153**, 25.
8 A. Corma, M. Iglesias and F. Sanchez, *J. Chem. Soc., Chem. Commun.*, 1995, 1635.
9 S. Shimizu, N. Abe, N. Goto, T. Niwa and A. Iguchi, *Jap. Pat.*, JP 01261367A, 1988.
10 X. Rabasseda, J. Silverstre and J. Castaner, *Drugs. Fut.*, 1999, **24**, 375.
11 A. F. Littke, C. Dai and G. C. Fu, *J. Am. Chem. Soc.*, 2000, **122**, 4020.
12 Y. G. Lim, J. B. Kang and Y. H. Kim, *J. Chem. Soc., Perkin Trans. 1*, 1996, 2201.
13 Y. G. Lim, J. B. Kang and Y. H. Kim, *J. Chem. Soc., Chem. Commun.*, 1994, 2267.
14 B. Heller and G. Oehme, *J. Chem. Soc., Chem. Commun.*, 1995, 179.
15 A. Ortlam, J. Rathousky, G. Schulz-Ekloff and A. Zukal, *Microporous Mater.*, 1996, **6**, 171.

Highly diastereoselective synthesis of 1,3-oxazolidines under thermodynamic control using focused microwave irradiation under solvent-free conditions

Nikolai Kuhnert* and Timothy N. Danks*

Synthetic and Biological Organic Chemistry Laboratory, Department of Chemistry, University of Surrey, Guildford, UK GU2 7XH. E-mail: n.kuhnert@surrey.ac.uk

Received 6th November 2000
First published as an Advance Article on the web 5th March 2001

A number of 1,3-oxazolidines, derived from enantiomerically pure amino alcohols such as (−)-ephedrine and (+)-pseudoephedrine, have been synthesised under solvent-free conditions using a focused microwave reactor. The condensation reaction between the amino alcohol and an aldehyde yields 1,3-oxazolidines in excellent yields and diastereoselectivities. Prolonged microwave irradiation increases the diastereoselectivity of the reaction and produces the thermodynamically more stable diastereomer.

Introduction

Modern focused microwave reactors are an efficient tool to effect selective organic synthesis often accompanied by a considerable increase of the reaction rates. Under solvent-free conditions this technique often reduces or eliminates the use and generation of hazardous solvent waste. In recent years an ever growing interest in the application of microwave irradiation in organic synthesis has lead to the development of a variety of extremely useful synthetic transformations.[1] Despite this interest, the area of diastereoselective synthesis under microwave conditions appears to have been neglected.

There are a number of isolated reports to date of diastereoselectivity under microwave irradiation conditions, including diastereoselective cycloaddition reactions,[2] diastereoselective Michael addition,[3] diastereoselective ß-lactam synthesis[4,5] and diastereoselective glycosidation reactions.[6] The diastereoselectivities reported are however only moderate and no comprehensive study has been reported to date.

The rapid superheating, which accompanies microwave irradiation, should be ideally suited to conducting diastereoselective synthesis under thermodynamic control. We decided to probe this concept as part of a research programme concerned with the application of focused microwave irradiation in organic synthesis. We chose the condensation of enantiomerically pure amino alcohols with aldehydes to give 1,3-oxazolidines as a suitable model reaction. This reaction seemed to be particularly suited to the purpose of our investigation as the two potential diastereomers are in thermal equilibrium with one another *via* an iminium ion intermediate,[7,8] thus allowing the equilibration of the diastereomeric oxazolidines in the absence of any other reagent. Furthermore, homochiral 1,3-oxazolidines have been used as valuable chiral auxiliaries in a number of asymmetric transformations[9–13] and have been employed to effect separation of enantiomers of α-chiral aldehydes.[14,15]

Results and discussion

Initially we considered enantiomerically pure amino alcohols derived from amino acids such as (*R*)-(−)-2-phenylglycinol **1a**, (*R*)-(−)-leucinol **1b** and (*R*)-(−)-2-amino-3-phenylpropanol **1c**. The aminal forming reaction between the amino alcohol **1a-c** and 4-fluorobenzaldehyde **2** or trimethylacetaldehyde **3**, respectively in the absence of solvent was conducted at a MW power setting of 200 W [eqn. (1)]. The reaction was monitored by ^{1}H NMR spectroscopy, allowing the determination of

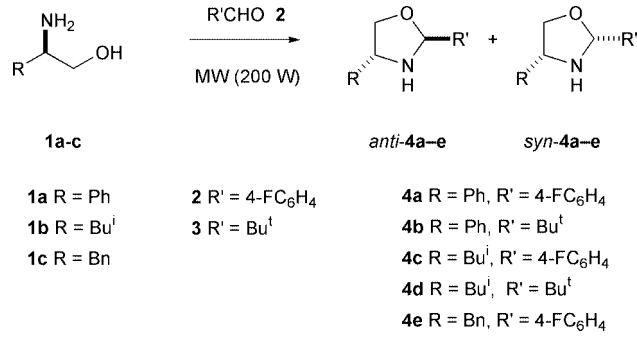

conversion and diastereoselectivity of the reaction products **4a-e** and results are summarised in Table 1 (entries 1–3 and 5–9). Modest conversions and diastereoselectivities were observed after short reaction times (usually 60–80 s at 200 W), whereas complete conversion and excellent diastereoselectivities were observed after irradiation for an additional 60–100 s (120–180 s in total). The reaction that yields compound **4b** is a notable

Green Context

The use of microwave reactors to reduce chemical process times and to enable solvent-free conditions are well known in the context of green chemical technology. Their use can also offer often unexpected additional benefits especially with regard to reaction control. This article describes what is believed to be the first example of stereoselective synthesis under thermodynamic control using microwave irradiation. Condensation reactions between enantiomerically pure amino alcohols and aldehydes occur in excellent yields and diastereoselectivities. Apparently, the rapid superheating which accompanies microwave irradiation, is ideally suited to conducting diastereoselective synthesis under thermodynamic control. ***JHC***

 DOI: 10.1039/b008866h

Table 1 Reaction times, conversions, diastereoselectivities and yields of aminals **4a–e and 6a,b** and **8a,b** and reference compounds from the literature (entries 4, 11, 17, 18)

Entry	Amino alcohol	Aldehyde	Product	Reaction time (200 W)	Diastereomeric ratio[a]	Conversion[a] (%)	Yield (%)
1	**1a**	**2**	**4a**	60 s	65:35[g]	64	—
2	**1a**	**2**	**4a**	120 s	>98:2[g]	100	98[e]
3	**1a**	**3**	**4b**	80 s	>98:2[g]	100	99[e]
4[b]	**1a**	PhCHO	—	2 h[f]	—	—	70-80
5	**1b**	**2**	**4c**	60 s	Undetermined[h]	60	—
6	**1b**	**2**	**4c**	140 s	>98:2[g]	100	96[e]
7	**1b**	**3**	**4d**	140 s	>98:2[g]	100	97[e]
8	**1c**	**2**	**4e**	60 s	70:30[g]	—	—
9	**1c**	**2**	**4e**	180 s	>98:2[g]	100	98[e]
10	**5**	**2**	**6a**	80 s	96:4[i]	55	—
11	**5**	**2**	**6a**	160 s	>98:2[i]	100	78[k]
11[c]	**5**	PhCHO	—	30 min[f]	—	—	76
12	**5**	**3**	**6b**	80 s	70:30[i]	70	—
13	**5**	**3**	**6b**	160 s	96:4[i]	100	98
14	**7**	**2**	**8a**	140 s	>98:2[j]	100	98
15	**7**	**3**	**8b**	80 s	65:35[j]	60	—
16	**7**	**3**	**8b**	180 s	>98:2[j]	100	99
17[c]	**7**	PhCHO	—	30 min[f]	—	-	92
18[d]	**7**	4-BrC_6H_4CHO	—	90 min[f]	—	—	98

[a] Determined by NMR spectroscopy by integration of H-2 signal. [b] Reference 13. [c] Reference 15. [d] From reference 16. [e] Compounds are initially isolated as 1,3-oxazolidines, and yield is based on this conversion. They revert on standing to a mixture of imine and 1,3-oxazolidine. [f] Reactions in solution. For details see references. [g] Major diasteromer is assigned *syn*-**4a–e** (as discussed in text). [h] Diasteromeric ratio could not be determined due to overlapping signals of H-2 in the ^{1}H NMR spectrum. [i] Major diastereomers were assigned as *syn-syn*-**6a,b** by nOe difference spectroscopy (see text). [j] Major diastereomers were assigned as 2,5-*syn*-4,5-*anti*-**8a,b** by nOe difference spectroscopy (see text). [k] The yield is lower due to leakage of small amounts of aldehyde from the vessel. Hence the reaction required an aqueous work-up followed by recrystallisation from diethyl ether–light petroleum.

exception exhibiting complete conversion and excellent diastereoselectivity even after only 80 s irradiation. It is worth noting that when equimolar amounts of starting materials were used, the reaction yielded the product directly in excellent purity, without requiring any further work-up. The 1,3-oxazolidines **4a-e** hydrolysed on standing in solution or in the solid state to yield a mixture of imine and 1,3-oxazolidine as previously observed.[16]

Assignment of stereochemistry in this series of compounds was not straightforward. The nOe difference spectra of compound **4a** gave ambigious results showing no notable nOe effect after irradiation of H-2 and H-4. *N*-Unsubstituted 1,3-oxazolidines have been previously reported but without spectroscopical data or an assignment of stereochemistry.[10,11] However, it has been reported that the related *N*-tosyl-1,3-oxazolidine series form the *syn* diastereomer preferentially.[7]

Having experienced difficulties with the stability of the products and the assignment of stereochemistry for **4a–e** we then turned our attention to the reaction between (−)- ephedrine **5** or (+)-pseudoephedrine **7** as the amino alcohol component and trimethylacetaldehyde **3** or 4-fluorobenzaldehyde **2** as the carbonyl component [eqns. (2) and (3)]. These amino alcohols

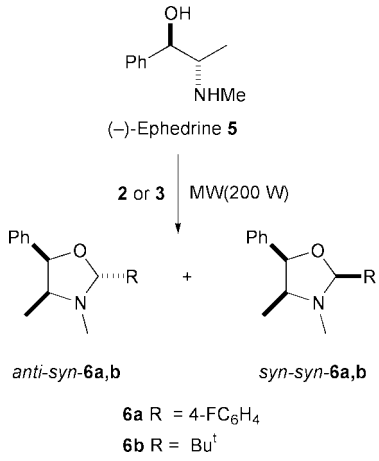

(2)

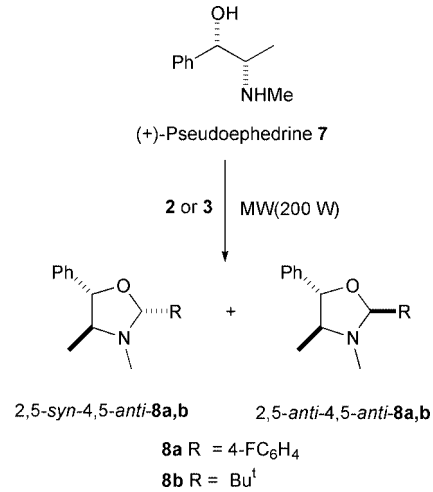

(3)

are known to form stable aminals, which are frequently used in asymmetric synthesis.[8,16,17]

Solvent-free conditions and short irradiation times (80 s) at a power setting of 200 W led to moderate conversions to the 1,3-oxazolidines **6a,b** and **8a,b** with moderate diastereoselectivities (see entries 10, 12 and 15 in Table 1). Continued irradiation (140–180 s in total), also at 200 W, led to a complete conversion of the products to yield the 1,3-oxazolidines **6a,b** and **8a,b** in excellent diastereoselectivities and quantitative yields (see entries 11, 13, 14 and 16 in Table 1). The course of the reaction was again monitored by ^{1}H NMR spectroscopy, which allowed the determination of conversion and diastereoselectivity during the course of the reaction. Diastereoselectivities were determined by integration of the H-2 signals. Obviously the conditions are suitable to drive the equilibrium between the two diastereomers towards the thermodynamically more stable diastereomer. In a separate experiment, to exclude any possible detrimental effect of the remaining starting materials, we irradiated a 3:1 mixture of diastereomers **6a** for 80 s at 200 W. We observed an identical shift of the reaction equilibrium, as seen for the reaction mixture containing the 1,3-oxazolidine in the presence of aldehyde and amino-alcohol

starting material to give a single diastereomer. Presumably the reaction proceeds *via* an iminium ion or imine intermediate, to give the thermodynamically more favoured diastereomer. This experiment gives further evidence that the two diastereomers are in thermal equilibrium under microwave heating.[18]

Assignment of the stereochemistry of the major diastereomers is based on nOe difference spectra of selected compounds **6a** and **8a** .[19] The stereochemistry of the major diastereomers can be unambigiously assigned as *syn*-*syn*-**6a** and 2,5-*syn*-4,5-*anti*-**8a**. The assignment of stereochemistry in the remaining two compounds is based on the assumption that the stereochemical course of the reaction is equivalent to these two examples. Furthermore the assigned stereochemistry is in full agreement with configurations assigned in previous work[16,17] on very similar compounds. This earlier work allows us draw the conclusion that under focused microwave irradiation the reaction rate is increased and yields are improved in comparison to previously published procedures using conventional heating.[15,17]

Conclusion

In conclusion we have shown that enantiomerically pure 1,3-oxazolidines can be obtained under solvent-free conditions using focused microwaves in excellent yields and diastereoselectivities from the reaction of an enantiomerically pure amino alcohol and an aldehydes. The reaction does not require any further work up. Under the conditions of microwave irradiation, presumably due to rapid heating of the reaction mixture, the equilibrium between the two possible diastereomeric products is shifted to the thermodynamically more stable diastereomer. This thus allows highly diastereoselective synthesis under thermodynamic control. To our knowledge this is the first example of stereoselective synthesis under thermodynamic control using microwave irradiation. All products synthesised are useful building blocks for organic synthesis. Our new protocol yields compounds which are homochiral and perfectly suited for further elaboration in asymmetric synthesis.

Experimental

Typical experimental procedure for synthesis under focused microwave irradiation

330 mg (0.20 mmol) (−)-Ephedrine **5**, 224 mg (0.20 mmol) and 4-fluorobenzaldehyde **2** were mixed in a 10 ml glass tube, sealed with a screw cap containing a Teflon septum, irradiated at 200 W for 160 s and left to solidify to yield the 1,3-oxazolidine (*syn*-*syn*-**6a**) in quantitative yield as a white solid. After 20 s pulses, irradiation was discontinued for safety considerations and the reaction vessel was checked against development of excessive pressure. The reaction mixture forms a homogenous melt after 20–25 s of irradiation at 200 W. The conversion was monitored by ^{1}H NMR and TLC.

2(*S*)-(4-Fluorophenyl)-5(*R*)-phenyl-3,4(*S*)-dimethyl-1,3-oxazolidine (*syn*-*syn*-6a)

Mp 71 °C. $[\alpha]_D$ = −48.0 (*c* = 0.1 in $CHCl_3$); $C_{17}H_{18}FNO$ (MW 271.14) calc.: C, 75.25; H, 6.69; N, 5.16. Found: C, 75.18; H, 6.70; N, 5.09%; $\delta_H(CDCl_3)$: 7.51–7.58 (m, 2H, Ar), 6.91–7.38 (m, 7H, Ar), 5.08 (d, *J* = 7.9 Hz, 1H, H-5), 4.64 (s, 1H, H-2), 2.93 (m, 1H, H-4), 2.12 (s, 3H, NMe), 0.74 (d, *J* = 7.9 Hz, 3H, Me). $\delta_C(CDCl_3)$: = 163.4 (d, J_{CF} = 247.5 Hz), 139.8, 134.1, 130.2 (d, J_{CF} = 8.3 Hz), 128.2, 128.0, 126.3, 115.2 (d, J_{CF} = 15 Hz), 98.1 (C-2), 82.5 (C-5), 63.9 (C-4), 35.7 (NMe), 15.1 (Me).

Acknowledgements

We thank the Royal Society and the University of Surrey Foundation Fund for financial support and Personal Chemistry AB for the provision of the Microwell 10 microwave reactor. We also thank Drs R. Bolton and S. Faulkner for helpful discussions.

References

1 For recent reviews on microwave assisted chemical reactions, see: R. S. Varma, *Green Chem.*, 1999, **1**, 43; S. Chaddick, *Tetrahedron*, 1995, **51**, 10403; C. R. Strauss and R. W. Trainor, *Aust. J. Chem.*, 1995, **48**, 1665; C. R. Strauss, *Aust. J. Chem.*, 1999, **52**, 83.
2 M. Avalos, R. Babiano, P. Cintas, F. R. Clemente, J. L. Jimenez, J. C. Palacios and J. B. Sanchez, *J. Org. Chem.*, 1999, **64**, 6297.
3 B. C. Ranu, S. K. Guchhait, K. Ghosh and A. Patra, *Green Chem.*, 2000, **2**, 5.
4 B. Das, B. Venkataiah and A. Kashinatham, *Tetrahedron*, 1999, **55**, 6585.
5 M. Kidwai, K. Kumar and P. Kumar, *J. Indian Chem. Soc.*, 1998, **75**, 102.
6 Y. Lakhrissi, C. Taillefumier, M. Lakhrissi and Y. Chapleur, *Tetrahedron: Asymmetry*, 2000, **11**, 417.
7 F. Steif, B. Wibbeling, O. Meyer and D. Hoppe, *Synthesis*, 2000, 743 and references therein.
8 C. Agami, F. Couty and C. Lequesne, *Tetrahedron Lett.*, 1999, **40**, 1977.
9 M. K. Mokhallalati, K. R. Muralidhavan and L. N. Pridgen, *Tetrahedron Lett.*, 1994, **35**, 4267.
10 L. N. Pridgen, M. K. Mokhallalati and M.-J. Wu, *J. Org. Chem.*, 1992, **57**, 1237.
11 M.-J. Wu and L. N. Pridgen, *J. Org. Chem.*, 1991, **56**, 1341.
12 E. Bergmann and A. Kaluszyner, *Recl. Trav. Chim. Pays-Bas*, 1959, **78**, 315.
13 F. J. Urban and B. S. Moore, *Tetrahedron: Asymmetry*, 1992, **3**, 731.
14 F. Fülöp, G. Bernath, J. Mattinen and K. Pihlaja, *Tetrahedron*, 1989, **45**, 4317.
15 M. E. A. Astudillo, N. C. J. Chokotho, T. C. Jarvis, C. D. Johnson, C. C. Lewis and P. D. McDonnell, *Tetrahedron*, 1985, **41**, 5919.
16 G. Just, P. Potvin and P. Uggowitzer, *J. Org. Chem.*, 1983, **48**, 2923.
17 C. Agami and T. Rizk, *Tetrahedron*, 1985, **41**, 537.
18 For other reaction equilibria under thermodynamic control see, *e.g.*, J. Eames, N. Kuhnert and S. Warren, *Synlett*, 1999, **8**, 1211.
19 In the NOE difference spectra all resonances were irradiated with the exception of the aromatic signals in **6a**.

Novel inorganic oxide supported organotin hydrides for fine chemical catalysis

Qi Jia Fu, Andrew M. Steele and Shik Chi Tsang*

The Surface and Catalysis Research Centre, Department of Chemistry, University of Reading, Reading, UK RG6 6AD. E-mail: s.c.e.tsang@reading.ac.uk

Received 30th October 2000
First published as an Advance Article on the web 28th February 2001

Chemically tethered organotin hydride on various acid pre-treated metal oxide surfaces has been prepared through reaction of surface hydroxyl groups with the hydrostannated product of trimethoxyvinylsilane with dibutyltin dihydride. It was found that some support oxides, typically hydroxylated silicas, clearly show hydride carrying capacities comparable to the best polymer supported hydrides reported but with expected advantages in mechanical and thermal stability. It is also shown, for the first time, that these oxide-supported hydrides can be used as cleaner and genuine heterogeneous catalysts. In the presence of sodium borohydride, the depleted hydrides can be regenerated *in situ* and complete the catalytic cycle. Therefore, novel heterogeneous catalytic hydrogenation reactions and intramolecular coupling reactions using the supported organotin hydride catalyst are demonstrated.

Introduction

The Sn–H bond in organotin hydride species is chemically labile and generates organotin and hydrogen radicals by homolytic cleavage. The exceptional capability and versatility of organotin hydrides, both for radical production and kinetically controlled radical trapping is well documented. Hence, new free-radical C–C bond coupling reactions, both intra- and inter-molecular, have become a powerful tool for impressive chemo-, regio- and even stereo-selective control within multi-step organic syntheses. Radical assisted hydrogenation reactions including replacement of halogen or hydroxyl groups from organic compounds with the hydrogen from organotin hydride are of great synthetic importance. Thus, the soluble forms of organotin hydrides are now conventionally employed for a wide range of important organic syntheses in industry.[1,2] However, the preparation and the regeneration of the hydride produce a significant amount of waste.[3–6] It is also known that total separation of these highly toxic organotin hydride compounds from products is rarely accomplished. These considerations have deemed such reagents unsuitable for the pharmaceutical and cosmetic industries. In order to eliminate, or substantially reduce the residual tin contamination in the products, attempts to support the organotin hydrides onto insoluble materials have been carried out. In particular, some progress has been made in the use of polymers as hydride carriers.[3,6,7] Although the use of polymers may give synthetic advantages, there are concerns over tin leaching, solvent swelling, mechanical stability and reagent regenerability over these materials.[6,7,9,10] Here, we report a study on the use of typical high surface area inorganic oxides as the organotin hydride carriers and explore their uses as catalysts for hydrogenation and intramolecular coupling reactions in ethanolic solutions of $NaBH_4$.

Experimental

Here, we report a study on the use of typical high surface area inorganic oxides as the organotin hydride carriers. We have employed a modified methodology based on the early work of Schumann and Pachaly.[8] The experimental procedure involved the following steps: dibutyltin dihydride was freshly prepared from the $LiAlH_4$ reduction of dibutyltin dichloride. 2.5 mmol dihydride was then allowed to react with an equivalent molar quantity of trimethoxysilane at 60 °C for 24 h in order to produce a silane-functionalised tin hydride complex [eqn. (1)].

$$Bu_2SnH_2 + CH_2{=}CHSi(OMe)_3 \xrightarrow{AIBN} (MeO)_3Si(CH_2)_2SnHBu_2 \quad (1)$$

Prior to the hydride attachment all the oxides were washed in 2 M nitric acid overnight in order to maximise the number of surface hydroxyl groups. The dried oxide powder (3.0 g) was then reacted with the silane complex in 40 ml refluxing diethyl ether for 24 h as shown in eqn. (2). The reactive hydride content

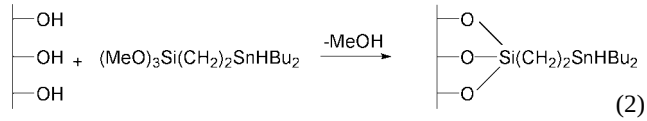

(2)

on the filtered and washed supports (MeOH and diethyl ether) was then determined indirectly by reacting with an excess of 1-iodooctane as shown in the eqn. (3). The amount of *n*-octane

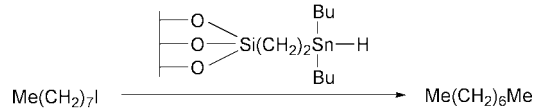

(3)

Green Context

Tributyl tin hydride is a very useful organic reagent. However, it has appallingly low atom economy (it transfers one hydrogen, but has a molecular mass of *ca.* 300). It is also toxic, and difficult to remove from products. The work described here relates to the development of a supported tin hydride, leading to better separation and purification. The reagent can also be regenerated *in situ*, which makes it catalytically active, and thus a far more attractive option for fine chemicals applications. ***DJM***

produced *via* the stoichiometric reduction reaction at 35 °C in 40 cm^3 diethyl ether was measured by gas chromatography.

Results and discussion

Table 1 shows that the active Sn–H content (μmol m^{-2}) varied greatly over different support materials. The hydride carrying capacities follow the order SiO_2 > Al_2O_3 > TiO_2 > C > ZrO_2 (with ZrO_2 and activated C being particularly poor). It is noted that the active Sn–H content on our hydroxylated ultra-high pore silica (810 μmol g^{-1}) is much higher than found in previous work using untreated silica and alumina[8] (*ca.* 170 μmol g^{-1}). Our Sn–H value matched well with atomic absorption and XPS studies (Table 2), which suggested that almost full coverage of the close packed hydroxyl groups (≈ 1 × 10^{20} m^{-2}) on silica surface had been achieved. This result indicates that most of the tin species are actually connected with the active hydrogen as supported tin hydride [eqn. (2)]. We discount the possibilities that the absorbed tin–hydrogen species on the silica is mainly due to weak hydrogen bonding interactions of the hydride with the surface silanol groups (extensive washing with MeOH and ether should have removed them) or to electrophilic attack of the silanol groups with hydride as shown in eqn. (4) (this should lead to a low value of the active Sn–H content).

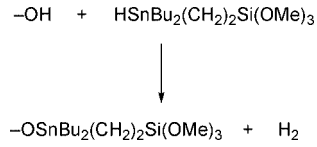

(4)

Despite the fact that the reaction described in eqn. (4) is well known for evaluating the number of surface acidic –OH groups on inorganic oxides[13] we believe that the high tin hydride loading is primarily due to the enhanced concentration of surface hydroxyl groups resulting from the nitric acid pre-treatment, which are then available for further attachment of the tin–hydride silane complex [eqn. (2)]. Comparing the hydride contents on the oxide supports with those of polymer supports reported in the literature, the oxides are as good, if not better than the best polymers[7,9,10] to date (Table 1). However, there have been some reports detailing swelling problems of polymer carriers[10] and tin leaching problems due to their weak mechanical stability.[9] We envisage that the use of inorganic supports may give some advantages in terms of mechanical, thermal and solvent stability relative to polymer supports.

Table 2 shows that the silica supported tin hydride can be recovered after the reduction and reused (*ex situ* regeneration using 1 M diisobutylaluminium hydride, (DIBAH) in hexane followed by exhaustive washing with diethyl ether). Despite the initial loss (16.7%) of the active Sn–H content (15.2% loss in the surface tin content) after the fresh sample is tested (some loosely bound Sn–H is initially present), there is no further significant loss of either reactivity or bulk/surface tin content in subsequent regeneration experiments (1st and 2nd washes) (Table 2). It is noted that the extent of tin leaching from the final stabilised oxide solid, if at all, occurs to a much lower extent as compared with previous polymer carriers.[7,10] Strikingly, from our experiment, the mild sodium borohydride solution, which does not lead to any 1-iodooctane reduction under our reaction conditions, can be used to regenerate *in situ*, the silica supported tin hydride and thereby sustains a fast catalytic hydrogenation of 1-iodooctane to *n*-octane. The unusually high Sn–H content of the silica sample in borohydride solution confirms the catalytic hydrogen transfer where $NaBH_4$ acts as the actual reductant (Table 2). More details on the rate of hydrogen transfer reduction will be presented elsewhere.

It was also found that the used silica-supported organotin hydride material (2.9 g of the 'spent' solid hydride) when immersed into sodium borohydride (10 mmol) solution with 6-bromohex-1-ene (5 mmol) in 40 cm^3 isopropyl alcohol at 40 °C resulted in the formation of principally methylcyclopentane (MCP) and small amounts of hex-1-ene as monitored by GC–MS (Scheme 1). The MCP is formed as a consequence of a kinetically favourable intramolecular coupling reaction[11,12] under our reaction conditions. A similar yield of MCP was obtained upon repeated testing of the solid materials. This result again suggests that the new, modified inorganic solid materials

Table 2 *Ex situ* and *in situ* regeneration of the active tin hydride on silica surface

Sample	Active Sn–H content/μmol g^{-1}	Sn surface composition[a] (%)
Fresh sample	810[b]	3.960
1st wash (DIBAH)	675	n.d.
2nd wash (DIBAH)	680	3.355
In situ regeneration ($NaBH_4$)	7146[c]	n.d.

[a] Results based on the XPS measurement of Sn $3d_{5/2}$, O $1s_{1/2}$, Si $2p_{3/2}$ and C $1s_{1/2}$ signals. [b] In comparison to the fresh sample the difference in the bulk tin content after reaction determined by AA was found to be < 0.1%. [c] Molar ratio of Sn–H : 1-iodooctane : $NaBH_4$ = 1 : 7 : 14, sample kept at 60 °C in EtOH for 87 h.

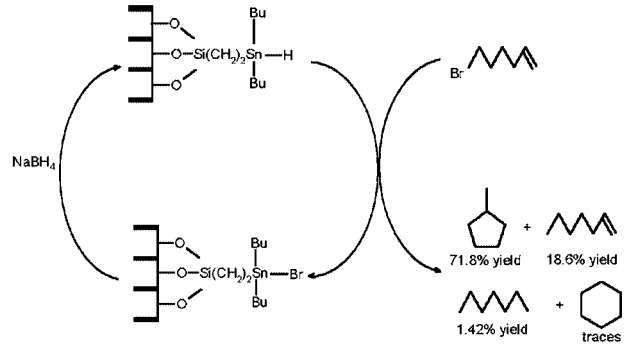

Scheme 1

Table 1 Reduction of 1-iodooctane with supported organotin hydride

Support material (Supplier)	Particle size/average pore size (pore volume)	BET surface area/m^2 g^{-1}	Active Sn–H content/μmol g^{-1}	Active Sn–H content/μmol m^{-2}
Al_2O_3 (Aldrich)	20 μm/58 Å	135	115	0.852
ZrO_2 (MEL Chemicals)	15 μm/n.a.	117	5.4	0.046
Activated carbon, (G-60, Aldrich)	150 μm /n.a. (0.25 cm^3 g^{-1})	845	43.2	0.051
TiO_2 (Aldrich)	5 μm/n.a.	62	47.5	0.766
SiO_2 (Silica gel, Davisil)	20 μm/150 Å (1.15 cm^3 g^{-1})	282	810	2.872
Polymer resin–organotin hydride[10]	n.a.	19	500	—
Polystyrene–DVB–organotin hydride[6]	n.a.	—	700–900	—

can catalyse heterogeneous intramolecular coupling reactions in sodium borohydride solution and that this could be a very useful synthetic tool. We therefore believe that the *in situ* regeneration of supported organotin hydride in the presence of $NaBH_4$ is both interesting and practically important. Proof of the supported organotin hydride acting as a genuine catalyst is demonstrated using two model reactions (hydrogenation of 1-iodooctane, cyclization of 6-bromohex-1-ene). The transformation of more useful molecules on a large scale using this concept in a manner that is useful for industrial chemists should be further addressed.

Conclusions

To summarise, the use of a small amount of inorganic oxide supported organotin hydride showed high activity for hydrogenation and intramolecular coupling reactions.

In situ regeneration of these inorganic oxide supported organotin hydrides under mild conditions affords a truly heterogeneous catalytic cycle. This will significantly reduce the tin pollution level, while retaining a high activity for hydrogenation reactions and intramolecular coupling reactions. In addition, the present novel inorganic oxide supported organotin hydride system may be applicable for use in the pharmaceutical and cosmetic industries. The transformation of more industrially important molecules on a large scale using this concept should be viable.

Acknowledgements

This work was supported by the EPSRC through the Catalysis Managed Programme (GR/L57302/01). S. C. T. is grateful to the Royal Society of London for a research fellowship.

References

1 W. P. Neumann, *Synthesis*, 1987, 665.
2 M. Pereyre, J. P. Quintard and A. Rahm, *Tin in Organic Synthesis*, Butterworths, London, 1987.
3 N. M. Weinshenker, G. A. Crosby and J. Y. Wong, *J. Org. Chem.*, 1975, **40**, 1966.
4 Y. Ueno, K. Chino, M. Watanabe, O. Moriya and M. Okawara, *J. Am. Chem. Soc.*, 1982, **194**, 5564.
5 G. Ruel, N. K. The, G. Dumartin, B. Delmond and M. Pereyre, *J. Organomet. Chem.*, 1993, **444**, C18.
6 G. Dumartin, G. Ruel, J. Kharboutli, B. Delmond, M. F. Connil, B. Jousseaume and M. Pereyre, *Synlett.*, 1994, 952.
7 M. Gerlach, F. Jördens, H. Kuhn, W. P. Neumann and M. Peterseim, *J. Org. Chem.*, 1991, **56**, 5971.
8 H. Schumann and B. Pachaly, *Angew. Chem., Int. Ed. Engl.*, 1981, **20**, 12.
9 G. Dumartin, M. Pourcel, B. Delmond, O. Donard and M. Pereyre, *Tetrahedron Lett.*, 1998, **39**, 4663.
10 A. Chemin, H. Deleuze and B. Maillard, *J. Chem. Soc., Perkin Trans. 1*, 1999, 137.
11 A. L. J. Beckwith, *Tetrahedron*, 1981, **37**, 3073.
12 C. Walling, J. H. Cooley, A. A. Ponaras and E. J. Racah, *J. Am. Chem. Soc.*, 1966, 5361.
13 A Choplin, *J. Mol Catal.*, 1994, **86**, 501.

Catalytic dehydrochlorination of chloro-organic compounds from PVC containing waste plastics derived fuel oil over $FeCl_2/SiO_2$ catalyst

N. Lingaiah,[a] Md. A. Uddin,[a] K. Morikawa,[a] A. Muto,[a] K. Murata[b] and Y. Sakata*[a]

[a] *Department of Applied Chemistry, Faculty of Engineering, Okayama University, 3-1-1 Tsushima Naka, Okayama, 700-8530, Japan. E-mail: yssakata@cc.okayama-u.ac.jp*
[b] *Japan Eco Environment Products, 1-1-18 Toranomon, Minato-Ku, Tokyo, 105-0001, Japan*

Received 27th November 2000
First published as an Advance Article on the web 5th March 2001

A highly selective and stable $FeCl_2/SiO_2$ catalyst system was studied for the dehydrochlorination of various chloro-organic compounds from the fuel oil derived from polyvinyl chloride (PVC) containing waste plastics.

Introduction

The disposal of waste plastics is recognized as a serious environmental problem as they are not biodegradable. The conversion of waste plastics into useful fuel oil has been considered to be the most promising of the recycling methods.[1] The main problems associated with the recycling of waste plastics are those associated with PVC. The pyrolysis of PVC-containing mixed waste plastics (PVMIX) leads to the production of chloro-organic compounds[2] which is necessary to remove to refine the PVMIX-derived oil. At present, catalytic dechlorination is the preferred method for the removal of chloro-organic compounds rather than incineration and chemical degradation.[3] Dehydrochlorination (DHC) is one of the important reactions for the conversion of chloro-organic compounds. A large number of research papers have reported the DHC reaction.[4] The main problem associated with catalytic DHC is the deactivation of the catalyst by the HCl that is produced during the reaction. In most studies the catalyst was deactivated within 2–4 h.[5] We have been working on the development of a stable catalyst system for the removal of chloro-organic compounds found in mixed plastics derived fuel oil.[6] Here we report a stable and active $FeCl_2/SiO_2$ catalyst system for the vapour-phase dehydrochlorination of various chloro-organic compounds from the fuel oil derived from PVC-containing waste plastics. This catalyst system was also tested for the dehydrochlorination of model chloroalkanes to understand more about their activity in this reaction.

Experimental

The waste plastic derived oil was prepared by degrading a mixed plastic sample containing polyethylene (PE) (33%), polypropylene (PP) (33%), polystyrene (PS) (33%) and PVC (1%) in a continuous stirred tank reactor at 410 °C as a model sample. The PVC-waste plastic derived oil contains various chloro-organic compounds (*ca.* 1600 ppm) such as 2-chloro-2-methylpropane, 2-chloro-2-methylpentane, chloroethylbenzene and 2-chloro-2-phenylpropane.

The $FeCl_2/SiO_2$ catalysts were prepared by an impregnation method using the required amount of an aqueous iron(II) chloride solution. After adsorbing iron(II) chloride on silica (surface area: 326 $m^2\ g^{-1}$) overnight, the excess solution was evaporated and the samples dried in an air oven at 120 °C for 12 h. The catalysts were calcined in an inert atmosphere at 350 °C for 3 h.

The dehydrochlorination reaction was carried out on a fixed-bed microreactor at atmospheric pressure as described elsewhere.[7] In brief, the required amount of catalyst (*ca.* 1 g) was loaded in the quartz reactor (300 mm length, 10 mm diameter) between two quartz wool plugs and pretreated in He atmosphere (60 $cm^3\ min^{-1}$) at a reaction temperature of between 300 and 350 °C before admitting the PVMIX-derived oil with a feed flow rate of 10 ml h^{-1} using a micro-feeder. A constant He flow of 10 $cm^3\ min^{-1}$ was maintained throughout the reaction. The products were collected at the outlet of the reactor in an ice-cold trap. The chlorine content was measured using a GC equipped with atomic emission detector (GC–AED). The amount of liberated HCl from the reaction was estimated using ion chromatography after absorbing it in an alkali trap.

Results and discussion

The catalytic activity of $FeCl_2/SiO_2$ as a function of $FeCl_2$ loading for the DHC reaction was studied using model chloroalkanes. Chlorocyclohexane (CCH) and 1-chloroheptane (1-CH) were used as model chloro-organic compounds as they both are similar types of chloro-organic compounds to those found in waste plastic derived oil. The effect of iron(II) chloride content for the DHC of CCH and 1-CH are presented in Fig. 1. The DHC of CCH and 1-CH over these catalysts lead to the

Green Context

Achieving a second use for a product is an important aspect of its life cycle assessment. In the case of non-biodegradable waste plastics, this is becoming a particularly important feature of product use and design. Fixed plastic wastes are not easily recycled as products or depolymerised into useful chemical feedstocks. They do have value as fuel oil feedstocks but tightening legislation makes it essential to remove organochlorine components. Thus dechlorination methods, and catalytic dechlorination methods in particular, are very important. The major limitation with the catalysts developed to date has been their stability, particularly under conditions where a large amount of HCl is produced. In this article, a new, very stable and effective, catalytic dehydrochlorination system based on the supported reagent $FeCl_2/SiO_2$, is described. ***JHC***

 DOI: 10.1039/b009471o

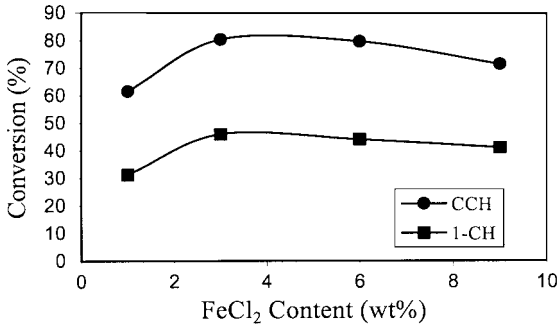

Fig. 1 Effect of $FeCl_2$ loading on the dehydrochlorination activity of chlorocyclohexane and 1-chloroheptane (reaction temperature: 300 °C; gas hourly space velocity: 2367 h^{-1}).

formation of cyclohexene and hept-1-ene as major products, respectively, with a selectivity of 98% in each case. In the reaction carried out by replacing the catalyst with quartz wool, chlorocyclohexane conversion was only *ca.* 1.6%, implying that the reaction is catalytic. These catalysts selectively dechlorinate the chloroalkanes with high activity. Chlorocyclohexane was more dechlorinated compared to 1-chloroheptane. The results from Fig. 1 suggests that the dechlorination activity is highest at a $FeCl_2$ loading of *ca.* 3–6 wt%. Further studies were carried out mainly using 6 wt% catalyst.

In the past, the main problem associated with the dechlorination reaction has been the deactivation of catalyst by HCl, produced during the reaction.

The time on stream over 6 wt% $FeCl_2/SiO_2$ catalyst was measured to clarify the stability of these catalysts. For clarity, only the DHC of CCH activity with reaction time is presented in Fig. 2, along with the amount of HCl liberated with time. It is important to note that the catalyst showed high activity and stability except for a slight initial deactivation. Tavoularis *et al.*[8] studied the DHC of chlorocyclohexane over Ni/SiO_2 catalysts using hydrogen gas. They reported that the deactivation of the catalyst occurred within 2–4 h even though hydrogen was used, which is generally believed to keep the metal surface clean by reducing the metal chloride. They also studied the DHC of CCH without hydrogen gas, which showed a more substantial deactivation than the hydrogen-containing system where the initial activity was reduced by up to 60% within 4 h.

The amount of HCl liberated *vs.* reaction time was also measured and these results are also shown in Fig. 2. It was

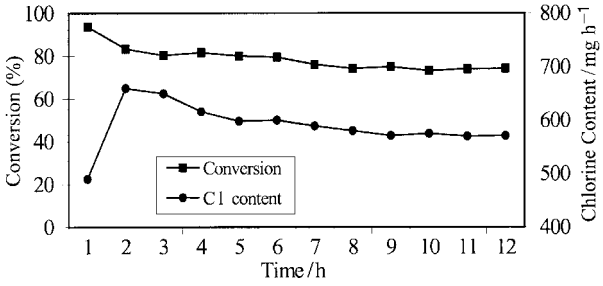

Fig. 2 Conversion and the amount of HCl liberated with time during the dehydrochlorination of chlorocyclohexane over 6 wt% $FeCl_2/SiO_2$ catalyst (reaction temperature: 300 °C; gas hourly space velocity: 2367 h^{-1}).

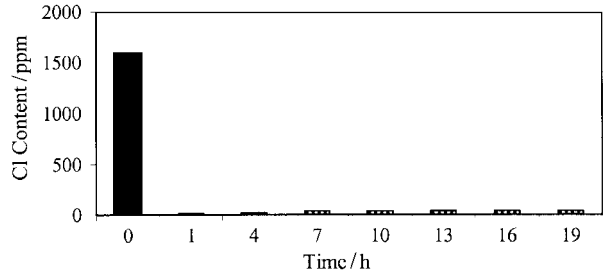

Fig. 3 Time on stream analysis: dehydrochlorination of PVMIX-derived oil over 6 wt% $FeCl_2/SiO_2$ catalyst (reaction temperature: 350 °C; liquid hourly space velocity: 10 h^{-1}).

observed that the amount of HCl liberated in the first hour was low even though the DHC activity was high, which would suggest that the liberation of HCl should be high. The HCl produced initially might be adsorbed on the catalyst surface. After the initial hour the amount of HCl liberated was constant. The small decrease in activity after the initial hour might be due to HCl adsorption on the catalyst surface. It is known that the adsorption of HCl tends to decrease the catalyst activity.[9]

This catalyst was used for the dechlorination of chloro-organic compounds present in fuel oil derived from waste plastics containing PVC. The dechlorination of the fuel oil was carried out over 6 wt% $FeCl_2/SiO_2$ catalyst at 350 °C and the results are summarized in Fig. 3 as a function of reaction time. It was observed that even after 20 h of reaction time the catalyst showed stable activity. The $FeCl_2/SiO_2$ catalyst effectively removed chloro-organic compounds selectively from the waste plastic derived oil, which contains a large number of hydrocarbons (C_5 to C_{20}). It is noteworthy that the carbon number distribution of the fuel oil did not change considerably during the dehydrochlorination. A detailed investigation to investigate the relationship between the physico-chemical characteristics of the catalyst to that of its activity is under way.

Acknowledgements

We are grateful for financial support of this work through the Regional Consortium Project by New Energy and Industrial Technology Development Organization (NEDO), Japan.

References

1 M. Blazso, B. Zelei and E. Jakab, *J. Anal. Appl. Pyrolysis*, 1995, **35**, 221.
2 Md. Azhar Uddin, Y. Sakata, Y. Shiraga, A. Muto and K. Murata, *Ind. Eng. Chem. Res.*, 1999, **38**, 1406.
3 E. N. Balko, E. Zybylski and F. V. Trentini, *Appl. Catal. B: Environ.*, 1993, **2**, 1.
4 I. Mochida, T. Akagi and H. Fujitsu, *Appl. Catal.*, 1985, **18**, 105.
5 G. Tavoularis and M. A. Keane, *Appl. Catal. A*, 1999, **182**, 309.
6 N. Lingaiah, Md. Azhar Uddin, A. Muto, Yusaku Sakata, T. Imai and K. Murata, *Appl. Catal. A: Gen.*, 2001, **207**, 79.
7 N. Lingaiah, Md. Azhar Uddin, Y. Shiraga, H. Tanikawa, A. Muto, Y. Sakata and T. Imai, *Chem. Lett.*, 1999, 1321.
8 G. Tavoularis and M. A. Keane, *J. Mol. Catal. A*, 1999, **142**, 187.
9 B. Coq, G. Ferrato and F. Figueran, *J. Catal.*, 1986, **101**, 434.

Palladium-catalysed carbonylation of aryl halides in ionic liquid media: high catalyst stability and significant rate-enhancement in alkoxycarbonylation

Eiichiro Mizushima, Teruyuki Hayashi and Masato Tanaka*

National Institute of Advanced Industrial Science and Technology, Tsukuba Central 5, Tsukuba, Ibaraki 305-8565, Japan. E-mail: mtanaka@home.nimc.go.jp

Received 29th January 2001
First published as an Advance Article on the web 27th March 2001

Palladium-catalysed carbonylation of aryl halides with alcohols or NEt_2H proceeds in ionic liquid media (1-butyl-3-methylimidazolium tetrafluoroborate or hexafluorophosphate). The catalyst/ionic liquid mixture could be recycled, after separation of the product by either distillation or extraction with ether. Carbonylation with alcohols forming benzoates was greatly accelerated by the use of ionic liquid.

Introduction

Palladium-catalysed carbonylation of aryl halides is a highly effective method for the synthesis of various carbonyl compounds such as carboxylic acids, esters, amides, aldehydes and ketones.[1] Double carbonylation forming α-keto acid derivatives has also been known since 1982.[2] However, the separation of the products and the catalyst still is problematic as in other homogeneous catalytic reactions. To circumvent this drawback, there have been several proposals relating to the use of alternate reaction media such as water,[3] supercritical fluids,[4] and fluorous solvents,[5] which allow easier separation. Another class of new media of considerable potential are ionic liquids,[6] which have been successfully exploited as alternatives to molecular solvents in transition metal-catalysed reactions, such as hydrogenation, isomerization, hydroformylation, dimerization of buta-1,3-diene, hydroesterification, Heck reaction, epoxidation, polymerisation of methyl methacrylate and Suzuki cross-coupling reaction.[7] To the best of our knowledge, however, carbonylation of organic halides in such media has not been reproted. We report herein the first examples of palladium-catalysed single and double carbonylation of aryl halides in 1-butyl-3-methylimidazolium tetrafluoroborate ($[bmim]^+BF_4^-$; **1**) and hexafluorophosphate ($[bmim]^+PF_6^-$; **2**) shown in Fig. 1.[8]

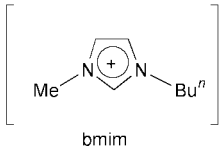

1 $[bmim]^+BF_4^-$
2 $[bmim]^+PF_6^-$

Fig. 1

Results and discussion

In a standard procedure, a mixture of bromobenzene (2.66 mmol), an alcohol (13.3 mmol) and triethylamine (2.66 mmol) was added to a solution of palladium acetate (0.5 mol%) and PPh_3 (2.0 mmol) dissolved in an ionic liquid (**1** or **2**; 2 ml). The mixture was heated under 30 kg cm^{-2} of carbon monoxide at 150 °C for 3 h to form the corresponding benzoate (Scheme 1). In control experiments to study the performance of the reaction media, 2 ml of the reactant alcohol was used as a diluent in place of the ionic liquid to compare the results at the same catalyst concentration. Preliminary results to evaluate the performance of ionic liquids in alkoxycarbonylation of bromobenzene are summarized in Table 1.

What is immediately seen in Table 1 is the high yields of the ester products obtained in ionic liquid media. Thus the reaction with methanol in ionic liquid **1** (entry 1) worked efficiently to form methyl benzoate in 82% yield. Another reaction run in ionic liquid **2** (entry 2) also gave methyl benzoate in 68% yield. However, the control experiment run in methanol (entry 3) resulted in only 30% yield, suggesting the higher performance of the ionic liquid as reaction medium. Alkoxycarbonylation with other alcohols also showed similar difference between the ionic liquid and the respective alcohol. Accordingly even *tert*-butyl alcohol, which reluctantly participates in carbonylation of bromobenzene, reacted more smoothly in **1**.

The recyclability of the catalyst species generated in the reactions run in an alcohol as diluent or without the use of a diluent was very low. As noted above, the reaction in MeOH as the diluent afforded only 30% yield of the ester even in the first run (run 1, entry 1, Table 2). In an attempt to reuse the catalyst species recovered from run 1 resulted in a very low yield of the ester (entry 1, run 2). Another set of reactions were run without

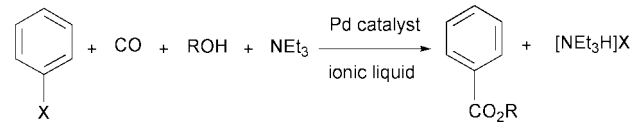

Scheme 1 X = Br or I.

Green Context

Palladium is an extraordinarily versatile catalyst for organic synthesis. It is however very expensive and it is important that it can be very efficiently recovered from reactions and subsequently recycled. Traditional homogeneous Pd catalysts can be very difficult to separate efficiently. Heterogenisation and the use of easily separable solvents are widely cited approaches to ease the problem. Here the authors demonstrate, for the first time, the use of non-volatile ionic liquid solvents in the Pd-catalyst carbonylation of arylhalides. The product can be removed directly by distillation or indirectly using an ether. The solvent–catalyst system can be easily recycled. ***JHC***

 DOI: 10.1039/b100951f

the use of a diluent (entry 2). Since the catalyst concentration was much higher in this procedure, the yield in the first run was high, forming the ester in 98% yield, but the second run using the recovered catalyst species gave only 6%, suggestive of serious deterioration of the catalyst. On the other hand, the activity of the catalyst species was more sustainable in the ionic liquid media to allow recycling at least twice (entries 3 and 4) without such a significant decrease in the yield as was found in entries 1 and 2. In the reactions of entries 1–4, the formation of metallic palladium was more or less evident by inspection, independent of the reaction medium. To prevent the decomposition of the palladium species to metallic palladium, the PPh_3/Pd ratio was increased from 4 to 20. As anticipated, the recyclability in MeOH was dramatically improved (entry 5), but still was inferior to those in the ionic liquids. Thus, in ionic liquid **1** (entry 6), the increase of the ratio not only improved the yield in the first run, but allowed recycling and exhibited catalytic activity even in the seventh run (25% yield). Total turnovers after the seventh run reached *ca*. 1100. The reaction in **2** also behaved similarly (entry 7).

Table 1 Palladium-catalysed carbonylation of bromobenzene[a]

Entry	ROH	Medium	Reaction time/h	Yield (%)[b]
1	MeOH	**1**	3	82
2	MeOH	**2**	3	68
3	MeOH	MeOH	3	30
4	EtOH	**1**	6	91
5	EtOH	EtOH	6	32
6	Pr^iOH	**1**	6	88
7	Pr^iOH	Pr^iOH	6	26
8	*c*-$C_6H_{11}OH$	**1**	6	64
9	*c*-$C_6H_{11}OH$	*c*-$C_6H_{11}OH$	6	32
10	Bu^tOH	**1**	6	28
11	Bu^tOH	Bu^tOH	6	7

[a] *Reaction conditions*: PhBr (2.66 mmol), ROH (13.3 mmol), $Pd(OAc)_2$ (0.5 mol%), PPh_3 (2 mol%), NEt_3 (2.66 mmol), reaction medium (ionic liquid or alcohol; 2 ml), P_{CO} = 30 kg cm^{-2}, 150 °C. [b] Based on bromobenzene and determined by GC using *n*-decane as internal standard.

Table 2 Pd complex catalyzed carbonylation of bromobenzene: Recycling experiments[a]

Entry	Medium	PPh_3/Pd ratio	Yield (%)[b] Run 1	Run 2	Run 3	Run 4
1	MeOH	4	30	12	—	—
2	—[c]	4	98	6	—	—
3	**1**	4	82	57	35	—
4	**2**	4	68	57	53	36
5	MeOH	20	93	88	69	51
6	**1**	20	99	96	82	74
7	**2**	20	99	93	92	78

[a] *Reaction conditions*: PhBr (2.66 mmol), $Pd(OAc)_2$ (0.5 mol%), PPh_3 (2 mol%), NEt_3 (2.66 mmol), reaction medium (MeOH or ionic liquid; 2 ml), P_{CO} = 30 kg cm^{-2}, 150 °C, 3 h. [b] Based on iodobenzene and determined by GC using *n*-decane as internal standard. [c] Run without using a diluent as reaction medium.

One of us has reported that the carbonylation of aryl halides with isopropyl alcohol under higher pressures in a molecular solvent (a large excess of isopropyl alcohol in this case) forms, in addition to the ester (**3**), the α-keto ester (**4**) *via* double carbonylation as shown in entries 1 and 2 of Table 3 (150 kg cm^{-2}, 18 h).[2d] As in the reaction of bromobenzene with various alcohols (*vide supra*), the use of ionic liquids **1** and **2** as reaction media significantly enhances the reactivity of the carbonylation. Thus, the conversion, which was only 12% in the control experiment at 80 °C (entry 1), increased to 83 or 100% when **1** or **2** was used, respectively (entries 3 and 4). However, the single carbonylation forming **3** was more accelerated than the double carbonylation forming **4**, and hence the selectivity to **4** [100 × **4**/(**3** + **4**)] decreased when the reaction was run in ionic liquids, **2** in particular. A similar and distinct change in the selectivity to the single carbonylation was also observed in the reaction at 120 °C (entries 2 and 5). The double carbonylation involves a nucleophilic attack of an alcohol molecule to a carbon monoxide ligand bound to a cationic palladium intermediate.[2e] The ionic liquid was envisioned to enhance the generation of the cationic palladium intermediate by dissociation of the halide ligand, resulting in an increase in the selectivity of the double carbonylation. The reality, however, was the reverse.[9] Clearly the role of ionic liquids in metal complex-catalysed reaction remains to be further clarified.

The performance of the ionic liquid was also studied in the amidation of iodobenzene by using diethylamine (13.3 mmol) in place of triethylamine and isopropyl alcohol. The results are summarized in Table 4. Both single and double carbonylations proceeded to form *N*,*N*-diethylbenzamide **5** and *N*,*N*-diethyl-

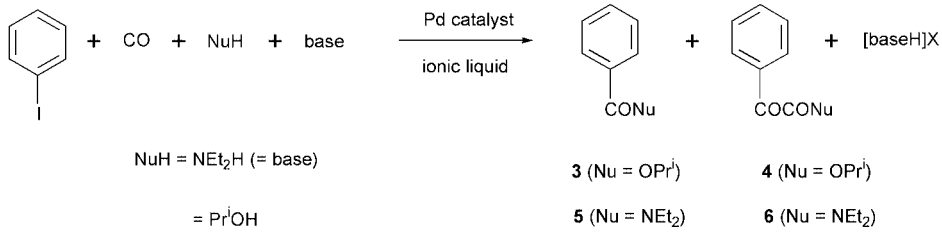

Scheme 2

Table 3 Palladium-catalysed single and double carbonylation of iodobenzene with Pr^iOH[a]

Entry	Medium	Temp./°C	PPh_3/Pd ratio	Conversion (%)[b]	Yield (%)[b] **3**	**4**	Selectivity of **4** (%)
1	Pr^iOH	80	4	12	5	7	58
2	Pr^iOH	120	4	100	70	25	26
3	**1**	80	4	83	58	25	30
4	**2**	80	4	100	93	6	6
5	**2**	120	4	100	95	5	5

[a] *Reaction conditions*: PhI (2.66 mmol), $Pd(OAc)_2$ (1.0 mol%), PPh_3 (4 mol%), NEt_3 (2.66 mmol), Pr^iOH (13.3 mmol), reaction medium (Pr^iOH or ionic liquid; 2 ml), P_{CO} = 150 kg cm^{-2}, 18 h. [b] Based on iodobenzene and determined by GC using *n*-decane as internal standard.

Table 4 Carbonylation of iodobenzene in the presence of NEt_2H[a]

Entry	Medium	P_{CO}/ kg cm^{-2}	Conversion (%)[b]	Yield (%)[b] 5	Yield (%)[b] 6	Selectivity to **6** (%)
1	NEt_2H	40	100	18	82	82
2[c]	NEt_2H	5	100	36	62	63
3	**1**	40	100	17	83	83
4	**2**	40	100	24	76	76
5[c]	**2**	5	24	10	14	58

[a] *Reaction conditions*: ionic liquid (2 ml), $Pd(OAc)_2$ (0.5 mol%), PPh_3 (2 mol%), PhI (2.66 mmol), NEt_2H (13.3 mmol), 80 °C, 3 h. [b] Based on iodobenzene and determined by GC using *n*-decane as internal standard. [c] For 6 h.

phenylglyoxylamide **6**, respectively. Under a higher CO pressure (40 kg cm^{-2}), the total yield of **5** and **6** was quantitative and **6** was the major product, independent on the reaction medium (entries 1, 3 and 4). The variance of the selectivity depending on the reaction media was also marginal. On the other hand, when the reaction was run under a low CO pressure (5 kg cm^{-2}, entries 2 and 5), the ionic liquid displayed much lower performance in the reactivity than diethylamine. After the reaction of entry 3, the mixture was treated with ether to extract the products and excess NEt_2H remaining in the system. The extraction residue, after stripping of ether, could be reused twice if triphenylphosphine (0.053 mmol, 4 equiv. relative to the quantity of palladium used in the first run) was supplemented each time. The yields of **5** and **6** were respectively 7 and 50% in the third run, suggesting that the majority of the palladium species was retained in the ionic liquid layer and was not extracted with ether.

In conclusion, we have shown that carbonylation of aromatic halides proceeds in ionic liquid media. The palladium catalyst in the ionic liquid could be recycled, after appropriate treatment (distillation/extraction with ether of the products). The use of ionic liquid media significantly enhances alkoxycarbonylation. However, there remain some aspects that need further study to clarify the roles of ionic liquids.

Experimental

Typical procedure: alkoxycarbonylation of bromobenzene with methanol in 1-butyl-3-methylimidazolium hexafluorophosphate 2

Palladium acetate (3 mg, 0.5 mol%), triphenylphosphine (14 mg, 2 mol%) and 2 ml of $[bmim]^+PF_6^-$ **2** were added to an autoclave under nitrogen atmosphere, and the mixture was heated to 100 °C for 10 min with stirring to ensure the formation of a solution of the catalyst in the ionic liquid. After cooling to room temperature, bromobenzene (0.28 ml, 2.66 mmol), triethylamine (0.37 ml, 2.66 mmol) and methanol (0.54 ml, 13.3 mmol) were added to the autoclave, which was pressurized with CO of 30 kg cm^{-2} at room temperature. The autoclave was heated at 150 °C for 3 h. The reaction mixture was taken out from the autoclave under nitrogen atmosphere. Evaporation and distillation of the mixture under a reduced pressure (100–120 °C/1 Torr) gave methyl benzoate to leave a residue comprising triethylammonium bromide and palladium species in **2**. After complete removal of volatiles, fresh starting materials were added to the residue. The mixture was transferred to the autoclave to resume a second run under the same conditions as in the first run.

In a control experiment, 2 ml of the corresponding alcohol was used as a diluent instead of ionic liquid. In this case, triethylammonium bromide and palladium species, which remained in the vessel as solids after distillation, were completely dissolved in fresh starting materials. The mixture was transferred to the autoclave.

Acknowledgments

We thank the Japan Science and Technology Corporation (JST) for financial support through the CREST (Core Research for Evolutional Science and Technology) program and the New Energy and Industrial Technology Development Organization (NEDO) for a postdoctoral fellowship to E. M.

References

1 J. Tsuji, *Palladium Reagents and Catalysts*, John-Wiley & Sons, Chichester, 1995, ch. 4; A. Mullen, *New Syntheses with Carbon Monoxide*, ed. J. Falbe, Springer-Verlag, West Berlin, 1980; A. Schoenberg, I. Bartoletti and R. F. Heck, *J. Org. Chem.*, 1974, **39**, 3318; J. K. Stille and P. K. Wong, *J. Org. Chem.*, 1975, **40**, 532; M. Hidai, T. Hikita, Y. Wada, Y. Fujikura and Y. Uchida, *Bull. Chem. Soc. Jpn.*, 1975, **48**, 2075; L. Cassar, M. Fòa and A. Gardano, *J. Organomet. Chem.*, 1976, **121**, C55; A. Schoenberg and R. F. Heck, *J. Org. Chem.*, 1974, **39**, 3327; A. Schoenberg and R. F. Heck, *J. Am. Chem. Soc.*, 1974, **96**, 7761; T. Kobayashi and M. Tanaka, *J. Chem. Soc., Chem. Commun.*, 1981, 333.

2 (*a*) T. Kobayashi and M. Tanaka, *J. Organomet. Chem.*, 1982, **233**, C64; (*b*) F. Ozawa, H. Soyama, T. Yamamoto and A. Yamamoto, *Tetrahedron Lett.*, 1982, **23**, 3383; (*c*) F. Ozawa and A. Yamamoto, *Chem. Lett.*, 1982, 865; (*d*) M. Tanaka, T. Kobayashi, T. Sakakura, H. Itatani, S. Danno and K. Zushi, *J. Mol. Catal.*, 1985, **32**, 115; (*e*) A. Yamamoto, *Bull. Chem. Soc. Jpn.*, 1995, **68**, 433 and references therein.

3 *Organic Synthesis in Water*, ed. P. A. Grieco, Blackie, London, 1998; *Aqueous Organometallic Chemistry and Catalysis*, ed. I. T. Horváth and F. Joó, Kluwer, Dordrecht, 1995; C.-J. Li, *Chem. Rev.*, 1993, **93**, 2023.

4 P. G. Jessop, T. Ikariya and R. Noyori, *Science*, 1995, **269**, 1065; P. G. Jessop, T. Ikariya and R. Noyori, *Chem. Rev.*, 1999, **99**, 475.

5 I. T. Horváth and J. Rábai, *Science*, 1994, **266**, 72; I. Klement, H. Lütjens and P. Knochel, *Angew. Chem., Int. Ed. Engl.*, 1997, **36**, 1454; E. G. Hope and A. M. Stuart, *J. Fluorine Chem.*, 1999, **100**, 75.

6 Y. Chauvin and H. Olivier-Bourbigon, *CHEMTECH*, 1995, **25**, 26; K. R. Seddon, *J. Chem. Technol. Biotechnol.*, 1997, **68**, 351; T. Welton, *Chem. Rev.*, 1999, **99**, 2071; P. Wasserscheid and W. Keim, *Angew. Chem., Int. Ed.*, 2000, **39**, 3772.

7 Y. Chauvin, L. Mussmann and H. Olivier, *Angew. Chem., Int. Ed. Engl.*, 1995, **34**, 2698; P. J. Dyson, D. J. Ellis, D. G. Parker and T. Welton, *Chem. Commun.*, 1999, 25; W. Keim, D. Vogt, H. Waffenschmidt and P. Wasserscheid, *J. Catal.*, 1999, **186**, 481; S. M. Silva, P. A. Z. Suarez, R. F. de Souza and J. Dupont, *Polym. Bull.*, 1998, **40**, 401; J. E. L. Dullius, P. A. Z. Suarez, S. Einloft, R. F. de Souza and J. Dupont, *Organometallics*, 1998, **17**, 815; D. Zim, R. F. de Souza, J. Dupont and A. L. Monteiro, *Tetrahedron Lett.*, 1998, **38**, 7071; D. E. Kaufmann, M. Nouroozian and H. Henze, *Synlett*, 1996, 1091; W. A. Herrmann and V. P. W. Böhm, *J. Organomet. Chem.*, 1999, **572**, 141; A. J. Carmichael, M. J. Earle, J. D. Holbrey, P. B. McCormac and K. R. Seddon, *Org. Lett.*, 1999, **1**, 997; C. E. Song and

E. J. Roh, *Chem. Commun.*, 2000, 837; A. J. Carnmichael, D. M. Haddleton, S. A. F. Bon and K. R. Seddon, *Chem. Commun.*, 2000, 1237; C. J. Mathews, P. J. Smith and T. Welton, *Chem. Commun.*, 2000, 1249.

8 P. A. Z. Suarez, J. E. L. Dullius, S. Einloft, R. F. de Souza and J. Dupont, *Polyhedron*, 1996, **15**, 1217.

9 A phosphine-free catalyst system, *i.e.* the use of $Pd(OAc)_2$ alone as catalyst precursor, displayed reverse medium-dependence on the selectivity. This appears to suggest that the detailed mechanism can be dependent on whether or not the catalyst ligates phosphines and/or that the influence of the ionic liquid is dependent on the structure of the catalyst.

Generation of hydrogen peroxide directly from H_2 and O_2 using CO_2 as the solvent

Dan Hâncu and Eric J. Beckman

Chemical Engineering Department, University of Pittsburgh, Pittsburgh, PA, USA.
E-mail: beckman@engrng.pitt.edu

Received 23rd October 2000
First published as an Advance Article on the web 27th March 2001

Hydrogen peroxide is a 'green' oxidant whose relatively high cost has prevented it from being applied to commodity chemical processing. In large part, those attributes of the current process (the anthraquinone route) that contribute to the cost of H_2O_2 also contribute to its non-sustainable features; by-product streams, energy input, and multiple required unit operations. We have explored the generation of hydrogen peroxide directly from hydrogen and oxygen using liquid CO_2 as the solvent and a CO_2-soluble palladium catalyst. Producing H_2O_2 directly from H_2 and O_2 eliminates unit operations and reduces raw material costs significantly. Further, homogeneous reaction in liquid CO_2 allows for contact between significant concentrations of O_2 and H_2, high rate of reaction, and ready recovery of the product *via* stripping into water. Both Pd(II) and Pd(0) catalysts were explored for the reaction; our results suggest that future work should focus on optimization of a CO_2-soluble or dispersible Pd(0) catalyst.

Introduction

Hydrogen peroxide is widely accepted as a green oxidant, as it is easy to handle, is relatively non-toxic, and breaks down readily in the environment to benign byproducts.[1] However, the process by which most of the world's H_2O_2 is produced (the anthraquinone, or AQ process) employs multiple unit operations, generates considerable waste and requires significant energy input, lowering the sustainability of the process and raising the production cost. Hydrogen peroxide is a green alternative to conventional oxidants, but its cost limits its application to higher value operations or areas where replacement of chlorinated oxidants produces a powerful market pull, as in paper bleaching.

The sequential hydrogenation and oxidation of an alkyl anthraquinone (in an organic solvent), a process essentially unchanged since the 1940s, is currently used to produce over 95% of the world's hydrogen peroxide (Fig. 1). A 2-alkylanthraquinone is dissolved in a mixture of an aromatic plus a long chain alcohol (a mixture often called the 'working solution') and then hydrogenated over a palladium catalyst in a three-phase reactor. The resulting anthrahydroquinone is oxidized by air in a subsequent reactor (two-phase, no catalyst), producing hydrogen peroxide and regenerating the anthraquinone. The H_2O_2 is stripped from the organic working solution into water in a counter-current column, producing a solution that is usually 30% by weight H_2O_2. The aqueous H_2O_2 is then distilled to remove impurities introduced during the production process and also to raise the concentration to as high as 70%. The AQ process has supplanted all of its competitors (electrochemical, secondary alcohol oxidation) because it generates H_2O_2 continuously at mild temperatures (40–60 °C) while preventing contact between H_2 and O_2 during production. The AQ process, however, suffers from innate inefficiencies owing to transport limitations in both reactors and organic contamination of the product during recovery by liquid–liquid extraction. Diffusional limitations to reaction mandate use of larger equipment and higher temperatures than are desired. Control of hydrogen:AQ stoichiometry and anthraquinone residence time during hydrogenation is difficult, promoting by-product formation. Over-hydrogenation of the AQ and the solvent during the process cycle requires constant disposal of non-reactive by-products and AQ make-up. Contact between the water and working solution in the stripping column cross-contaminates the phases; this, plus a non-optimal partition coefficient (of H_2O_2 between organic and aqueous phases), mandates use of

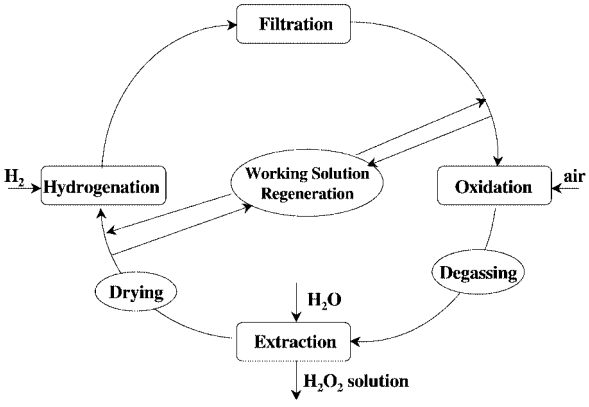

Fig. 1 Flow diagram for the AQ-AQH_2 process.

Green Context

Among the many chemical oxidants available to the organic chemist hydrogen peroxide is one of the 'greenest' since the only by-product is water (unlike toxic metal compounds from reagents such as chromate). As we should increasingly make a life cycle assessment of chemical processes we need to also consider the manufacture of the oxidant and here the current anthraquinone route does not have good green credentials since it generates by-products, has a high energy demand and requires multiple unit operations. Here the authors consider the viability of an alternative route to hydrogen peroxide based on the catalysed direct reaction of H_2 and O_2 in carbon dioxide as solvent. ***JHC***

 DOI: 10.1039/b008515o

distillation to both concentrate and purify H_2O_2, a major energy sink in the process.[2]

Gelbein has estimated that of the 17$/lb-mol cost of hydrogen peroxide, only $2/lb-mol derives from O_2 and H_2 cost while $5.40/lb-mol is needed for solvent and anthraquinone make-up and $1.50/lb-mol for energy. Because H_2O_2 plants incorporate numerous unit operations, they have relatively large capital costs (and hence fixed costs of over $7.00/lb-mol of H_2O_2, according to Gelbein). Hence, an intensified process (fewer operations) that uses less energy and wastes less raw material would be both greener and produce H_2O_2 less expensively. Production of H_2O_2 is thus an interesting target for green chemistry/design, in that those features that render the process "less than green" also contribute to added costs, both capital and operating. For H_2O_2 to successfully break into new markets, such as commodity chemical production, the process must become cheaper, and hence greener. Physically smaller plants would also facilitate applications such as on-site generation for microelectronics processing and would eliminate the need for transportation of aqueous H_2O_2.

In this paper, we show how direct production of H_2O_2 from oxygen and hydrogen using liquid carbon dioxide as a solvent is potentially a greener and less expensive route to this benign oxidant. This route also requires fewer unit operations, and hence the process would be greatly intensified.

Background

Direct production of H_2O_2 from O_2 and H_2 is being investigated by researchers at many companies, as shown by the large number of patents issued since 1980.[4] Clearly, direct contact between H_2 and O_2 presents a significant safety hazard, and yet a potential process *must* employ these two reactants above certain concentrations, and generate H_2O_2 at a certain rate, in order for the process to be of economical size and productivity. Hence many of the patents generated since 1980 present innovations whose aim is to balance H_2O_2 productivity with plant safety. The lack of commercial processes employing the direct route suggests that an adequate balance between these requirements has yet to be achieved.

Early work on the direct route involved the reaction of H_2 and O_2 in the gas phase, where the H_2O_2 was then quickly stripped into water. Because the explosive regime for O_2–H_2 coincides with the stoichiometry providing the best selectivity to H_2O_2 (5 : 1 to 20 : 1), large quantities of nitrogen were added for safety, but quite naturally this greatly reduced productivity.[5] Recent work has emphasized the dispersal of the gases in water to maximize the safety of the process, yet because the solubility of both H_2 and O_2 in water are very low, productivity is still below the point desired. Generation of "microbubbles" of H_2 and O_2, for example, has been proposed to deal with the inherent transport limitations of the process.[6] The Pd catalysts employed for the direct route will also catalyze the decomposition of H_2O_2 in water, and hence a number of patents disclose means of stabilizing the aqueous H_2O_2, although there is little discussion of the ultimate fate of these stabilizers.[7] New catalysts and catalyst supports are often described,[8] and recently catalytic membranes have also been introduced.[9]

In the early 1980s, Air Products and Chemicals patented a process where H_2O_2 was produced in a biphasic mixture of water and an organic solvent, later a fluorinated solvent.[10] Ligands for the Pd(II) catalyst were prepared such that the catalyst was soluble in the solvent yet not in water. Hydrogen and oxygen were dissolved in the organic (or fluorinated) phase, and the H_2O_2 stripped into the water. While H_2O_2 was produced using this route, use of organic solvent/O_2 mixtures is clearly problematic, and further the catalyst was degraded during the reaction. Finally, contamination of the aqueous phase by the organic solvent was still a problem. Mitsubishi has also disclosed a process for the direct generation of H_2O_2 where an organic solvent is used.[11]

Researchers at EniChem recently published a variation of the direct route to H_2O_2, where oxygen, CO, and water are reacted over a palladium catalyst (plus various promoters) to produce H_2O_2 plus CO_2.[12] Although nominally different from the previously mentioned work, research by Sen's group[13] and others would suggest that the first step in such a process is the reaction of CO and water to generate H_2 and CO_2, followed by the combination of hydrogen and oxygen to form H_2O_2. Patents on this route have been issued to Enichem and Halcon.[14]

In order to gain the advantages of the direct route to H_2O_2 (no impurities, low cost for raw materials), maintain safe operation, and achieve high productivity, we have investigated the homogeneous production of H_2O_2 from H_2 and O_2 in carbon dioxide. In our system, a palladium catalyst is developed whose ligands allow miscibility with CO_2 at moderate pressures, as shown in Fig. 2. Above 31 °C, H_2 and O_2 are miscible with CO_2 in all proportions (even under sub-critical conditions, the solubility of H_2 and O_2 in CO_2 is much higher than in organic solvents or water). Further, the heat capacity of CO_2 under our conditions is liquid-like, and hence the safe operating regime of a H_2–O_2 mixture is much broader in pressurized CO_2 than in a gas. CO_2 is immune to further oxidation, overcoming a significant drawback of using organic solvents in contact with O_2. Further, Solymosi and colleagues have shown that CO_2–H_2 mixtures will not form CO over a Pd catalyst at temperatures below 100 °C.[15] Operating the reaction homogeneously (*i.e.*, *via* a CO_2-soluble catalyst) eliminates the transport limitations to reaction inherent to all of the water-based processes described in the patent literature while maintaining safe operation through use of inert, non-flammable CO_2 as the solvent.

Hydrogen peroxide is soluble in conventional 'working solutions' at levels of 4% and greater. Given the relatively feeble solvent power of CO_2, it is likely that the solubility of H_2O_2 in CO_2 will be substantially less than that in organic solvents. Hence, we assume that H_2O_2 will rapidly partition to the aqueous phase, minimizing the chances for product degradation through prolonged contact with the CO_2-soluble catalyst. CO_2 readily dissolves in water, lowering the pH to 2.85, within the range (2–4) typically used to stabilize aqueous hydrogen peroxide. 'Contamination' of the aqueous phase by the organic (CO_2) in our case clearly does not require remediation through distillation. Finally, the product (H_2O_2) in our system is recovered from CO_2 without resorting to a large pressure drop. Although depressurization of CO_2 will lead to essentially complete precipitation of dissolved material, use of a significant pressure drop for product recovery greatly elevates operating costs (CO_2 recompression). The well-known CO_2-based coffee decaffeination process operates economically partly because dissolved caffeine is removed from carbon dioxide through countercurrent extraction against water, allowing the CO_2 to travel in a loop at relatively constant pressure.

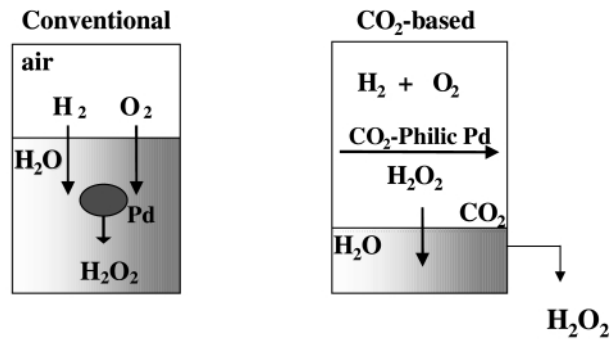

Fig. 2 Direct reaction of hydrogen and oxygen.

In summary, we believe that identification of an active, CO_2-soluble catalyst for this system will allow construction of H_2O_2 plants that incorporate significantly fewer unit operations (and are hence more compact), will use much less energy, and will produce a cleaner product with less waste. In this paper we explore the use of two model catalysts, modified triphenylphosphine Pd(II) and dibenzylideneacetone Pd(0), to generate hydrogen peroxide homogeneously in carbon dioxide.

Experimental

1,4-Dibromobenzene (98%; Aldrich), 1-bromo-4-iodobenzene (98%; Aldrich), magnesium (turnings, 99.98%; Aldrich), perfluorohexyl iodide (99%; Aldrich), 1,1,1,2,2,3,3,4,4,5,5,6,6-tridecafluoro-8-iodooctane (96%; Aldrich), copper(I) chloride (99.995%; Aldrich), phosphorus trichloride (99.9%; Aldrich), *tert*-butyllithium (1.7 M solution in pentane; Aldrich), trichlorosilane (99%; Aldrich), triethylamine (99.5%; Fluka), bis(acetonitrile)dichloropalladium(II) (99.99%; Aldrich), dichlorobis(triphenylphosphine)palladium(II) (99.99%; Aldrich), cyclohexene (Aldrich), tris(dibenzylideneacetone)dipalladium(0) (Stream) and Pd/C (1% Pd, Aldrich) were used as received. The TS-1 catalyst (0.97% Ti) was a gift from Lyondell Chemical Company, synthesized according to the published procedures.[16] Reactions involving air- or moisture-sensitive materials were performed under argon using Schlenk techniques. All NMR spectra were recorded on a Bruker DMX300 instrument at the base frequency of 121.49 MHz for ^{31}P and 300.13 MHz for ^{1}H. The samples were prepared in 8 mm NMR tubes placed coaxially in standard, thin-walled, 10 mm tubes containing $CDCl_3$ as chemical shift standard. Chemical shifts were reported in ppm relative to TMS for ^{1}H NMR and to 85% H_3PO_4 for ^{31}P NMR.

1-Bromo-4-(tridecafluorohexyl)benzene 2a[17]

In a typical experiment, a solution of $F(CF_2)_6I$ (8.92 g, 0.02 mol) in hexafluorobenzene (20 ml) was added dropwise to a mixture of 4-bromoiodobenzene **1a** (5.77 g, 0.02 mol), 2,2′-pypyridine (0.24 g, 1.5 mmol), Cu powder (3.23 g, 0.05 mol), DMSO (20 ml) and hexafluorobenzene (30 ml) at 70 °C, under Ar atmosphere. The reaction mixture was stirred for 72 h at 70 °C. After filtration of the catalyst and hydrolysis with 100 ml of water, the product was extracted with dichloromethane (100 cm^3), and the organic layer was subsequently washed with water, and dried over $MgSO_4$. Then, the product was extracted with perfluoro-1,3-dimethylcyclohexane (3 × 20 cm^3) and the solvent was removed under vacuum. Distillation gave the product as a colorless liquid (bp 45–47 °C at 5 10^{-3} mmHg) (72%). ^{1}H NMR (δ, $CDCl_3$, 300 MHz) 7.72 (2 H, d, 2,6-ArH), 7.48 (2 H, d, 3,5-ArH).

1-Bromo-4-(1*H*,1*H*,2*H*,2*H*-Perfluorooctyl)benzene 2b[18]

A 100 ml three-neck flask equipped with a dropping funnel and thermometer, previously evacuated and then filled with Ar was charged with Mg turnings (2.07 g, 0.0862 mol) and Et_2O (*ca*. 5 ml) such that the solvent fully covered the magnesium particles. A solution of *p*-dibromobenzene (18.06 g, 0.075 mol) in Et_2O (*ca*. 35 ml) was added dropwise to the reaction mixture slowly enough to maintain a gentle boiling of the solvent. The mixture was subsequently stirred at room temperature overnight. After filtration, the yellowish resulting solution was added dropwise to 1,1,1,2,2,3,3,4,4,5,5,6,6-tridecafluoro-8-iodooctane (31.9 g, 0.0675 mol) and CuCl (0.2 g) in dry tetrahydrofuran (*ca*. 45 ml) over 1 h at −20 °C. The slightly yellow reaction mixture was allowed to warm slowly to room temperature in a 4 h period. The mixture was hydrolyzed with 10% aqueous NH_4Cl (50 cm^3) and the organic layer was collected, washed with water (2 × 30 cm^3), and dried over $MgSO_4$. The solvent was then removed under vacuum affording 19 g of a brown–yellow oil. Distillation gave the product as a colorless liquid (9.5 g (28%); bp 95–100 °C/10^{-2} mmHg). ^{1}H NMR (δ, $CDCl_3$, 300 MHz) 7.42 (2 H, d, 2,6-ArH), 7.06 (2 H, d, 3,5-ArH), 2.84 (2 H, m, H_2C^{α}), 2.30 (2 H, m, H_2C^{β}).

Tris(4-tridecafluorohexylphenyl)phosphine 3a[19]

A three-neck flask equipped with a dropping funnel and thermometer was charged with **2a** (4 g, 8.4 mmol) in anhydrous diethyl ether (50 cm^3), cooled in a liquid nitrogen–acetone bath at −78 °C, evacuated for 10 min and then filled with dry Ar. A 1.7 M pentane solution of *tert*-butyllithium (9.9 cm^3, 0.017 mol) was added dropwise under stirring over 1 h at −78 °C, and the slightly yellow resulting mixture was stirred at this temperature for 30 min. Subsequently, phosphorus trichloride (0.424 g, 3.1 mmol) in diethyl ether (5 cm^3) was added dropwise over 1 h at −78 °C, and the reaction mixture was kept at this temperature (−78 °C) for an additional hour and then allowed to warm at room temperature over a 12 h period. After hydrolysis with 10% aqueous NH_4Cl (50 cm^3), the organic layer was washed with water and dried over $MgSO_4$. The water phase was washed with diethyl ether (3 × 20 cm^3). The combined organic layers were concentrated to 5 cm^3 and then passed through a silica gel column, using a 95% hexane–5% ethyl acetate mixture as eluent. Evaporation of the solvent yields **3a** as white solid (2.1 g (53%), mp 63 °C). ^{1}H NMR (δ, $CDCl_3$, 300 MHz) 7.6 (6 H, d, 2,6-ArH), 7.4 (6 H, t, 3,5-ArH). $^{31}P\{^{1}H\}$ NMR (δ, $CDCl_3$, 121.49 MHz) −5.6.

Tris(4-(3,3,4,4,5,5,6,6,7,7,8,8,8-tridecafluoro-1-octylphenyl))phosphine 3b

This was prepared by the same method as that used for **3a** by using **2b** (4.23 g, 8.4 mmol) affording **3b** as a white solid (1.8 g (45%), mp 58 °C). ^{1}H NMR (δ, $CDCl_3$, 300 MHz) 7.3 (6 H, d, 2,6-ArH), 7.1 (6 H, t, 3,5-ArH), 2.84 (6 H, m, H_2C^{α}), 2.30 (6 H, m, H_2C^{β}). $^{31}P\{^{1}H\}$ NMR (δ, $CDCl_3$, 121.49 MHz) −7.1.

Tris(4-trifluoromethylphenyl)phosphine 3c

This was prepared by the same method as that used for **3a** by using 4-trifluoromethylbromobenzene **2c** (1.89 g, 8 mmol) affording **3c** as a white solid (0.79 g (55%), mp 70 °C). ^{1}H NMR (δ, $CDCl_3$, 300 MHz) 7.6 (6 H, d, 2,6-ArH), 7.4 (6 H, t, 3,5-ArH). $^{31}P\{^{1}H\}$ NMR (δ, $CDCl_3$, 121.49 MHz) −5.3.

Dichlorobis(tris(4-tridecafluorohexylphenyl)-phosphine))palladium(II) 4a

A solution of **3a** (1.3 g, 1 mmol) in chloroform (15 cm^3) was mixed with $[Pd(MeCN)_2]Cl_2$ (0.13 g, 0.5 mmol) for 15 min. The resulting yellow–orange solution was concentrated, and passed through a silica gel column using a hexane–ethyl acetate mixture of increasing polarity as eluent. Evaporation of the solvent from the fractions obtained with 10% ethyl acetate–90% hexane mixture gave the product **4a** as yellow solid (0.79 g, 55%). ^{1}H NMR (δ, $CDCl_3$, 300 MHz) 7.6 (12 H, d, 2,6-ArH), 7.4 (12 H, t, 3,5-ArH). $^{31}P\{^{1}H\}$ NMR (δ, $CDCl_3$, 121.49 MHz) 23.8.

Dichlorobis(tris-(4-(3,3,4,4,5,5,6,6,7,7,8,8,8-tridecafluoro-1-octyl)phenyl)phosphine)palladium(II) 4b

This was prepared by the same method as described for **4a** by using **3b** (1.37 g, 1 mmol) affording **4b** as yellow solid (0.91 g, 62%). ^{1}H NMR (δ, $CDCl_3$, 300 MHz) 7.6 (12 H, d, 2,6-ArH), 7.3 (12 H, t, 3,5-ArH),), 2.9 (6 H, m, H_2C^{α}), 2.3 (6 H, m, H_2C^{β}). ^{31}P{^{1}H} NMR (δ, $CDCl_3$, 121.49 MHz) 22.5.

Dichlorobis(tris(4-trifluoromethylphenyl)phosphine)-palladium(II) 4c

This was prepared by the same method as described for **4a** by using **3c** (0.5 g, 1 mmol) affording **4c** as yellow solid (0.36 g, 62%). ^{1}H NMR (δ, $CDCl_3$, 300 MHz) 7.61 (12 H, d, 2,6-ArH), 7.4 (12 H, t, 3,5-ArH). ^{31}P{^{1}H} NMR (δ, $CDCl_3$, 121.49 MHz) 23.9.

Solubility of catalysts in carbon dioxide

The phase behavior measurements of the 'CO_2-philic' Pd-catalysts in liquid CO_2 were conducted as described elsewhere.[21,22]

Reaction of H_2 and O_2 in carbon dioxide

Direct reaction of H_2 and O_2 in liquid CO_2 was conducted in a high-pressure batch reactor at room temperature and P = 170 bar. The experimental setup (Fig. 3) consists of: (1) a 35 cm^3 high-pressure batch reactor (Univ. of Pittsburgh) whose walls were previously passivated with 35% HNO_3 at 65 °C for 2 h to avoid decomposition of H_2O_2 on the stainless steel, (2) two manual syringe pumps (HIP, Erie, Pa) where H_2–CO_2 and air–CO_2 mixtures were prepared, and (3) two high-pressure HPLC injection valves (Rheodyne) for precise measurement of the amount of air and H_2 added to the system.

In a typical experiment, the reactor was charged with deionized water (3.5 cm^3), H_2SO_4 (96%, 0.04 g, 0.3 mmol), Pd-catalyst ($PdCl_2[P(C_6H_5)_3]_2$, 0.0188 g, 0.017 mmol), and NH_4Cl (0.0077 g, 0.1 mmol). After 15 min evacuation, air (31 cm^3 air at P = 10.9 bar) was injected into the reactor and one of the syringe pumps (SP1) was charged with hydrogen (2 cm^3, P = 90 psi). The system (SP1 and the reactor) was then pressurized with CO_2 (P = 2500 psi) and the reaction was started by injecting the CO_2–H_2 mixture into the reactor. After 3 h of reaction (T = 25 °C, P = 2500 psi) the system was slowly depressurized, and Pd-catalyst extracted with $CDCl_3$. The aqueous phase (3 cm^3) was diluted with deionized water to 15 cm^3 and titrated with 0.05 M $KMnO_4$ in the presence of 96% H_2SO_4 to determine the concentration of hydrogen peroxide.

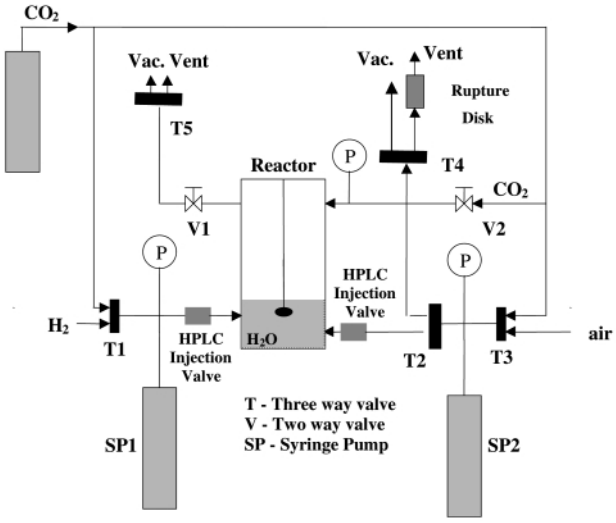

Fig. 3 Experimental set-up for direct synthesis of H_2O_2 in liquid CO_2.

Epoxidation of cyclohexene in CO_2

Epoxidation of cyclohexene by H_2 and O_2 was conducted using a Pd-based catalyst in conjunction with the titania silicate catalyst TS-1. Reactions were run in liquid CO_2 in a high-pressure batch reactor (Fig. 3) at room temperature and P = 1900 psi. In a typical experiment, the reactor was charged with deionized water (5.0 cm^3), TS-1 (0.15 g), a Pd-based catalyst (1% Pd with respect to TS-1) and cyclohexene (0.8 g, 9.75 mmol). After 15 min evacuation, air (80 cm^3 air at P = 10.9 bar) was injected into the reactor and one of the syringe pumps (SP1) was charged with hydrogen (20 cm^3, P = 90 psi). The system (SP1 and the reactor) was then pressurized with CO_2 and the reaction was started by injecting the CO_2–H_2 mixture into the reactor. After 3 h of reaction (T = 25 °C, P = 1900 psi) the system was slowly depressurized, and the organic phase was extracted with $CHCl_3$ and then analyzed by GC for cyclohexene oxide. No cyclohexene oxide was produced in the absence of palladium.

Safety issues

The experiments described in this paper were conducted at high pressure using mixtures of hydrogen, oxygen and carbon dioxide. The vessels used in this project were designed and constructed at the University of Pittsburgh with a safety margin (5:1) with regards to pressure. Vessels were hydrostatically tested at a pressure twice that of the anticipated maximum operating pressure prior to being placed into service. A rupture disk was attached to each reactor in use during the experiments. Regarding the use of mixtures of hydrogen and oxygen, the concentrations employed (of the order of 5mM in the reactor) were sufficiently dilute (and the heat capacity of liquid CO_2 is sufficiently high) such that if all of the hydrogen and oxygen reacted to form water, the temperature rise within the reactor would be < 5 °C. Both hydrogen and oxygen were added (*via* manual syringe pumps) as mixtures with CO_2, further reducing the risk of undesired reaction. Regulators for both the hydrogen and oxygen cylinders were those recommended by the gas supplier for this type of service.

Results and discussion

The patent literature is divided as to the most appropriate catalyst to use for the direct conversion of hydrogen and oxygen to H_2O_2; both Pd(0) and Pd(II) catalysts are recommended.[10,20] We consequently explored the use of each type.

Pd(II) catalysts

A large body of previous work[21] has shown that use of fluorinated ligands creates organometallic catalysts with significantly higher solubility in carbon dioxide than their hydrocarbon analogs. Increasing the fluorine content of the ligand tends to lower the miscibility pressure of the catalyst (by rendering the molecule on balance more 'CO_2-philic'), yet can also greatly increase the cost. Use of fluorinated ligands may also change the electronic character of the active center of the catalyst; this effect will increase as the extent of fluorination increases. We generated a series of fluorinated Pd(II) catalysts to examine the role of fluorine content, plus the presence or absence of a spacer between the metal and the fluorinated 'tails', on CO_2 solubility, activity in the reaction between H_2 and O_2 in

CO_2, and cost (as evidenced by ease of synthesis). The catalysts and the synthetic procedures used to prepare them are shown in Scheme 1.

Increasing the length of a fluorinated 'ponytail' tends to decrease the pressure required for miscibility as the enthalpy of mixing (between solute and CO_2) becomes more favorable.[22] This is also true for our fluorinated Pd(II) catalysts (Fig. 4). Eventually, a point of diminishing returns will be reached, such that further increases to the length of the fluorinated tail will increase miscibility pressures (owing to unfavorable entropic effects). Further, it should be noted that the trifluoromethyl variant, although not as 'CO_2-philic' as the version with the longer tail, was assembled using commercially available materials while the other required a multi-step synthesis to construct. Hence, we are confronted with an optimization problem, where increasing the length of the fluorinated tail raises the cost of the ligand but lowers the required miscibility pressure, and hence the capital cost of a process. It should be noted that previous patents on the direct route employed total pressures (usually N_2–O_2–H_2 mixtures) in the 50–200 bar range.[23]

Reactions were conducted in a biphasic system (water/CO_2) where H_2, O_2 and the catalyst reside in the CO_2 phase (nitrogen was also present as we employed air as our reactant). We employed an O_2:H_2 ratio of 7:1, as suggested by the previous patent literature as a means to suppress formation of water from H_2 and O_2. Stabilizers were added to the water to inhibit degradation of H_2O_2 *via* contact with the steel walls of the reactor vessel. Samples of the aqueous phase were removed after 3 h (at room temperature) and titrated against potassium permanganate to find the H_2O_2 concentration. In general (Fig. 5), we found that all of the Pd(II) catalysts were active in the generation of H_2O_2, and that neither the length of the fluorinated tail nor the presence of a spacer between fluorinated tail and metal significantly affected the yield of H_2O_2 after 3 h. Further, as noted in Fig. 5, simple hydrocarbon versions of the catalysts also produced H_2O_2, although only half as much as their fluorinated cousins. The hydrogenated catalysts do exhibit some solubility in CO_2, but unlike their fluorinated cousins, only part of the initial catalyst charge is actually dissolved in the carbon dioxide. The turnover frequencies for the reactions described in Fig. 5 are not high, only *ca.* 10 h^{-1}, but they do demonstrate that H_2O_2 can be generated using this type of system despite operating at only 22 °C. Because we could not sample the system on-line, we do not as yet know the selectivity of the reaction to H_2O_2 (*vs.* water).

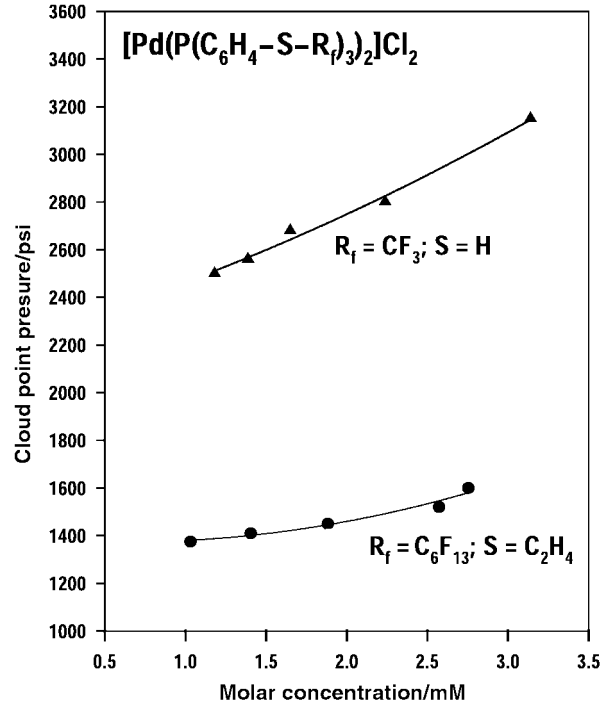

Fig. 4 Phase behavior of $[Pd(P(C_6H_4–S–R_f)_3)_2]Cl_2$ in CO_2 (T = 25 °C): (●) R_f = $(CF_2)_6F$; S = C_2H_4; (▲) R_f = CF_3; S = H.

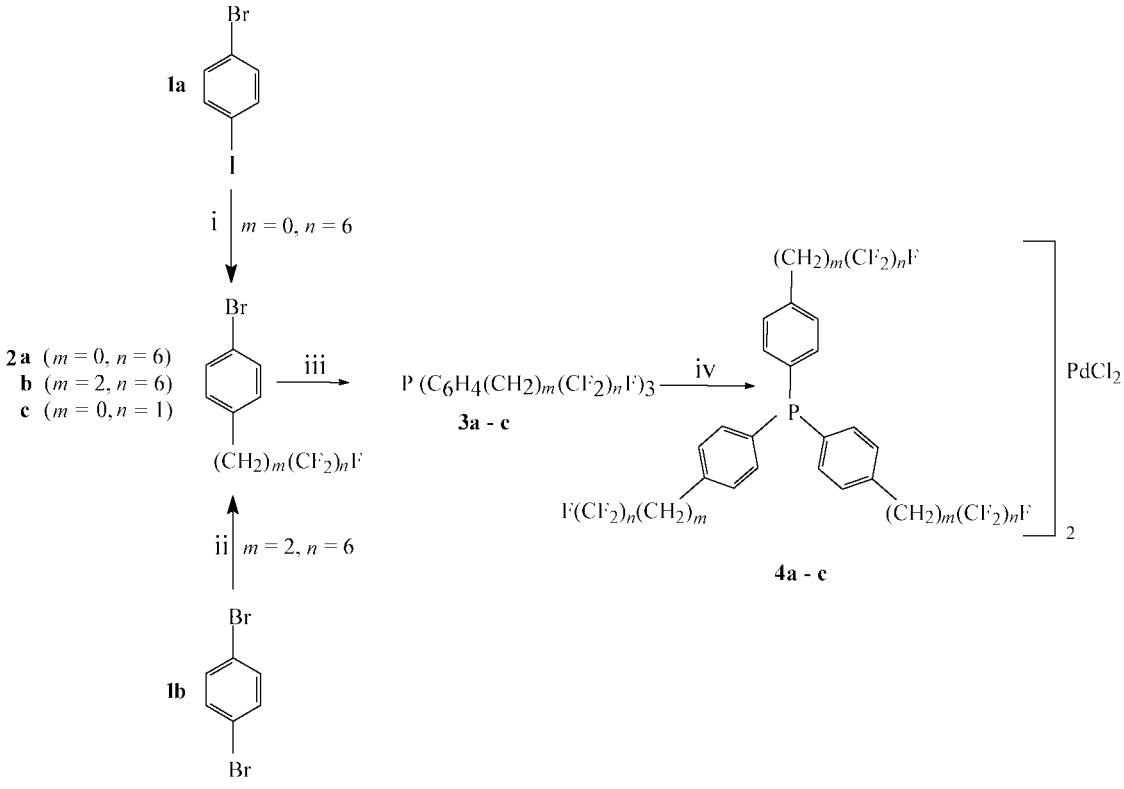

Scheme 1 Synthetic route for 'CO_2-philic' Pd^{II}-catalysts ($[Pd(P(C_6H_4–S–R_f)_3)_2]Cl_2$; R_f = CF_3, C_6F_{13}; S = H, C_2H_4) *Reagents and conditions*: i, $C_6F_{13}I$, Cu, DMSO, 70 °C; ii, Mg, Et_2O and then $C_6F_{13}C_2H_4I$, CuCl, THF; iii, Bu^tLi, Et_2O, −78 °C and then PCl_3; iv, $[Pd(MeCN)_2]Cl_2$.

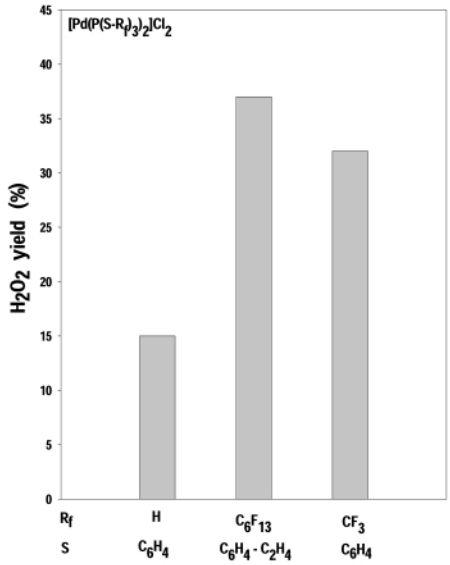

Fig. 5 Reactivity of $[Pd(P–S–R_f)_3)_2]Cl_2$ (S = $–C_6H_4–$ or $–C_6H_4–C_2H_4$; R_f = H, C_6F_{13}, CF_3) in the synthesis of H_2O_2 from elements in liquid CO_2–H_2O biphasic system (P = 2500 psi, T = 25 °C; 3 h; O_2 : H_2 = 7 : 1 (molar); C_{H_2} = 0.012 M; $C_{[Pd(P–S–Rf)_3)_2]Cl_2}$ = 0.5 mM).

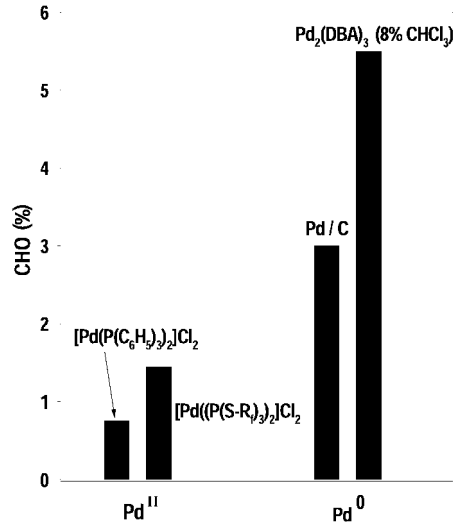

Fig. 6 Performance of Pd catalysts in epoxidation of cyclohexene to cyclohexene oxide (CHO) over TS-1 by H_2–O_2 mixture (T = 25 °C; P = 1900 psi; 4.28 g/L TS-1; 1% Pd (with respect to TS-1); H_2 : O_2 : C_6H_{10} = 1 : 1.25 : 0.5 (molar); C_{H_2} = 0.2 M) (DBA = dibenzylideneacetone).

We examined the stability of the catalysts against oxygen and hydrogen by exposing them to a ten-fold molar excess of hydrogen and oxygen (in CO_2) for 24 h at room temperature; subsequent analysis by ^{31}P NMR shows no degradation after 24 h.

Pd(0) catalysts

Although we found that we could produce H_2O_2 in CO_2, the methodology in the previous section was less than ideal because we could not sample for the product online, and hence it is likely, despite our best efforts, that some of the product decomposed through interactions with the steel reactor and tubing. Hence, we examined an indirect method for measuring H_2O_2 production. Here we took advantage of the known rapid reaction of H_2O_2 with cyclohexene oxide over a titania silicate catalyst (TS-1) to produce cyclohexene oxide. The rapid reaction of H_2O_2 with cyclohexene thus provides less opportunity for H_2O_2 degradation. We compared the performance of two Pd(II) catalysts (both fluorinated triphenyl phosphine and the unfluorinated analog) to two Pd(II) catalysts (heterogeneous palladium on carbon and a dibenzylideneacetone Pd complex). Rather than synthesizing a fluorinated version of the DBA–Pd catalyst, we added a co-solvent (here 8% chloroform) to allow the catalyst to dissolve in CO_2 at the operating temperature and pressure.

Results (Fig. 6) after 3 h show that Pd(0) catalysts are superior in activity in the generation of H_2O_2 (and hence cyclohexene oxide) than the Pd(II) catalysts we have employed previously. Interestingly, simple Pd/C produced significant amounts of product, likely owing to the solubilization of H_2 and O_2 in water under the high pressures employed and the rapid reaction of any H_2O_2 formed with cyclohexene. Nevertheless, these results suggest that a Pd(0) catalyst that can be dissolved or dispersed in CO_2 will ultimately prove to be the most useful for this system.

Summary

The production of hydrogen peroxide directly from O_2 and H_2 using CO_2 as the solvent could provide a route to H_2O_2 that is both less expensive than the current process and significantly 'greener'. Our results show that one can produce H_2O_2 in CO_2 using either CO_2-soluble Pd(II) or Pd(0) catalyst, although it appears at this point that Pd(0) catalysts will ultimately prove more useful. Conducting the reaction homogeneously in CO_2 addresses the key issue involved in the direct route to H_2O_2; how to adequately balance productivity with safety. Further, the reaction of H_2 and O_2 to form H_2O_2 takes full advantage of the properties of carbon dioxide as solvent. First, the reaction employs gaseous reactants (completely miscible with CO_2), including oxygen (CO_2 is a non-oxidizable organic solvent, and non-flammable); we can eliminate all transport limitations by employing a homogeneous catalyst. The product, H_2O_2, can be recovered from CO_2 without resorting to large (and expensive) pressure drops. Contact between water and CO_2, unlike that between water and organic solvents, present us with no remediation problems. Finally, the pH of a CO_2–water biphasic system is 2.85, within the 2–4 range used in H_2O_2 stabilization.

Future work will focus on the use of Pd(0) catalysts in CO_2, to try to optimize H_2O_2 production.

References

1 C. W. Jones, *Applications of Hydrogen Peroxide and Derivatives*, *Clean Technology Monographs*, Royal Society of Chemistry, Cambridge, 1999; Y. Deng, Z. Ma, K. Wang and J. Chen, *Green Chem.*, 1999, **1**, 277.

2 T. E. Guenter, *Hydrogen Peroxide*, in *Encyclopedia of Chemical Processing and Design*, ed. J. J. McKetta and W. A. Cunningham, Marcel Dekker, Inc., 1988; vol. 27, p. 27.

3 A. P. Gelbein, *CHEMTECH*, 1998, **28**, 1.

4 H. T. Hess, *Hydrogen Peroxide*, in *Kirk-Othmer Encyclopedia of Chemical Engineering*, ed. I. Kroschwitz and M. Howe-Grant, John & Sons, Inc., New York, 4th edn., 1995, vol. 13, p. 961.

5 M. A. Paoli, *US Pat.*, 5 194 242, 1993 (E.I. DuPont de Nemours & Co.); W. F. Brill, *US Pat.*, 4 661 337, 1987 (The Halcon SD Group, Inc.).

6 H. A. Huckins, *US Pat.*, 5 641 467, 1997 (Princeton Advanced Technologies); H. A. Huckins, *US Pat.*, 6 042 804, 2000 (Advanced Peroxide Technology, Inc.)

7 L.W. Gosser and M. A. Paoli, *US Pat.*, 5 135 731, 1992 (E.I. DuPont de Nemours & Co.); L.W. Gosser and J. T. Schwartz, *US Pat.*, 4 772 458, 9/20/88 (assigned to E.I. DuPont de Nemours & Co).

8 M. E. Thompson, J. L. Snover, V. Joshi and L. A. Vermuelen, *US Pat.*, 5 480 629, 1996 (Princeton University); F. Goto, K. Tanaka and

T. Sasaki, *US Pat.*, 5 965 101, 1999 (Sumitomo Chemical Co.); M. E. Thompson, V. V Krishnan, A. G. Dokoutchaev, F. Abdel-Razzaq and S. Rice, *US Pat.*, 5 976 486, 1999 (University of Southern California); K. T. Chuang, *US Pat.*, 5 082 647, 1992 (Atomic Energy of Canada, Ltd.); C. Pralus and J-P. Schirmann, *US Pat.*, 4 996 039, 1991 (Atochem); J. Van Weynbergh, J-P. Schoebrechts and J-C. Colery, *US Pat.*, 5 447 706, 1995 (Solvay Interox); H. Nagashima, Y. Ishiuchi, Y. Hiramatsu and M. Kawakami, *US Pat.*, 5 292 496, 1994 (Mitsubishi Gas Chemical Co).

9 S. P. Web and J. A. McIntyre, *US Pat.*, 5 800 796, 1998 (Dow Chemical Co.).

10 F. Moseley and P. N. Dyer, *US Pat.*, 4 369 128, 1983 (Air Products & Chemicals Inc); P. N. Dyer and F. Moseley, *US Pat.*, 4 128 627, 1978 (Air Products & Chemicals Inc.); F. Moseley and P. N. Dyer, *US Pat.*, 4 336 240, 1982 (Air Products & Chemicals, Inc).

11 M. Kawakami, Y. Ushiuchi, H. Nagashima, T. Tomita and N. Hiramatsu, *US Pat.*, 5 399 334, 1995 (Mitsubishi Gas Chemical Co).

12 D. Bianchi, R. Bortolo, R. D'Aloisio and M. Ricci, *Angew. Chem., Int. Ed.*, 1999, **38**, 706; D. Bianch, R. Bortolo, R. D'Aloisio, M. Ricci and S. Soattini, *US Pat.*, 5 783 164, 1998 (Enichem S.p.A).

13 M. Lin and A. Sen, *J. Am. Chem. Soc.*, 1992, **114**, 7307; A. Sen, *Acc. Chem. Res.*, 1998, **31**, 550; M. Lin, T. Hogan and A. Sen, *J. Am. Chem. Soc.*, 1997, **119**, 6048.

14 W. F. Brill, *US Pat.*, 4 462 978, 1984 (The Halcon SD Group, Inc.).

15 F. Solymosi, A. Erdöhelyi and M. Lancz, *J. Catal.*, 1985, **95**, 567; A. Erdöhelyi, M. Pásztor and F. Solymosi, *J. Catal.*, 1986, **98**, 166.

16 M. Taramasso, G. Perego and B. Notari, *US Pat.*, 4 410 501, 1983.

17 P. Bhattacharyya, D. Gudmunsen, E. G. Hope, R. D. W. Kemmitt, D. R. Paige and A. M. Stuart, *J. Chem. Soc., Perkin Trans. 1*, 1997, 3609.

18 S. Kainz, Z. Y. Luo, D. P. Curran and W. Leitner, *Synthesis*, 1998, 1425.

19 D. P. Curran and Q. Zhang, personal communication.

20 R. C. Michaelson, *US Pat.*, 4 347 232, 1982 (FMC Corporation).

21 J. M. DeSimone, Z. Guan and C. S. Elsbernd, *Science*, 1992, **257**, 945; D. A. Newman, T. A. Hoefling, R. R. Beitle, E. J. Beckman and R. M. Enick, *J. Supercrit. Fluids*, 1993, **6**, 205; P. G. Jessop, T. Ikariya and R. Noyori, *Chem. Rev.*, 1999, **99**, 475.

22 A. V. Yazdi and E. J. B. Beckman, *Ind. Eng. Chem. Res.*, 1996, **35**, 3644.

23 A. I. Dalton and R. W. Skinner, *US Pat.*, 4 336 239, 1982 (Air Products & Chemicals); L. W. Gosser, *US Pat.*, 4 681 751, 1987 (E.I. DuPont de Nemours & Co.); L. W. Gosser and J. T. Schwartz, *US Pat.*, 4 832 938, 1989 (E.I. DuPont de Nemours & Co.); Y. Izumi, H. Miyazaki and S. Kawahara, *US Pat.*, 4 009 252, 1977 (Tokuyama Soda K.K).

Synthesis of dimethyl carbonate from carbon dioxide and methanol in the presence of methyl iodide and base catalysts under mild conditions: effect of reaction conditions and reaction mechanism

Shin-ichiro Fujita,[a] Bhalchandra M. Bhanage,†[a] Yutaka Ikushima†[b] and Masahiko Arai*†[a]

[a] *Division of Materials Science and Engineering, Graduate School of Engineering, Hokkaido University, Sapporo 060-8628, Japan. E-mail: marai@eng.hokudai.ac.jp*
[b] *Tohoku National Industrial Research Institute, Sendai 983-8551, Japan*

Received 9th January 2001
First published as an Advance Article on the web 26th March 2001

The synthesis of dimethyl carbonate (DMC) from methanol and CO_2 was studied in the presence of methyl iodide and various base catalysts. Among the catalysts used, potassium carbonate was found to be most active. Dimethyl ether (DME) is formed as a byproduct. When the reaction was carried out at various pressure of CO_2, two maxima in DMC formation were observed at 4.5 and 8 MPa, while DME formation decreased monotonically with increasing the CO_2 pressure. The effects of the amounts of methyl iodide and potassium carbonate on the DMC and DME formation were also investigated. Mechanistic studies suggest that DMC and DME are produced in parallel pathways and methyl iodide is involved in the formation of both DMC and DME. Other alcohols show less reactivity than methanol.

Introduction

Recently, it has been well recognized that the utilization of carbon dioxide as a carbon resource is important.[1–4] Direct synthesis of dimethyl carbonate (DMC) from carbon dioxide is one of the promising reactions for this purpose.[2,5–7] DMC can be used as a solvent and an octane enhancer. Besides these applications, DMC is a non-toxic carbonylation and methylation reagent replacing poisonous phosgene and dimethyl sulfate.[8–14] In addition, DMC is a precursor for polycarbonate resins.[10] Polycarbonate has been commercially produced by the polycondensation between bisphenol-A and phosgene.[10] Thus, DMC can be regarded as a safe replacement for phosgene.

Currently, DMC is synthesized by phosgenenation of methanol, by oxidative carbonylation of methanol (non-phosgene route)[15] or by a reaction of carbon monoxide with methyl nitrite.[16,17] Methyl nitrite is produced from methanol, oxygen and nitric oxide. These routes use poisonous and/or corrosive gases such as phosgene, hydrogen chloride, nitric oxide and carbon monoxide, and also bear potential explosion hazards in the case of methanol carbonylation. Hence, the direct synthesis of DMC from carbon dioxide and methanol is an attractive alternative.

Several researchers report that the direct synthesis of DMC from carbon dioxide and methanol proceeds in the presence of organometallic complexes.[18–22] Fang and Fujimoto[23] reported that several inorganic bases catalyzed DMC synthesis in the presence of methyl iodide as a promoter. Among the base catalysts examined, potassium carbonate was most effective. Although the yield of DMC obtained with this catalyst was higher than those with organometallic complexes, the range of reaction conditions used was quite limited. Tomishige *et al.* found that zirconia catalyzed the reaction in the absence of methyl iodide;[24–26] however, the yield was far from satisfactory. Indirect synthesis of DMC was also studied. Sakakura *et al.* reported the synthesis of DMC from orthoesters[27] and acetals[28,29] using an organotin catalyst. The yields of DMC reported in these systems were high; however, these systems have disadvantages due to the high cost of the starting materials and the difficulty in the catalyst–product separation due to the homogeneous nature of the catalyst. Under these circumstances, it is important to study the base catalyzed reaction between methanol and carbon dioxide along with methyl iodide in more detail.

In the present study, the base catalyzed synthesis of dimethyl carbonate was carried out in the presence of CO_2 and methyl iodide at mild operating conditions. Effects of the CO_2 pressure and the amounts of methyl iodide and potassium carbonate on the reaction were investigated. Results for other alcohols are also reported.

Results and discussion

Reaction with various carbonates

When the reaction of methanol and methyl iodide was carried out in the presence of inorganic basic compounds, dimethyl

Green Context

Dimethyl carbonate is gaining importance as a replacement for phosgene. Significant effort is thus being expended in the development of clean synthetic methods for the production of dimethyl carbonate, and of other related carbonates. This paper deals with the synthesis of dialkyl carbonates in carbon dioxide as reagent and solvent. Methanol and methyl iodide are both required for the reaction, and it is shown that methyl iodide is a reagent rather than a promotor/catalyst. The use of CO_2 as solvent and reactant allows a clean reaction and separation to be achieved without the need for organic solvent. ***DJM***

† CREST, JST.

Table 1 Reaction of methanol and methyl iodide with various carbonate compounds[a]

Catalyst	DMC/mmol	DME/mmol
K_2CO_3	4.04	0.90
$KHCO_3$	2.0	0.70
Na_2CO_3	0.97	0.58
$(NH_4)_2CO_3$	Trace	0.65
Li_2CO_3	0.53	0.39
$BaCO_3$	0.0	0.25
$CaCO_3$	0.0	0.28

[a] Methanol, 198 mmol; CH_3I, 24 mmol; catalyst, 3 mmol; CO_2 pressure, 8 MPa; temperature, 70 °C, time, 4 h.

carbonate (DMC) and dimethyl ether (DME) were formed. The results are summarized in Table 1. Among the catalysts listed in Table 1, the DMC yield is highest with K_2CO_3, in accordance with the previous results of Fang and Fujimoto.[23] Surprisingly, the activities of Na_2CO_3 and $(NH_4)_2CO_3$ are very low as compared with K_2CO_3. Although not shown in Table 1, the reaction was also conducted with nickel, copper and cobalt hydroxycarbonates. However, these compounds showed no activity for the reaction. Considering these results, an important factor for the reaction process is the basicity of the catalyst.[23] The difference in the reactivity among the carbonate salts could be well ascribed to the different basicities induced by various sizes of alkali metal ions. On the basis of these results, further experiments were conducted by the use of K_2CO_3.

Effects of reaction conditions

Fig. 1 illustrates the effect of CO_2 pressure upon the yields of DMC and DME in the presence of K_2CO_3. In the absence of CO_2, *i.e.* in nitrogen atmosphere, DMC and DME are formed in comparable quantities. Probably, DMC should be produced *via* the transesterification of carbonate ions of K_2CO_3. As the CO_2 pressure is raised, the amount of DME decreases monotonically. In contrast with this, the DMC formation shows two maxima near 4.5 and 8 MPa. It has been sometimes reported that, when CO_2 is used as a solvent or a reactant, reaction rates are maximal near the critical pressure (7.3 MPa) of CO_2.[22,27,30] Fig. 1 also indicates that high CO_2 pressures are not required for the DMC formation and supercritical conditions are detrimental for the reaction.

To elucidate the reason for the pressure dependence, the reaction mixture was visually examined by using a reactor

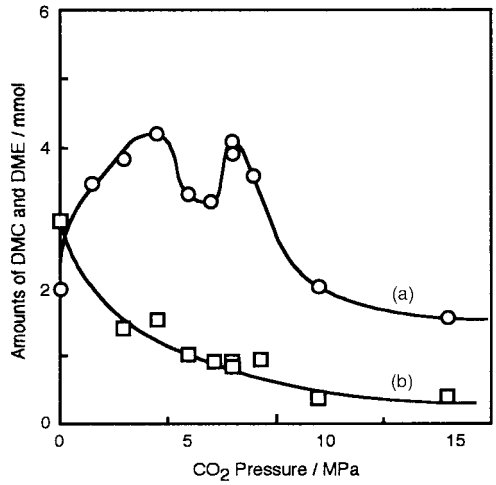

Fig. 1 Effect of CO_2 pressure upon the formation of (a) DMC and (b) DME. Methanol, 200 mmol; methyl iodide, 24 mmol; K_2CO_3, 3 mmol; temperature, 70 °C; time, 4 h.

attached with sapphire windows. Fig. 2 shows photographs of the reactant mixture taken at various CO_2 pressures in the absence of the catalyst. At low pressures of CO_2, liquid and gaseous CO_2 coexist in the reactor. With increasing the CO_2 pressure, the volume of the liquid phase increases. Probably, the increase in the liquid volume should arise from absorption of CO_2 into the liquid.[31] Around 14 MPa, CO_2 and the liquid take the form of a homogeneous phase. Fig. 3 plots the volume of the liquid phase estimated *vs.* the CO_2 pressure. The volume increases slightly with increasing the pressure up to 6 MPa and significantly increases above 10 MPa.

The solid catalyst did not affect the behavior of the reactant mixture and the volume of the liquid phase. In the presence of the catalyst, the reaction mixture is a triphasic system which consists of gaseous CO_2, liquid of the reactants mixture and the solid catalyst at CO_2 pressures below 14 MPa. Above 14 MPa, CO_2 and the liquid form the homogeneous phase, resulting in a biphasic reaction system. Hence, the decrease of DME formation with increasing the CO_2 pressure should be ascribed at least partly to the dilution effect of the reactants. On the other hand, the increase in the DMC yield observed up to 4.5 MPa should be ascribed to the absorption of CO_2, since both methanol and CO_2 are required for the DMC formation and the change in the liquid phase volume is small in this region of the CO_2 pressure. The decrease in the DMC yield observed between 4.5 and 7 MPa would result from the dilution effect. However, the DMC yield increases again near the critical pressure (7.4 MPa) of CO_2. This might be related to some effects of CO_2 on reactants and/or catalyst, as suggested previously by one of the present authors.[32] The decrease in the yield beyond 9 MPa should be again ascribed to the dilution effect.

The influence of other reaction conditions was also investigated at 8 MPa. Fig. 4 shows the effect of the amount of K_2CO_3 on the formation of DMC and DME. The amount of DMC formed increases in proportion with the amount of K_2CO_3 up to 3 mmol. Turnover number of DMC formation based on the amount of K_2CO_3 reaches 1.3, showing that the DMC formation is catalytic with respect to K_2CO_3. Above 3 mmol of K_2CO_3, the increase in the yield falls slightly. The formation of DME also increases with the increased amount of K_2CO_3; however, the extent of the increase is not appreciable as compared with the DMC formation.

Similar experiments were carried out with respect to methyl iodide (CH_3I). Fig. 5 shows the amounts of DMC and DEC produced relative to that of CH_3I. Both DMC and DME formation increase with an increased amount of CH_3I. The curve for DMC is slightly convex, while that for DME is concave. Hence the selectivity for DMC, DMC/(DMC + DME), is higher with smaller amounts of CH_3I.

Fig. 6 shows typical concentration–time profiles of the reactions. The curve of the DMC yield increases with time in a slightly convex manner, and the increase in the yield between 5 and 15 h is not substantial. These results mean that the rate of DMC formation decreases with time. This could be ascribed to the equilibrium of the reaction[33] or the deactivation of the catalyst. However, as shown in Fig. 4, the yield of DMC increases with an increased amount of K_2CO_3. Hence, the former possibility is excluded. To investigate the deactivation, the catalyst was extracted by water after the reaction and then reused for the next run. It was found that the activity of the reused catalyst was negligible. Thus, it was concluded that the catalyst was deactivated in the course of the reaction.

Reaction mechanism

For elucidation of the reaction mechanism, additional experiments were conducted at 8 MPa for 4 h. When lithium iodide was used instead of methyl iodide, neither DMC nor DME was

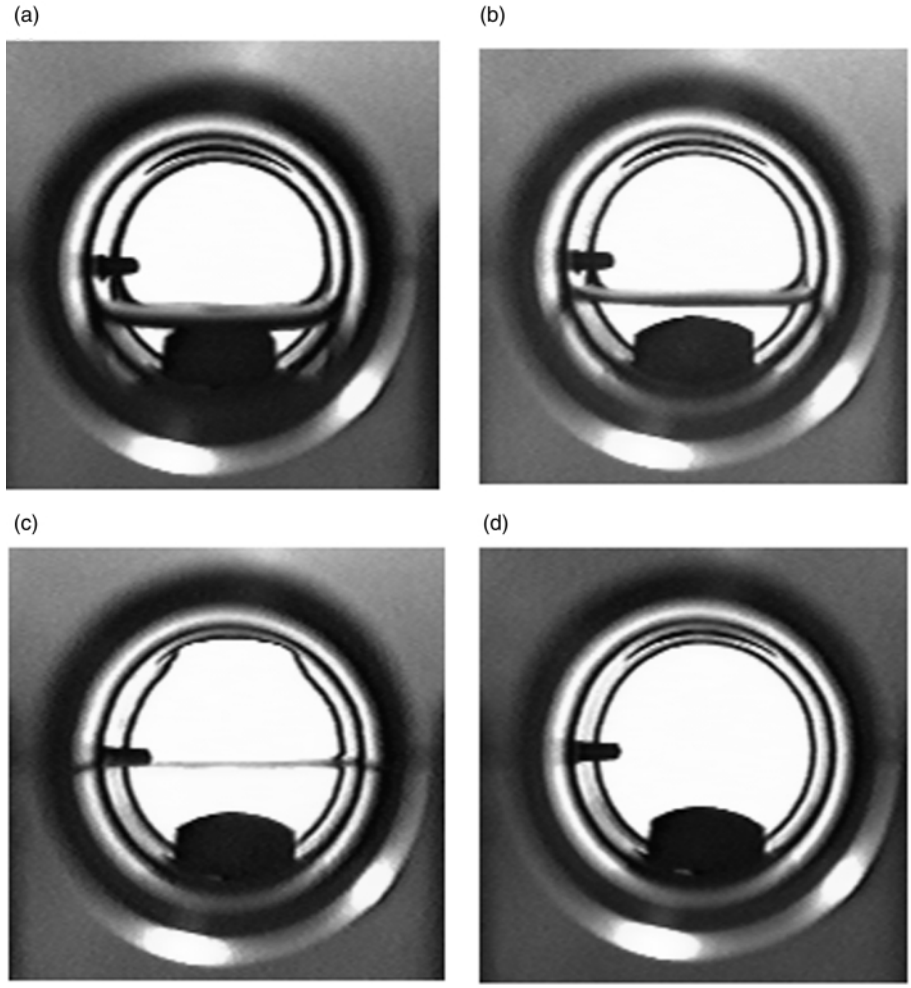

Fig. 2 Photographs of the reactant mixture taken at CO_2 pressure of (a) 1.5 MPa, (b) 8 MPa, (c) 12 MPa and (d) 15 MPa. For clarity, photographs were taken in the absence of the catalyst. The black object at the bottom of the reactor is a Teflon stirrer.

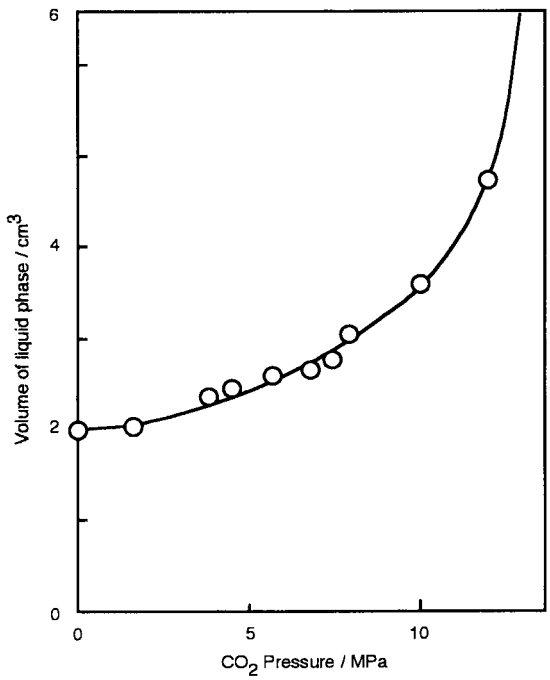

Fig. 3 Variation of the liquid phase volume with CO_2 pressure.

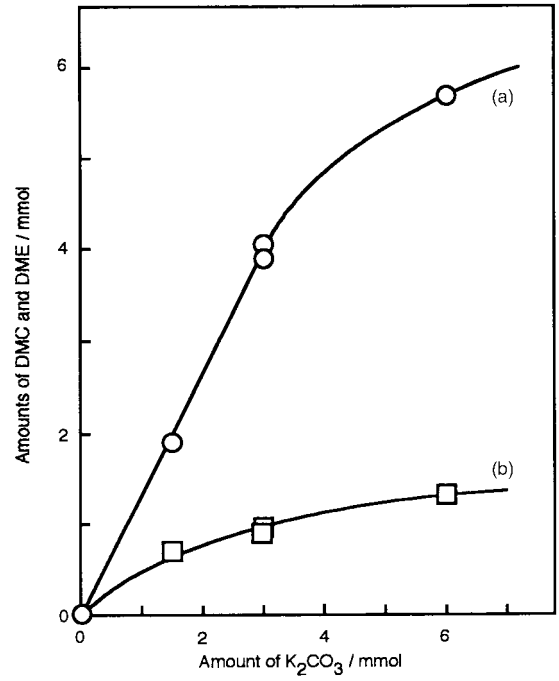

Fig. 4 The effect of the amount of K_2CO_3 on the formation of (a) DMC and (b) DME.

formed. As Fig. 5 shows, the amount of DMC formed does not exceed that of CH_3I. Furthermore, the amount of methyl iodide consumed was the same or larger as compared with the sum of the amounts of DMC and DME formed. When the amount of methyl iodide consumed was larger than the sum of the amounts of DMC and DME formed, the color of the liquid in the reactor changed from colourless to brown after the reaction. The

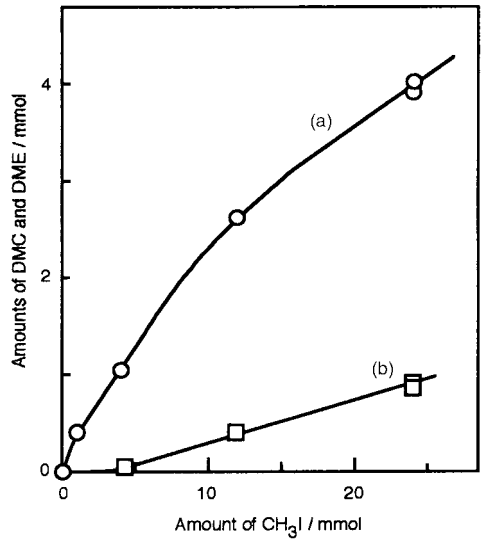

Fig. 5 The effect of the amount of CH_3I on the formation of (a) DMC and (b) DME.

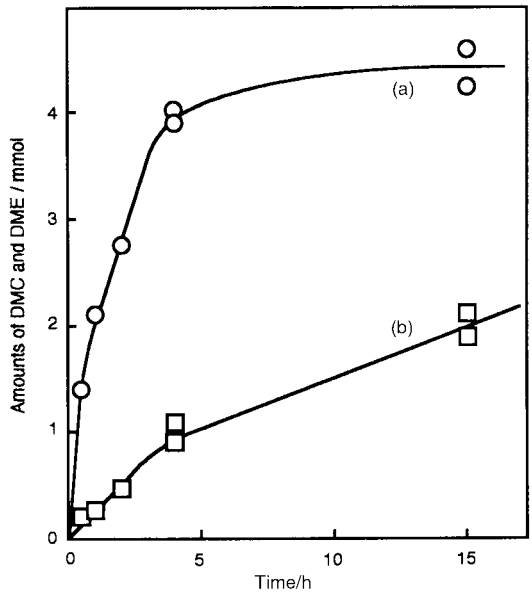

Fig. 6 Concentration–time profiles for (a) DMC and (b) DME formation.

excessive consumption of methyl iodide could have resulted from the decomposition of CH_3I to iodine. These observations strongly suggest that CH_3I is a reactant and not a promoter.

When the reaction was carried out with methyl iodide and ethanol or with ethyl iodide and methanol, ethyl methyl carbonate (EMC) was formed along with ethyl methyl ether. Neither DMC nor diethyl carbonate (DEC) was formed. The amounts of EMC produced were 2.4 mmol in the former case and 1.8 mmol in the latter. The reaction with CD_3OD and CH_3I produced $CD_3OCO_2CH_3$ and CD_3OCH_3, while $CD_3OCO_2CD_3$ and CD_3OCD_3 were not detected. These results also suggest that methyl iodide is merely one of the reactants for the reaction and not the promoter, and that DME is produced *via* the reaction between methanol and methyl iodide not *via* the dehydration of methanol. Furthermore, when dimethyl ether was used instead of methanol as a reactant, no DMC was detected. On the basis of these observations, it is concluded that the reactions of the DMC and DME formation proceed thorough parallel pathways, in which methyl iodide is incorporated in both the reactions.

The reaction mechanism could be represented as shown in Scheme 1. The hydroxy in methanol is abstracted by the base catalyst, producing the methoxy anion. This species reacts with

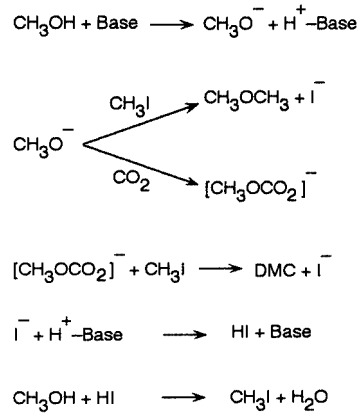

Scheme 1 Proposed reaction mechanism.

CH_3I or CO_2, leading to DME or methyl carbonate anion, respectively. The methyl carbonate anion successively reacts with CH_3I to give DMC. The iodo anion formed in the course of these elemental steps reacts with the proton abstracted by the base catalyst, and thus the catalyst is recycled. The product HI could further react with methanol reproducing CH_3I.

On the basis of the reaction mechanism proposed, CH_3I is recycled in the course of the reaction. However, the results obtained in the present study show that CH_3I acts as one of the reactants, not the promoter. This contradiction should be correlated with the catalyst deactivation. To study the deactivation, diffuse reflectance IR spectra of the catalyst were measured before and after the reaction for 15 h. Fig. 7 shows these spectra. In the spectrum obtained before the reaction [Fig.7(a)], strong bands assigned to carbonate species[34] are observed. It is seen that these bands disappeared after the reaction [Fig.7(b)]. Although not shown in Fig. 7, no band was observed in the OH stretching region for the catalyst after the reaction. These results strongly suggest that K_2CO_3 is converted to KI in the course of the reaction, as previously reported by Fang and Fujimoto.[23] As shown in Scheme 1, HI is cogenerated in the course of the elemental reactions. The product HI could react with methanol reproducing methyl iodide. However, this recycling would be difficult under the present reaction conditions, and the residual HI instead would react with K_2CO_3 [eqn. (1)]

$$K_2CO_3 + 2HI \longrightarrow 2KI + CO_2 + H_2O \quad (1)$$

Thus, the catalyst is deactivated in the course of the reaction. As described above, the turnover number of DMC formation based on the amount of K_2CO_3 reaches 1.3. This means that at least part of K_2CO_3 and CH_3I is recycled. Since the amounts of

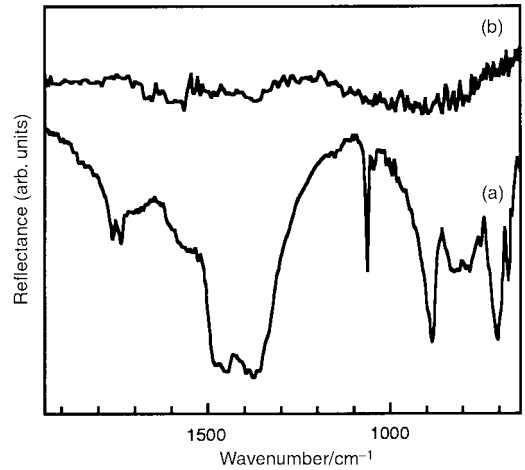

Fig. 7 Diffuse reflectance spectra for the K_2CO_3 catalyst obtained (a) before and (b) after the reaction, carried out at 8 MPa for 15 h.

K_2CO_3 and CH_3I recycled are low, $CD_3OCO_2CD_3$ was not detected in the products of the labeling experiment. Thus, CH_3I is essentially a reactant and not the promoter.

The formation of DME decreases monotonically with increase in CO_2 pressure (Fig. 1). The reason of this is partly ascribed to the dilution effect of the reactants, *i.e.* the variation of the volume of the reactants. However, as shown in Scheme 1, the formation of DMC and DME are considered to proceed through parallel pathways in which methyl carbonate anion reacts with CO_2 or CH_3I. Furthermore the ratio of CO_2/CH_3I would increase with increased CO_2 pressure. When this ratio increases, the relative rate of the DME formation would decrease. Thus, the decrease of the DME formation with increasing the CO_2 pressure should be ascribed to both the dilution effect and the changes of the CO_2/CH_3I ratio.

Reaction with other alcohols

Ethanol and ethyl iodide gave diethyl carbonate (DEC) as expected; however, the DEC yield was very small. Only 0.15 mmol of DEC was formed at 8 MPa for 4 h. Probably, the reactivities of ethanol and ethyl iodide were low compared with those of methanol and methyl iodide, causing the low yield of DEC. In the case of phenyl iodide/methanol or methyl iodide/phenol, no formation of methyl phenyl carbonate was observed. Also reaction between phenyl iodide and phenol failed to produce diphenyl carbonate. Hence, this reaction system is applicable only to the system of alkyl alcohols and alkyl halides. Reaction with ethylene glycol led to production of only a trace amount of cyclic carbonate instead of carbonate oligomer.

Conclusion

In the present study, the title reaction was carried out with potassium carbonate under various conditions. It was found that two maxima in the DMC formation were observed at 4.5 and 8 MPa of CO_2 pressure, while the formation of byproduct DME decreased monotonically with increasing the CO_2 pressure. DMC formation increases almost linearly with the amount of methyl iodide and potassium carbonate, when their concentration is low. Mechanistic studies suggest that DMC and DME are produced in parallel pathways and methyl iodide is involved in both the formation of DMC and DME. The catalyst is deactivated in the course of the reaction and methyl iodide is essentially a reactant rather than a promoter for the reaction. This is likely since the regeneration of methyl iodide from methanol and HI produced in the elemental reaction is difficult under the present reaction conditions. Other alcohols were found to have less reactivity than methanol for the reaction.

Experimental

The title reaction was carried out with various carbonates and hydroxycarbonate compounds as catalysts. These catalysts were used as purchased. All experiments were carried out in a 50 ml stainless steel autoclave. MeOH (200 mmol), the catalyst (3 mmol) and CH_3I (24 mmol) were charged into a reactor. Then CO_2 was injected to the reactor to *ca.* 0.8 MPa. The reactor was heated to 70 °C and then CO_2 was further injected to the desired pressure under stirring. An HPLC pump attached with a cooler was used for the supply of CO_2 and the pressure was monitored and controlled by a back pressure regulator.[35] After the reaction, the reactor was cooled to 0 °C and then the pressure was released by the back pressure regulator. The gases evolved were collected with a balloon. The gases collected and the liquid components in the reactor were analyzed by gas chromatography and mass spectrometry.

Visual observation of the reactant mixture was conducted with a 10 ml reactor attached with sapphire windows. Diffuse reflectance IR spectra of K_2CO_3 were measured with an IR spectrophotometer. Samples were diluted with KBr and a spectrum of KBr was used as background.

References

1 P. G. Jessop, T. Ikariya and R. Noyori, *Science*, 1995, **269**, 1065.
2 X. D. Xu and J. A. Moulijin, *Energy Fuels*, 1996, **10**, 305.
3 P. G. Jessop and W. Leitner, in *Chemical Synthesis Using Supercritical Fluids*, ed. P. G. Jessop and W. Leitner, Wiley-VCH, Weinheim, 1999, ch. 4.7, p. 351.
4 P. G. Jessop, T. Ikariya and R. Noyori, *Chem. Rev.*, 1999, **99**, 475.
5 M. A. Pacheco and C. L. Marshall, *Energy Fuels*, 1997, **11**, 2.
6 M. Aresta and E. Quaranta, *CHEMTECH*, 1997, **27**, 32.
7 A. A. Shaikh and S. Sivaram, *Chem. Rev.*, 1996, **96**, 951.
8 Y. Ono, *Appl. Catal. A.*, 1997, **155**, 133.
9 Y. Ono, *CATTECH*, 1997, **1**, 31.
10 Y. Ono, *Catal. Today*, 1997, **35**, 15.
11 P. Tundo and M. Selva, *Chemtech*, 1995, 31.
12 A. Bomben, M. Selva and P. Tudo, *J. Chem. Res. (S)*, 1997, 448.
13 P. Tundo, M. Selva and A. Bomben, *Org. Synth.*, 1999, **76**, 169.
14 A. Perosa, M. Selva and P. Tundo, *Synlett*, 2000, **7**, 71.
15 U. Romano, R. Tesei, M. M. Mauri and P. Rebora, *Ind, Eng, Chem. Prod. Res. Dev.*, 1980, **19**, 396.
16 K. Nishihira, T. Matsuzaki and S. Tanaka, *Shokubai*, 1995, **37**, 68.
17 T. Matsuzaki and A. Nakamura, *Catal. Surv. Jpn.*, 1997, **1**, 77.
18 J. Kizlink, *Collect. Czech. Chem. Commun.*, 1993, **58**, 1399.
19 J. Kizlink and I. Pastucha, *Collect. Czech. Chem. Commun.*, 1994, **59**, 2116.
20 J. Kizlink and I. Pastucha, *Collect. Czech. Chem. Commun.*, 1995, **60**, 687.
21 N. S. Isaacs, B. O. Sullivan and C. Verhaelen, *Tetradedron*, 1999, **55**, 11949.
22 T. Zhao, Y. Han and Y. Sun, *Fuel Processing Tech.*, 2000, **62**, 187.
23 S. Fang and K. Fujimoto, *Appl. Catal. A*, 1996, **142**, L1.
24 K. Tomishige, T. Sakaihori, Y. Ikeda and K. Fijimoto, *Catal. Lett.*, 2000, **58**, 225.
25 Y. Ikeda, T. Sakaihori, K. Tomishighe and K. Fujimoto, *Catal. Lett.*, 2000, **66**, 59.
26 K. Tomishige, Y. Ikeda, T. Sakaihori and K. Fujimoto, *J. Catal.*, 2000, **192**, 355.
27 T. Sakakura, Y. Saito, M. Okano, J. C. Choi and T. Sako, *J. Org. Chem.*, 1998, **63**, 7095.
28 T. Sakakura, J. C. Choi, Y. Saito, T. Masuda, T. Sako and T. Oriyama, *J. Org. Chem.*, 1999, **64**, 4506.
29 T. Sakakura, J. C. Choi, Y. Saito and T. Sako, *Polyhedron*, 2000, **19**, 573.
30 H. Kawanami and Y. Ikushima, *Chem. Commun.*, 2000, 2089.
31 I. Souvignet and S. V. Olesik, *J. Phys. Chem.*, 1995, **99**, 16800.
32 M. Arai, Y. Nishiyama and Y. Ikushima, *J. Supercrit. Fluids*, 1998, **13**, 149.
33 N. Cohen and S. W. Benson, *Chem. Rev.*, 1993, **93**, 2419.
34 L. H. Little, *Infrared Spectra of Adsorbed Species*, Academic Press, New York, 1966, p. 76.
35 B. M. Bhanage, Y. Ikushima, M. Shirai and M. Arai, *High Pressure Research*, in press.

Alkylation of dihydroxybenzenes and anisole with methyl-*tert*-butyl ether (MTBE) over solid acid catalysts

G. D. Yadav,* P. K. Goel and A. V. Joshi

Chemical Engineering Division, University Department of Chemical Technology (UDCT), Matunga, Mumbai - 400 019, India. E-mail: gdy@udct.ernet.in; gdyadav@yahoo.com

Received 8th January 2001
First published as an Advance Article on the web 26th March 2001

The synthesis of *tert*-butylated dihydroxy and alkoxy benzenes from catechol, resorcinol and anisole, with MTBE has been carried out in presence of variety of solid acid catalysts. The current work dealt with the efficacy of various solid acid catalysts in the alkylation of substituted benzenes and MTBE. MTBE is a better *tert*-butylating agent than isobutylene and *tert*-butyl alcohol. 20% w/w dodecatungstophosphoric acid (DTP) supported on K10 montmorillonite clay was found to be very effective in comparison with other solid acid catalysts used. A complete theoretical and experimental analysis is presented for the model studies of catechol/anisole with MTBE. The reaction follows a typical second order kinetics at a fixed catalyst loading, with weak adsorption of both the species. The energy of activation for catechol alkylation was found to be 8.86 kcal mol^{-1}, which was low and suggested that intraparticle diffusional resistance would set in for larger particle size. For anisole alkylation the energy of activation was 17.36 kcal mol^{-1} indicating that the reaction is intrinsically kinetically controlled.

Introduction

Alkylation of dihydroxy- and alkoxy-benzenes is a very important reaction from the industrial point of view since *tert*-butylated dihydroxy- and alkoxy-benzenes are used as anti-oxidants, dye developers and stabilisers for fats, oils, plastic, rubbers *etc*.[1] For instance, 4-*tert*-butylcatechol is used as a polymerization inhibitor during the manufacture and storage of monomers such as styrene and butadiene. Also, 4-alkyl-catechols are less toxic as compared to biologically active 3-alkylcatechols.[2] Commercial alkylation of aromatic compounds requires severe conditions since it proceeds through electrophilic substitution. The conventional acid catalysts like $AlCl_3$, $ZnCl_2$ and $FeCl_3$ *etc.*, are required to be employed in excessive amounts to carry out such reactions.[3] The use of these catalysts leads to many problems concerning handling, safety, corrosion and waste disposal.

The alkylation of catechol to obtain 4-*tert*-butylcatechol has been carried out by using Amberlyst-15,[2] silica-alumina,[4] sulfuric acid,[5] triflic acid,[6] acidic zeolites[7] and activated clay.[8] Alkylation of hydroquinone has been reported by Yadav and Doshi using dodecatungstophosphoric acid supported on K10 clay.[9] Similarly the alkylation of anisole to yield 4-*tert*-butylanisole has been carried out in presence of $ZrCl_4$[10] and trifluoroacetic acid.[11] The alkylation of anisole and phenol was carried out with *tert*-butyl acetate in presence of H_2SO_4[12] and with *tert*-butyl nitrate using $SnCl_4$.[13]

The alkylation of dihydroxybenzenes and anisole was thus considered as an important problem necessitating use of different solid acid catalysts and feedstocks. Owing to the problems associated with unavailability, transportation and handling of isobutylene, particularly for usage in low-tonnage fine chemical and speciality manufacture, it is advantageous to generate pure isobutylene *in situ*. MTBE and *tert*-butyl alcohol are attractive alkylating agents, which eliminate the problems associated with the transportation and storage of isobutylene and/or C-4 fractions. The dehydration of *tert*-butayl alchol generates isobutylene, but the co-product is water, which affects the activity of some of the catalysts. The *in situ* cracking of MTBE, which is more reactive, provides a convenient source of pure isobutylene required for alkylation with methanol as the co-product which can be reused easily. We have shown earlier that the rates of alkylation with MTBE are greater than those with *tert*-butyl alcohol.[9] The cracking of MTBE for the generation of isobutylene has been discussed.[14–17] Heteropoly acids (HPA) supported on clays have shown superior activity as catalyst in comparison to others in the alkylation and etherification reactions.[18–20]

It is thus clear that there is tremendous scope for devising a new catalytic process for the synthesis of *tert*-butylated catechols, resorcinol and anisole. This work deals with the alkylation of catechol, resorcinol and anisole with MTBE over a variety of catalysts including development of a kinetic model.

Experimental

Chemicals

MTBE was obtained from Texas Petrochemicals Corp., USA. K10 clay and filtrol-24 were obtained from Fluka, Germany. Zirconium oxychloride, dodecatungstophosphoric acid, dodecatungstosilicic acid, zinc chloride, 1,4-dioxane and anisole were obtained from M/s s.d. Fine Chemical Ltd., Mumbai, India. Catechol, 4-*tert*-butylcatechol and resorcinol were procured from Loba Chemie, Mumbai, India. All chemicals were analytical grade reagents and were used without further

Green Context

The synthesis of a range of stabilisers and anti-oxidants relies on the Friedel–Crafts alkylation of phenols. Clean processes have been developed, in which the homogeneous acid catalyst is replaced with a heterogeneous solid acid catalyst, leading to simpler and cleaner work-up, and the potential for catalyst reuse. This example shows the promise of combining heteropolyacids onto mineral supports as catalysts for such reactions, giving good conversions and selectivities. ***DJM***

 DOI: 10.1039/b100298h

purification. The catalysts used for the reaction were dried at 110 °C for 2 h before use.

Catalysts

Dodecatungstophosphoric acid (DTP)/K-10 was prepared by a well established procedure in our laboratory.[20] A measured quantity of montmorillonite clay (K10) was taken and dried in an oven for 2 h and dodecatungstophosphoric acid dissolved in methanol was added dropwise, with stirring by the so called incipient wetness technique. The catalyst was then dried in an oven for 2 h and subsequently calcined at 285 °C for 3 h. Similarly other heteropolyacids such as dodecatungstosilicic acid (DTS) were impregnated on K10 monmorillonite. Sulfated zirconia was also prepared by an established procedure.[21]

Reaction procedure

All experiments were carried out in a 100 ml stainless steel autoclave manufactured by Parr instruments Co, USA. A four bladed-pitched turbine impeller was used for agitation. The temperature was maintained at ±1 °C of the desired value with the help of an in-built proportional-integral-derivative (PID) controller. Predetermined quantities of reactants and the catalyst were charged into the autoclave and the temperature was raised to the desired value.

In a typical experiment, 0.05 mol of catechol or anisole and 0.15 mol of MTBE were used and 1,4-dioxane was added to make up the total volume to 50 cm^3. A typical catalyst loading of 0.75 and 1.5 g were used for catechol and anisole, respectively, while the corresponding temperatures were 150 and 170 °C. The reaction mixture was then allowed to reach the desired temperature and the initial/zero time sample was collected. Agitation was then commenced at a particular speed. Samples were withdrawn periodically for analysis.

Analysis

Analysis of the reaction mixture was done on a high-pressure liquid chromatogram (Tosho) for catechol, 4-*tert*-butylcatechol and 3,5-di-*tert*-butylcatechol under the following conditions: column = C-18 (reverse phase), mobile phase = methanol–water (70 : 30), detector wavelength = 280 nm, flow rate of mobile phase = 1 ml min^{-1}.

For anisole, analysis was done using GC (Chemito 8510) using a 10% OV-17 (2 m × 3.18 mm) column with FID.

The samples were analysed for anisole, 4-*tert*-butylanisole, 2-*tert*-butylanisole, 2,4-di-*tert*-butylanisole and 2,6-di-*tert*-butylanisole. Identification of products was done by GC–MS and by matching the retention time of reaction products to that of authentic compounds in all cases.

Reaction scheme

In the presence of an acid catalyst, MTBE cracks into isobutylene and methanol. Isobutylene thus produced reacts *in situ* with catechol and resorcinol to give 4-*tert*-butylcatechol (4-TBC), 3,5-di-*tert*-butylcatechol (3,5-DTBC) and 4-*tert*-butylresorcinol (4-TBR) whereas for anisole, 4-*tert*-butylanisole (4-TBA), 2-*tert*-butylanisole (2-TBA), 2,4-di-*tert*-butylanisole (2,4-DTBA) and 2,6-di-*tert*-butylanisole (2,6-DTBA) are obtained. Further, dimers and trimers of isobutylene can also be formed as side products. The reaction network is shown in Fig. 1.

Results and discussion

Efficacies of various catalysts

Various solid acid catalysts were employed to assess their efficacy in this reaction. Preliminary experiments had indicated that anisole alkylation required higher catalyst loading as well as temperature for significant conversions, *vis-à-vis* dihydroxybenzenes. A 0.015 and 0.03 g cm^{-3} loading of catalyst based on the organic volume of the reaction mixture were taken for catechol and anisole at 150 and 170 °C, respectively. The mole ratio of catechol or anisole to MTBE was kept at 1 : 3, with an agitational speed of 800 rpm. The catalysts used were K10 montmorillonite, 20% DTP/K10, 20% DTS/K10, sulfated zirconia and filtrol-24. Table 1 shows conversion of catechol and anisole, the limiting reactant, for the various catalysts. 20% DTP/K10 gave good conversion of catechol and anisole compared to other catalysts. The typical product distribution, as the reaction progresses, is given in Table 2.

A good cracking catalyst and a poor alkylation catalyst would result in loss of the generated isobutylene. A reverse phenomenon would result in poor yield of the required alkylated product. It was therefore necessary that the best catalyst should give a reasonable activity for the cracking of MTBE as well as the alkylation. Further, it is also essential that the rate of alkylation is faster than that of oligomerisation of the isobutylene generated *in situ* to get maximum selectivity of the alkylated product.

The use of MTBE as a butylating agent is advantageous. MTBE cracking starts beyond 75 °C in a significant way and no *O*-alkylated product is formed in the case of dihydroxybenzenes. Whatever, isobutylene generated *in situ* is consumed leading to *C*-alkylated product and no free isobutylene in the gas phase is detected nor does any oligomerisation take place at low temperatures. The co-product methanol is recyclable. The vapour pressure data at 150 °C for methanol showed that the pressure corresponded to that of the methanol partial pressure without any isobutylene in the gas phase. On cooling the reactor to room temperature the pressure immediately went down to atmospheric pressure which also suggested that the methanol in vapour phase was condensed and no noticeable isobutylene was in the vapour phase. In another set of experiments we had already proved, that in the absence of any substrate, the pressure rise is substantial due to cracking of MTBE to methanol and isobutylene.[19,20] In earlier studies, we had noticed that no *O*-alkylated product is formed beyond 50 °C when *p*-cresol was alkylated with isobutylene in the presence of sulfated zirconia and UDCaT-1 as catalysts,[21,22] since the rate of *C*-alkylation was very much faster than that of oligomerisation. In the present case, all standard experiments were done at 150 and 170 °C for catechol and anisole, respectively and the analysis showed no *O*-alkylated product was formed during alkylation of catechol or resorcinol.

Effect of speed of agitation

In order to assess the role of external mass transfer on the reaction rate, the effect of the speed of agitation was studied. The speed of agitation was varied from 800 to 1200 rpm (Fig. 2). It was observed that the conversion of catechol and anisole was practically the same in all cases without any change in selectivity. Thus, it was shown that external mass transfer effects did not influence the reaction. Hence, all further reactions were carried out at 800 rpm. A theoretical analysis of the assessment of external mass transfer resistance is given to support this observation. Details of this theory for general slurry reactions are given elsewhere.[21]

For catechol alkylation, when the maximum catalyst loading used (0.03 g cm^{-3}) for a particle size (d_p) of 0.006 cm, in the

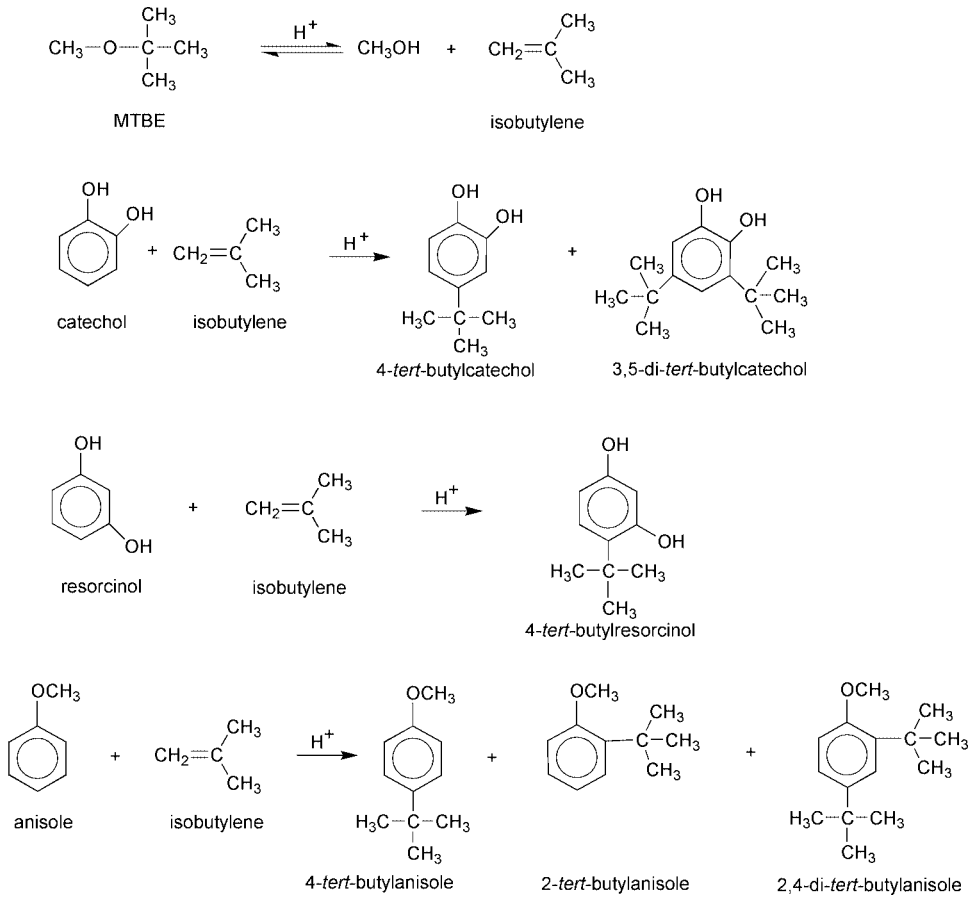

Fig. 1 Reaction scheme for alkylation of catechol, resorcinol and anisole with MTBE.

Table 1 Effects of various catalysts on conversion of catechol/anisole

	Conversion (%)		Selectivity (%)				
Catalyst	Catechol[a]	Anisole[b]	4-TBC	3,5-DTBC	4-TBA	2-TBA	2,4-DTBA
DTP	85	75	92	8	49	20.3	30.7
DTP(20%)/K10	42	59.5	82	18	57	22	21
DTS(20%)/K10	38	55.4	75	25	53	24	23
Filtrol-24	39	57	78	22	56	13.5	30.4
K10	28	32.7	87	13	69.4	18.2	12.4
Sulfated ZrO_2	22	17	88	12	70.4	23.7	5.9

[a] Catechol:MTBE = 1:3, catalyst loading = 0.015 g cm^{-3}, temperature = 150 °C, speed of agitation = 800 rpm, solvent = 1,4-dioxane, time = 4 h; autogeneous pressure = 0.7 MPa. [b] Anisole:MTBE = 1:3, catalyst loading = 0.03 g cm^{-3}, temperature = 170 °C, speed of agitation = 800 rpm, solvent = 1,4-dioxane, time = 5 h; autogeneous pressure = 1 MPa, DTP: dodecatungstophosphoric acid, DTS: tungstosilicic acid; 4-TBC: 4-*tert*-butylcatechol, 3,5-DTBC: 3,5-di-*tert*-butylcatechol, 4-TBA: 4-*tert*-butylanisole, 2-TBA: 2-*tert*-butyl anisole, 2,4-DTBA: 2,4-di-*tert*-butylanisole.

Table 2 Distribution of various products

	Conversion (%)		Selectivity (%)				
Time/min	Catechol[a]	Anisole[b]	4-TBC	3,5-DTBC	4-TBA	2-TBA	2,4-DTBA
15	4.1	18.5	83.5	16.5	66.1	25.7	8.2
30	7.9	30.6	83.5	16.5	64.8	25.1	10.1
60	14.7	44.0	83.0	17.0	63.1	23.7	13.2
90	19.9	48.5	83.0	17.0	61.8	23.3	14.9
120	24.3	51.4	83.0	17.0	61.1	22.8	16.1
180	34.0	53.9	82.5	17.5	60.7	22.2	17.1
240	42.0	56.2	82.0	18.0	59.0	22.2	18.8
300	—	59.5	—	—	57.0	22.0	21.0

[a] Catechol:MTBE = 1:3, catalyst = DTP(20%)/K10, temperature = 150 °C, speed of agitation = 800 rpm, solvent = 1,4-dioxane; autogeneous pressure = 0.7 MPa. [b] Anisole:MTBE = 1:3, catalyst = DTP(20%)/K10, temperature = 170 °C, speed of agitation = 800 rpm, solvent = 1,4-dioxane; autogeneous pressure = 1 MPa.

current studies, a_p = 18.75 cm^2 cm^{-3} liquid phase. The liquid phase diffusivity values of the reactants A (catechol) and B (MTBE), denoted by D_{AB} and D_{BA}, were calculated by using the Wilke–Chang equation[23] at 150 °C as 6.33 × 10^{-5} and 1.37 × 10^{-5} cm^2 s^{-1}, respectively. The solid–liquid mass transfer coefficients for both A and B were calculated from the limiting value of the Sherwood number (*e.g.*, Sh-A = $k_{SL\text{-}A}d_p/D_{AB}$) of 2. The actual Sherwood numbers are typically higher by order of magnitude in well agitated systems but for conservative estimations a value of 2 is taken.[21,24] The solid–liquid mass transfer coefficients $k_{SL\text{-}A}$ and $k_{SL\text{-}B}$ values were obtained as 2.11 × 10^{-2} and 4.56 × 10^{-3} cm s^{-1}, respectively. The initial rate of reaction was calculated from the conversion profiles. A typical calculation shows that for a typical initial rate of reaction was calculated as 4.38 × 10^{-8} gmol cm^{-3} s^{-1}. Therefore, putting the appropriate values in eqn. (1) (see ref. 25 for derivation of the following equation):

$$1/r_{obs} >> \frac{1}{k_{SL-A}a_p[A_0]} \text{ and } \frac{1}{k_{SL-B}a_p[B_0]} \quad (1)$$

i.e., 2.28 × 10^7 >> 2.53 × 10^3 and 3.90 × 10^3

Similarly, for anisole alkylation, calculations were performed to check the influence the effect of external mass resistance by putting the appropriate values in eqn. (1): *i.e.*, 5.88 × 10^6 >> 1.43 × 10^3 and 1.88 × 10^3.

The above inequality demonstrates that there is an absence of resistance due to the solid–liquid external mass transfer for both the species A and B and the rate may be either surface reaction controlled or intra-particle diffusion controlled. Therefore, the effects of catalyst loading at a fixed particle size and temperature were studied to evaluate the influence of intra-particle resistance.

Effect of catalyst loading

In the absence of external mass transfer resistance, the rate of reaction is directly proportional to catalyst loading based on the entire liquid phase volume. The catalyst loading was varied over the range 0.01–0.03 g cm^{-3} and 0.006–0.03 g cm^{-3} on the basis of total volume of the reaction mixture for catechol and anisole, respectively. Fig. 3 shows the effect of catalyst loading on the conversion of catechol and anisole. The conversion increases with increasing catalyst loading, which is obviously due to the proportional increase in the number of active sites. All further experiments were carried out at 0.015 and 0.03 g cm^{-3} of catalyst loading for catechol and anisole, respectively.

It is possible to calculate the values of [A_S] and [B_S] the external surface concentration of A and B, respectively [eqn. (2)]:

$$k_{SL\text{-}A}a_p\{[A_0] - [A_S]\} = r_{obs} \text{ at steady state} = 4.38 \times 10^{-8} \text{ gmol cm}^{-3} \text{ s}^{-1} \quad (2)$$

Thus putting in the appropriate values, it is seen that [A_S] ≈ [A_0], similarly [B_S] ≈ [B_0]. Thus, any further addition of catalyst is of no further consequence for external mass transfer.

Proof of absence of intra-particle resistance

The average particle diameter of the catalyst used in the reactions was 0.006 cm and thus a theoretical calculation was done based on the Wiesz–Prater criterion to assess the influence of intra-particle diffusional resistance.[26]

According to the Wiesz–Prater criterion, the dimensionless parameter C_{wp} which represents the ratio of the intrinsic reaction rate to intra-particle diffusion rate, can be evaluated from the observed rate of reaction, the particle radius (R_p), effective diffusivity of the limiting reactant (D_e) and concentration of the reactant at the external surface of the particle.

(i) If $C_{wp} = -r_{obs}\rho_p R_P^2/D_e[A_s] >> 1$, then the reaction is limited by severe internal diffusional resistance,

(ii) If $C_{wp} << 1$, then the reaction is intrinsically kinetically controlled.

The effective diffusivity of catechol ($D_{e\text{-}A}$) inside the pores of the catalyst was obtained from the bulk diffusivity (D_{AB}), porosity (ε) and tortuosity (τ) as 8.018 × 10^{-6} cm^2 s^{-1} where $D_{e\text{-}A} = D_{AB}\varepsilon/\tau$. In the present case, the value of C_{wp} was calculated as 3.93 × 10^{-5} for the initial observed rate and therefore the reaction is intrinsically kinetically controlled. Similarly, calculations were done for anisole and value of C_{wp} was calculated as 1.72 × 10^{-4}, which is also much less than unity and therefore proves that the reaction is intrinsically

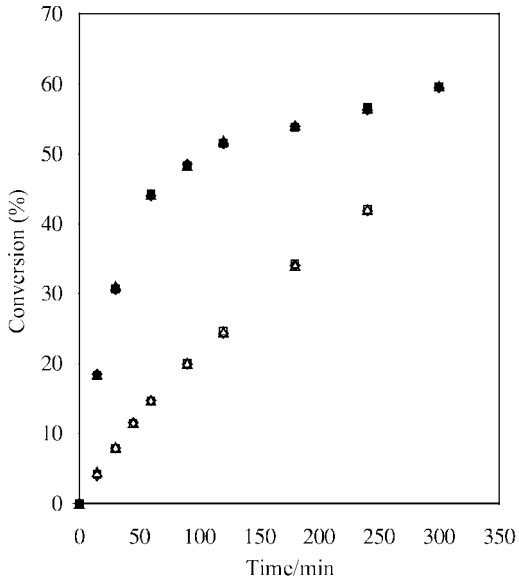

Fig. 2 Effect of speed of agitation: catechol:MTBE = 1:3, catalyst loading = 0.015 g cm^{-3}, temperature = 150 °C, time = 4 h; (◇) 800, (□) 1000, (△) 1200 rpm; anisole:MTBE = 1:3, catalyst loading = 0.03 g cm^{-3}, temperature = 170 °C, time = 5 h; catalyst = DTP(20%)/K10, solvent = 1,4-dioxane; (◆) 800, (■) 1000, (▲) 1200 rpm.

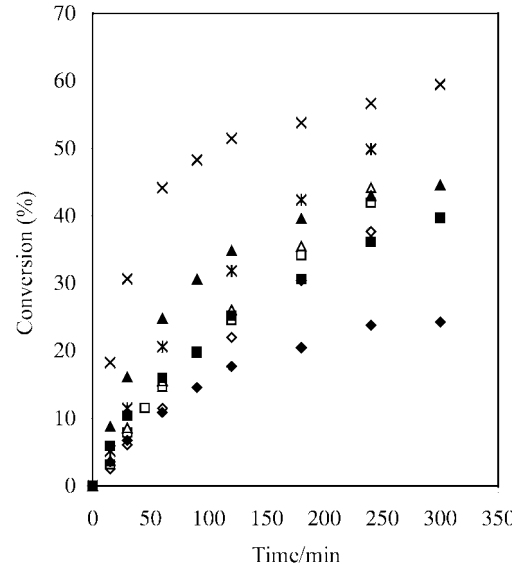

Fig. 3 Effect of catalyst loading: catechol:MTBE = 1:3, temperature = 150 °C, time = 4 h; (◇) 0.01, (□) 0.015, (△) 0.02, (*) 0.03 g cm^{-3}; anisole:MTBE = 1:3, temperature = 170 °C, time = 5 h; (◆) 0.01, (■) 0.015, (▲) 0.02 (×) 0.03 g cm^{-3}. Catalyst = DTP(20%)/K10, solvent = 1,4-dioxane, speed = 800 rpm.

kinetically controlled. A further proof of the absence of the intra-particle diffusion resistance was obtained through the study of the effect of temperature and this will be discussed later.

Effect of DTP loading on K10

In order to investigate the change in selectivity of alkylated products, different amounts of DTP were loaded on K10 montmorillonite. With an increase in DTP loading from 5 to 40% w/w of K10, the conversion of catechol also increased (Fig. 4). There was some formation of oligomers of isobutylene. However, further experiments were done with 20% DTP/K10 for which the selectivity to the mono-alkylated product was very high.

Since 20% DTP/K10 was the best catalyst, the effects of various parameters on conversion and yields were studied with this catalyst which has already been fully characterised by us[19,20] and a brief summary is provided here. The surface areas of the catalysts measured by the nitrogen BET method for K10 montmorillonite and DTP/K10 were found to be 230 and 107 $m^2\ g^{-1}$, respectively. Since both the catalysts were pre-treated in similar way prior to analysis, the reduction in surface area of DTP/K10 may be due to the blockage of the smaller pores by the active species. It appears that the active species are held in a few junctions of such dimensions from where the access to smaller pores is denied, thereby leading to the decrease in accessible surface area. The average particle size of both K10 and DTP/K10, as determined by image analysis, was in the range of 60 μm. XRD studies of DTP/K10 indicate that in the impregnation process, the clay lost some of its crystallinity compared to K10. The cation exchange capacity (CEC) of the catalyst DTP/K10 was observed to be higher than that of K10. This may be due to some additional surface protons, which arise from hetero-polyacid impregnation, which may be readily available for exchange reaction. We have earlier reported[19] that on the basis of the actual quantity of DTP loaded on the support in comparison with the same unloaded catalyst or the support K10 alone, the turnover frequency is greater for the supported catalyst. Thus, there is a synergism between DTP and K10 leading to higher activity. For DTP/K10 there are many dispersed particles on the surface of the support K10 as revealed by SEM photomicrographs. FTIR studies of K10 showed Si–O and Si–O–Al linkages and that OH groups are bonded to the Al atoms, whereas in DTP/K10, the presence of H_3O^+ (Bronsted acidity) and linkage of phosphorus. (P–O–P) was observed.

Effect of mole ratio

The mole ratio of catechol : anisole to MTBE was changed from 1 : 1 to 1 : 5 under otherwise similar conditions. The conversion of catechol and anisole was only 17 and 43% when the catechol and anisole to MTBE mole ratio was 1 : 1 (Fig. 5). With an increase in mole ratio (1 : 5), the conversion of catechol and anisole increased to 57 and 63%, respectively. All further experiments were carried out at catechol or (anisole) to MTBE mole ratio of 1 : 3.

Effect of temperature

The effect of temperature on conversion under otherwise similar conditions was studied in the temperature range 130–170 and 140–185 °C for catechol and anisole, respectively (Fig. 6). The conversion was found to increase substantially with increase in temperature. All further experiments were carried out at 150 and 170 °C, respectively, for catechol and anisole.

Effect of reusability of 20% DTP/K10

The reusability of 20% DTP/K10 was tested by employing it three times. After each run the catalyst was washed thoroughly with methanol and dried in an oven at 120 °C for 2 h. The results are shown in Fig. 7. In the presence of fresh catalyst, the conversion of catechol and anisole was 42 and 59%, respectively. During the third run, the conversion of catechol and anisole decreased to 31 and 41%, respectively. The catalyst was filtered off and then dried and weighed after each run to find that there was up to 10% loss of catalyst during filtration due to attrition (no make-up catalyst was added). Thus the catalyst was not deactivated and was reusable.

When a heteropoly acid (HPA) such as dodecatungstophosphoric acid (DTP) is supported on K10, a high activity of the catalyst is obtained which is due to the presence of the HPA on the support. We had reported earlier if the HPA is physically

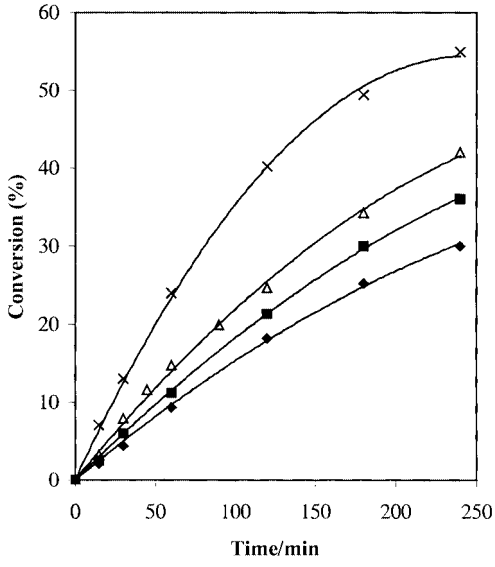

Fig. 4 Effect of DTP loading on K10; catechol : MTBE = 1 : 3, catalyst loading = 0.015 g cm^{-3}, temperature = 150 °C, speed of agitation = 800 rpm, solvent = 1,4-dioxane, time = 4 h; (◆) 5, (■) 10, (△) 20, (×) 40% DTP/K10.

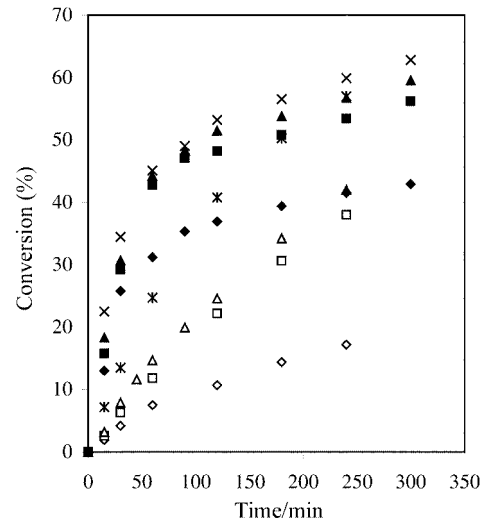

Fig. 5 Effect of mole ratio: catechol : MTBE, catalyst loading = 0.015 g cm^{-3}, temperature = 150 °C, time = 4 h; (◇) 1 : 1, (□) 1 : 2, (△) 1 : 3, (∗) 1 : 5; anisole : MTBE, catalyst loading = 0.03 g cm^{-3}, temperature = 170 °C, time = 5 h; (◆) 1 : 1, (■) 1 : 2, (▲) 1 : 3, (×) 1 : 5. Catalyst = DTP(20%)/K10, speed = 800 rpm, solvent = 1,4-dioxane.

adsorbed on the surface then the catalyst cannot be reused because of loss of active sites during usage of catalyst. It was found that the DTP/K10 showed consistent activity to a minimum of three runs even in the presence of highly polar solvents such as methanol and 1,4-dioxane because DTP is chemically bonded to the support. There was no leaching of DTP from the support. We have also confirmed the stability of this catalyst in other systems.[17–19]

It was necessary to study the stability of DTP on K10 in order to reuse the catalyst. Any leaching of the active sites from the catalyst would render it commercially unattractive. It was therefore decided to verify the possibility of leaching of DTP from the support under severe conditions.[20]

DTP can be analysed by the heteropoly blue which is observed when it is made to react with a mild reducing agent

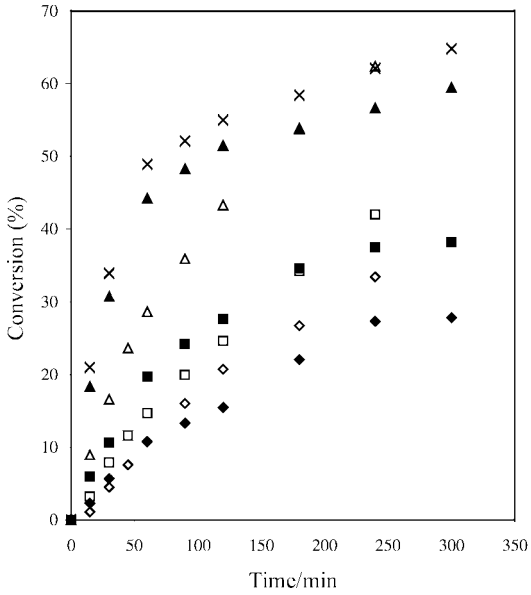

Fig. 6 Effect of temperature: catechol : MTBE = 1 : 3, catalyst loading = 0.015 g cm^{-3}, time = 4 h; (◇) 130, (□) 150, (△) 170 °C; anisole : MTBE = 1 : 3, catalyst loading = 0.03 g cm^{-3}, time = 5 h; (◆) 140, (■) 155, (△) 170, (×) 185 °C. Catalyst = DTP(20%)/K10, solvent = 1,4-dioxane, speed = 800 rpm.

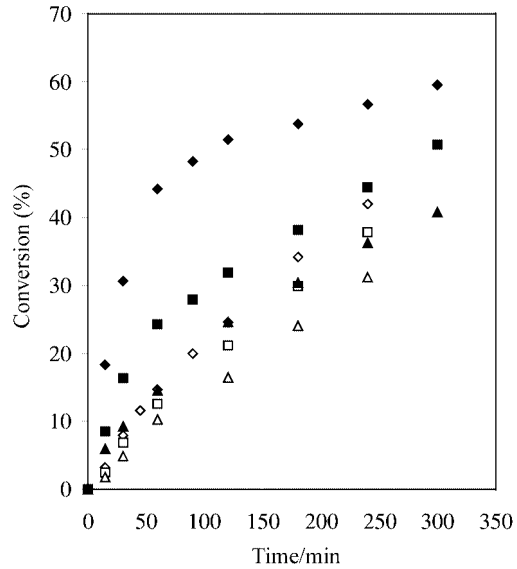

Fig. 7 Effect of reusability of catalyst: catechol : MTBE = 1 : 3, catalyst loading = 0.015 g cm^{-3}, temperature = 150 °C, time = 4 h; (◇) fresh, (□) 1st, (△) 2nd reuse; anisole : MTBE = 1 : 3, catalyst loading = 0.03 g cm^{-3}, temperature = 170 °C, time = 5 h; (◆) fresh, (■) 1st, (▲) 2nd reuse. Catalyst = DTP(20%)/K10, solvent = 1,4-dioxane, speed = 800 rpm.

such as ascorbic acid. Standard samples amounting to 1–5% of DTP in water were prepared. To 10 ml of the above samples 1 ml of 10% ascorbic acid was added. The mixture was diluted to 25 ml. The absorbance of the resulting solution was measured at λ_{max} of 785 cm^{-1}. A standard calibration curve was obtained by plotting the absorbance with of DTP in aqueous solution.

10 g of DTP/K10 was taken in 25 ml of methanol and the mixture was refluxed and a 1 ml aliquot of the refluxing solution was withdrawn to which 1 ml of 10% ascorbic acid solution was added. The solution was diluted to 25 ml and the absorbance was measured at the λ_{max} of 785 cm^{-1}. It was observed that up to a period of 3 h there was a loss of 3% of the loaded DTP. The above test was repeated to find that subsequent leaching was indeed negligible. It was thus that DTP was chemically adsorbed on the catalyst surface, no leaching of DTP from the support was observed, and there is no poisoning of the active sites.

Tsigdinos has reported that for impregnation of an activated carbon with a concentrated solution of HPA and consecutive drying, phosphotungstic acid could not be desorbed from the carbon support, although HPA is highly soluble in water, methanol and acetone. Prolonged extraction of impregnated carbon with methanol in a Soxhlet apparatus was reported to fail to remove a measurable amount of the adsorbed HPA.[27]

Mechanism and reaction kinetics

Several mechanisms have been considered by us[22] for the alkylation with MTBE and the mechanism of alkylation of *p*-cresol with MTBE was found to be adequate to describe the results. Since no dehydration of catechol was found to take place to give the corresponding ether or, for that matter, no *O*-alkylated product was formed with methanol generated *in situ*. This would suggest that there is adsorption of MTBE on the catalytic site which can react with catechol either from the adjacent site, or that MTBE first gets cracked to isobutylene which is then readsorbed on the catalytic site to react with catechol. The Eley–Rideal mechanism was considered adequate and the rate of alkylation is given by [eqn. (3)]:

$$-r_A = K_B k_R [A][B] w / \{1 + K_B [B]\} \quad (3)$$

Here K_B and k_R are the adsorption equilibrium constant for MTBE and intrinsic rate constant for the reaction in the absence of any external or internal resistance; w is the catalyst loading.

It was found that the weak adsorption of MTBE on the catalytic sites was confirmed wherein the surface reaction between adsorbed MTBE with catechol from the liquid phase controlled the overall rate of reaction. It could also mean that both species are weakly adsorbed as per the Langmuir–Hinshelwood–Hougen–Watson model. However, the key step is the adsorption of MTBE which is essential for *in situ* generation of isobutylene. Since there was no dehydration of catechol to form a symmetric ether as was confirmed from the mass balance and spectroscopic analysis, only MTBE was adsorbed as per the Eley–Rideal mechanism. Further, since $K_B << 1$, eqn. (3) reduces to that for a typical second order kinetic equation [eqn. (4)]:

$$-r_A = -\mathrm{d}[A]/\mathrm{d}t = k_2 [A][B] w \quad (4)$$

Upon substitution in terms of mole ratio (M_R) of MTBE to catechol and fractional conversion of catechol (X_C), eqn. (3) can be integrated to give eqn. (5):

$$\ln \{(M_R - X_C)/M_R (1 - X_C)\} = [A_0] (M_R - 1) w k_2 t = k_o t \quad (5)$$

Here, M_R = mole ratio of initial concentration of MTBE to that of catechol, X_C = fractional conversion of catechol and $[A_0]$ = initial concentration of catechol.

Plots of ln $\{(M_R - X_C) / M_R (1 - X_C)\}$ *vs.* time for catechol were made for different temperatures as shown in Fig. 8. It is found that this equation fits the data quite well. Similar plots were made for anisole alkylation at different loadings of catalyst and it was found that data fit well and the reaction conforms to the same model (Fig. 9). It was possible to evaluate the rate constant k_2 ($cm^6\ gmol^{-1}\ gcat^{-1}\ s^{-1}$) at different temperature. Arrhenius plots of ln k_2 *vs.* T^{-1} were made to obtain the apparent energy of activation as 8.86 and 17.36 kcal mol^{-1} for catechol and anisole, respectively (Fig. 10), thereby also suggesting the reaction was intrinsically kinetically controlled.

Alkylation of resorcinol

Alkylation of resorcinol was also carried out using MTBE as an alkylating agent over 20% DTP/K10 as a catalyst under otherwise similar conditions as were used for catechol.

The conversion of resorcinol was 97% in 4 h with a selectivity of 100% towards 4-*tert*-butylresorcinol. It was observed that the alkylation of resorcinol was faster relative to alkylation of catechol due to the fact that resorcinol is a more active species than catechol.

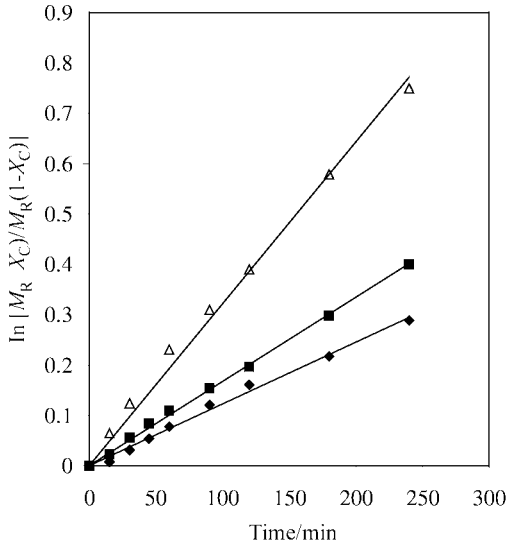

Fig. 8 Plot of ln $[(M_R - X_C)/M_R(1 - X_C)]$ *vs.* time for catechol alkylation; (◆) 130, (■) 150, (△) 170 °C.

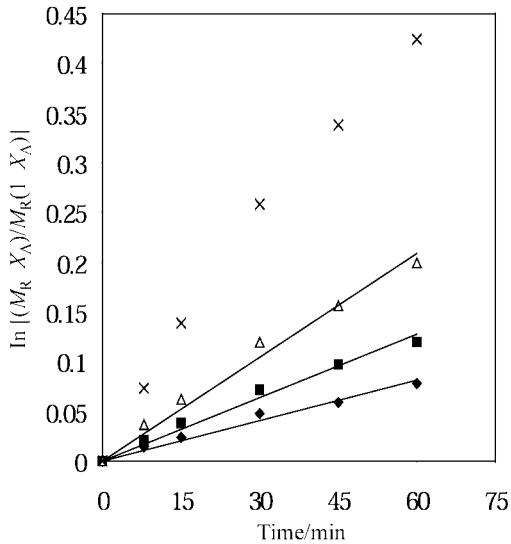

Fig. 9 Plot of ln$[(M_R - X_A)/M_R(1-X_A)]$ *vs.* time for anisole alkylation; (◆) 0.006, (■) 0.015, (△) 0.02, (×) 0.03 g cm^{-3}.

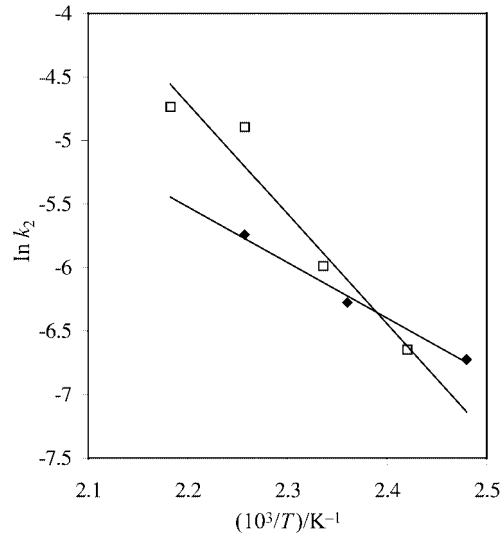

Fig. 10 Arrhenius plot; (◆) catechol, (□) anisole.

Conclusions

The current work has addressed the use of solid acid catalysts in the synthesis of *tert*-butylated products from alkylation of catechol, resorcinol and anisole with MTBE. Among the variety of catalysts used, 20% dodecatungstophosphoric acid supported on K10 (DTP/K10) was found to be the best. The effects of various parameters on the rates of reaction were studied systematically, and the reactions were found to be kinetically controlled. The best reaction conditions for catechol and resorcinol were: 20% DTPA/K10, 150 °C, mole ratio of catechol : MTBE = 1 : 3, catalyst loading 0.015 g cm^{-3} and for anisole were, 20% DTPA/K10, 170 °C, mole ratio of catechol: MTBE = 1 : 3, catalyst loading 0.03 g cm^{-3}. The reaction mechanism involves weak adsorption of MTBE on the catalyst followed by surface reaction with catechol leading to typical second order kinetics at a fixed catalyst loading. The values of the energy of activation were found as 8.86 and 17.36 kcal mol^{-1} for the alkylation of catechol and anisole, respectively.

Acknowledgement

P. K. G. thanks the University Grants Commission for the award of a Senior Research Fellowship. A. V. J. thanks AICTE for awarding Junior Research Fellowship. G. D. Y. thanks the Darbari Seth Professorship Endowment.

References

1 J. Kroupa, J. Podstata, V. Matous and V. R. Nechybova, *Czech Pat.*, 265262, 1990 (*Chem. Abstr.*, 1992, **117**, 48093).
2 D. B. Campbell, A. Onopchenko and D. C. Young, *Ind. Eng. Chem. Res.*, 1990, **24**, 642.
3 A. Schriesheim, *Friedel Crafts and Related Reactions*, ed. G. A. Olah, Interscience, London, 1964, vol. II, Part I, pp. 447–495.
4 T. Saito, T. Ito and H. Nishizawa, *Jap. Pat.*, 0782197, 1995.
5 H. Yamamoto, M. Hirai and K. Takahashi, *Jap. Pat.*, 08231452, 1996.
6 R. A. Rajadaksha and D. D. Chaudhari, *Ind. Chem. Eng. Res.*, 1987, **26**, 1276.
7 J. W. Yoo, C. W. Lee, S.-E. Park and J. Ko, *Appl. Catal. A*, 1999, **187**, 225.
8 T. Akoi and K. Sawa, *Jap. Pat.*, 04273838, 1992 (*Chem. Abstr.*, 1993, **118**, 83288).
9 G. D. Yadav and N. S. Doshi, *Catal. Today*, 2000, **60**, 263.

10 G. Sartori, F. Bigi, G. Casiraghi, G. Casnari, L. Chiesi and A. Arduini, *Chem. Ind.*, 1985, **22**, 762.
11 U. Svanholm and V. D. Parker, *J. Chem. Soc., Perkin Trans. 1*, 1973, **6**, 562.
12 H. Fernholz and H. J. Schimdt, *Angew. Chem.*, 1969, **8**, 521.
13 O. Noburu, Y. Tetsuya, A. Kamimura and K. Aritsune, *J. Chem. Soc., Chem. Commun.*, 1986, **16**, 1285.
14 F. Cunill, J. Tejero and J. F. Izquierdo, *Appl. Catal.*, 1987, **34**, 341.
15 J. Tajero, F. Cunill and S. Manzano, *Appl. Catal.*, 1988, **38**, 327.
16 B. Schleppinghoff, A. Stuewe, H. L. Niederberger, H. V. Scheef and J. Grub, *Eur. Pat.*, 407840, 1991 (*Chem. Abstr.*, 1991, **114**, 228348).
17 G. D. Yadav and N. Kirthivasan, in *Fundamental and Applied Aspects of Chemically Modified Surfaces*, ed. P. B. Jonathan and B. L. Charles, Royal Society of Chemistry, Cambridge, UK, 1999, pp. 254–269.
18 G. D. Yadav and N. Kirthivasan, *J. Chem. Soc., Chem Commun.*, 1995, 203.
19 G. D. Yadav and V. V. Bokade, *Appl. Catal. A*, 1996, **147**, 299.
20 G. D. Yadav and N. Kirthivasan, *Appl. Catal. A*, 1997, **154**, 29.
21 G. D. Yadav and T. S. Thorat, *Ind. Eng. Chem. Res.*, 1996, **35**, 721.
22 G. D. Yadav, A. A. Pujari and A. V. Joshi, *Green Chem.*, 1999, **1**, 269.
23 R. C. Reid, M. J. Prausnitz and T. K. Sherwood, *The Properties of Gases and Liquids*, 3rd edn., McGraw-Hill Book Company, New York, 1977.
24 P. S. Kumbhar and G. D. Yadav, *Chem. Eng. Sci.*, 1989, **44**, 2535.
25 G. D. Yadav and P. K. Goel, *Green Chem.*, 2000, **2**, 71.
26 H. S. Fogler, *Elements of Chemical Reaction Engineering*, Prentice-Hall, New Delhi, 1995.
27 G. A. Tsigdinos, *Ind. Eng. Chem. Prod. Res. Dev.*, 1974, **13**, 267.

Surface characterization of natural fibers; surface properties and the water up-take behavior of modified sisal and coir fibers

Alexander Bismarck,*†[a] Amar K. Mohanty,‡[b] Ibon Aranberri-Askargorta,†§[a] Syliva Czapla,[c] Manjusri Misra,‡[b] Georg Hinrichsen[b] and Jürgen Springer[a]

[a] *Technische Universität Berlin, Institut für Technische Chemie, Fachgebiet Makromolekulare Chemie, Sekr. TC6, Straße des 17. Juni 135, D-10623 Berlin, Germany*
[b] *Technische Universität Berlin, Institut für Nichtmetallische Werkstoffe, Polymerphysik, Sekr. ES5, Englische Str. 20, D-10587 Berlin, Germany*
[c] *Max-Planck-Institut für molekulare Pflanzenphysiologie, D-14424 Potsdam, Germany. E-mail: a.bismarck@chem.hull.ac.uk*

Received 9th January 2001
First published as an Advance Article on the web 30th March 2001

The influence of fiber surface modifications like dewaxing, alkali treatment and methyl methacrylate grafting on the thermal and electrokinetic properties of coir (coconut) and sisal fibers has been investigated. Additionally scanning electron microscopy was performed to follow changes in the fiber surface morphology. Electrokinetic properties were measured using the streaming potential method. The measured time dependence of the ζ-potential offers the possibility to characterize the water up-take, *i.e.* the swelling behavior of natural fibers. The investigated natural fibers, as expected, contain dissociable surface functional groups as verified by measuring the pH-dependence of the ζ-potential. The influence of fiber surface modifications on the ζ-potential was compared to the influence of fiber surface modifications on measured (tensile and flexural strength) mechanical biocomposite properties. The ζ-potential measurement is a very efficient technique to investigate the various changes effected by different surface modifications, which are necessary to improve the compatibility of such natural fibers and polymer matrices for making eco-friendly and low cost composite materials.

Introduction

Sisal fiber is a hard fiber extracted from the leaves of the sisal plant (*Agave sisalana*). Though native to tropical and sub-tropical North and South America, sisal plants are widely grown in tropical countries of Africa, the West Indies and the Far East,[1] Tanzania and Brazil being the two main producing countries.[2] Sisal fiber is one of the most widely used natural fibers[3] and accounts for almost half the total production of natural fibers. Though sisal fiber is the most widely used natural fiber, a large quantity of this economic and renewable resource is still under-utilized. It is mainly used as ropes in marine industry and agriculture.[4] Other applications of sisal fibers include twines, cords, upholstery, padding and mat making, fishing nets, fancy articles such as purses, wall hangings, tablemats *etc.*[5] It has also been used to manufacture corrugated roofing panels that are strong and cheap with good fire resistance.[6] Using sisal fiber as reinforcement in composites has raised great interest and expectations among material scientists and engineers.[7] However, sisal fiber-reinforced composites generally have poor interface and moisture resistance.[8] Sisal fiber is ligno-cellulosic in nature and the main constituents[9] as well as some mechanical properties of the fiber are summarized in Table 1 (from ref. 10). The presence of a large amount of hydroxy groups is responsible for the hydrophilic nature of sisal fiber. Several fiber surface treatment methods have been studied to improve the adhesion properties between sisal fibers and a surrounding matrix and simultaneously to reduce water absorption. Effective methods include alkali treatment to increase the roughness of fiber surface hence increasing the surface area available for contact with matrix, dewaxing, grafting *etc.*

Coir is a versatile ligno-cellulosic fiber obtained from coconut trees (*Cocos nucifera*), which grow extensively in tropical countries. The chemical constituents[11] and the mechanical properties of coir fibers are included in Table 1. Because of its hardwearing quality, durability and other advantages, it is used for making a wide variety of floor-furnishing materials, yarn, rope, *etc.*[12] However, these traditional coir products consume only a small percentage of the total world production of coconut husk. Coir is a cheap fiber, even cheaper than sisal

Green Context

The use of natural fibers to make low cost and eco-friendly composite materials is a subject of great importance. Nature provides us with an abundance of raw material including sisal fibre which comes from the widely grown sisal plant. The main problem with the use of such fibres is their hydrophilicity brought about by high surface hydroxy group concentrations which leads to poor interface and moisture resistance in composite materials. In this article, the effects of several surface modifications are considered in terms of their effects on the properties of fibres and fibre composites. The importance of ζ-potential measurements as a useful tool to follow the changes effected by such modifications is emphasised. ***JHC***

† Present Address: Surfactant & Colloid Group, Dept. of Chemistry, The University of Hull, Hull, UK HU6 7RX.
‡ Present Address: Composite Materials and Structures Center, Michigan State University, 2100, Engineering Building, East Lansing, MI 48824-1226, USA. E-mail: mohantya@egr.msu.edu
§ Research placement from Euskal Herriko Unibertsitatea, Zientzia Fakultatea, Bo Sarriena s/n-48940 Leioa, Spain.

 DOI: 10.1039/b100365h

and jute; the cost ratio being[13] coir : sisal : jute = 1 : 1.5 : 2. Coir fibers are not as brittle as glass fibers, are amenable to chemical modification, are non-toxic and possess no waste disposal problems, but unfortunately the performance of coir as a reinforcement in polymer composites is unsatisfactory and not comparable even with other natural fibers. This inferior performance of coir is due to various factors such as its low cellulose content, high lignin content, high microfibrillar angle, and large as well as variable diameter. Preliminary surface modification of coir has been reported recently.[14]

Zeta (ζ)-potential measurements are suitable for characterizing the 'normal wet-state' (because of the known hydrophilicity) of natural fibers.[15] ζ-Potential measurements allow following of changes in the fibers' surface composition (and therefore surface chemistry) caused by different modifications applied to improve fiber properties for textile[16–18] or composite applications.[19]

Especially for composite applications, *i.e.* natural fiber reinforced polymers, it is very important to know the degradation of the mechanical properties of the natural fibers[20] when they are exposed to processing temperatures (in air) of 180–200 °C for a certain time.[21] The thermal behavior of different natural fibers like coir[11] and jute[22,23] has been investigated. In order to compare the different modifications of coir and sisal fibers DSC and TG were performed. The known low thermal resistance of natural fibers does not allow an arbitrary choice of polymers as matrix materials during composite fabrications.

A deeper understanding of the complex nature of natural fibers and their surface properties is still needed in order to optimize natural fiber surface modification processes, which might help to increase the usefulness of those fibers as reinforcing material for polymers and to gain insights about the interaction between these materials.[24,25]

Experimental

Materials and fiber surface modifications

Coir fibers were supplied from Aerocom Pvt Ltd. (Orissa, India) and sisal fibers from the local sources of Orissa, India. The natural fibers were subjected to various surface modifications like dewaxing, alkali treatment (AT) and vinyl grafting. All chemicals like copper sulfate, sodium periodate, sodium hydroxide, ethanol, benzene were of analytical grade and were used without further purification. The monomer methylmethacrylate (MMA)[26] was purified prior to graft polymerization reactions with coir.[14]

The coir and sisal fibers were washed in 2% SURF (commercially available washing powder, Unilever, UK) detergent solution at 70 °C for 1 h, then washed overnight with rinsing tap-water and finally thoroughly washed with distilled water followed by a drying process in a vacuum oven at 70 °C. Different surface modifications of detergent washed natural fibers were used for the present studies on ζ-potential measurements. The surface modification consisted of dewaxing the detergent washed fibers in a 1 : 2 mixture of ethanol and benzene for 72 h at 50 °C, followed by washing with distilled water. The dewaxed and defatted fibers were treated in 2 and 5% NaOH solution for 30 min at 30 °C, then washed again thoroughly with distilled water and dried. The monomer methylmethacrylate (MMA) was grafted to coir as reported earlier.[14]

Fiber surface morphology

In order to evaluate changes in the surface morphology, all investigated natural fibers were analyzed by scanning electron microscopy (SEM) using a Hitachi S-2700 scanning electron microscope (Nissei Sangyo GmbH, Rathingen, Germany). The excitation energy was 10keV with a beam current of 0.5nA. All natural fibers were sputtered with gold before examination in order to ensure good conductivity.

Experimental thermoanalysis

The thermal behavior of modified coir and sisal fibers was investigated by simultaneous differential scanning calorimetry (DSC) and thermogravimetry (TG) with a Rheometric Scientific STA 1000 apparatus between 25 and 410 °C in an oxygen gas flow (50 cm^3 min^{-1}). The DSC measurements were calibrated using indium and tin standards. For each experiment, *ca.* 5 mg of the samples were weighted in an aluminium pan with one hole in the top. The experiments were carried at a heating rate of 10 K min^{-1}.

ζ-Potential measurements

The ζ-potential of the natural fibers was determined in 1 mM KCl-electrolyte solution at a constant temperature of 20 ± 1 °C using the electrokinetic analyzer EKA (Anton Paar KG, Graz, Austria) based on the streaming potential method. The theoretical background[27,28] and details of the ζ-potential measuring technique are reported elsewhere.[29,30]

By measuring the ζ-potential as a function of the pH, the acidity and basicity of solid surfaces can be determined qualitatively, if the dissociation of functional groups is the predominant mechanism forming the double-layer.

According to Kanamaru[31] the time-dependence of the ζ-potential can give information about the amount of adsorbed water. The quotient $\Delta\zeta = (\zeta_0 - \zeta_\infty)/\zeta_0$ is proportional to the water uptake at 100% relative humidity (RH) (the sorption capacity) of the investigated solid. The decrease of the ζ-potential as a function of time due to the water uptake can be described by eqn. (1):

$$-\frac{d\zeta}{dt} = k(\zeta - \zeta_\infty) \quad (1)$$

which leads to, eqn. (2):

$$-\mathrm{In}\frac{\zeta - \zeta_\infty}{\zeta_0 - \zeta_\infty} = kt \quad (2)$$

where ζ is the measured ζ-potential value at a certain time, ζ_∞ the ζ-potential value which reaches the function $\zeta = f(t)$

Table 1 Chemical composition and comparative mechanical properties of sisal (leaf) and coir (coconut, fruit) fibers

Fiber	Cellulose (%)	Lignin (%)	Hemicellulose (%)	Moisture content (%)	Tensile strength (MPa)	Young's modulus (GPa)	Elongation at break (%)	Microfibrillar spiral angle/°
Sisal	67–78	8.0–11.0	10.0–14.2	11.0	468–640	9.4–22.0	3–7	20.0
Coir	36–43	41–45	0.15–0.25	8.0	131–175	4.0–6.0	15–40	41–45

asymptotically and k the relative rate constant (a structure dependent constant) of the adsorption (swelling) process.[28]

Results and discussion

Fiber surface morphology; SEM analysis

Comparing all SEM-micrographs [Fig. 1(a)–(e)] taken of unmodified (standard) coir with modified coir fibers, hardly any difference in the surface structure between the fibers can be observed at low magnification (magnification factor ×250). The coir fibers [Fig. 1(a)–(e)] display many pinholes on the surface ('rotten wood'-like appearance). The diameter of natural fibers (coir as well as sisal) vary considerably. It seems that the fibers become smoother upon dewaxing and on treatment with 2% NaOH compared to the standard coir, whereas treatment with 5% NaOH seems to roughen the surface again. The cross-sections of the coir fibers, both untreated and dewaxed, are shown in Fig. 1(a) and (b), respectively. A larger number of surface cracks, or pit formations are observed in dewaxed coir [Fig. 1(b)] as compared to untreated sample [Fig. 1(a)]. These might occur because of the partial removal of wax or fatty substances (from which two major components can be distinguished; (i) components (up to 80% of their total mass),

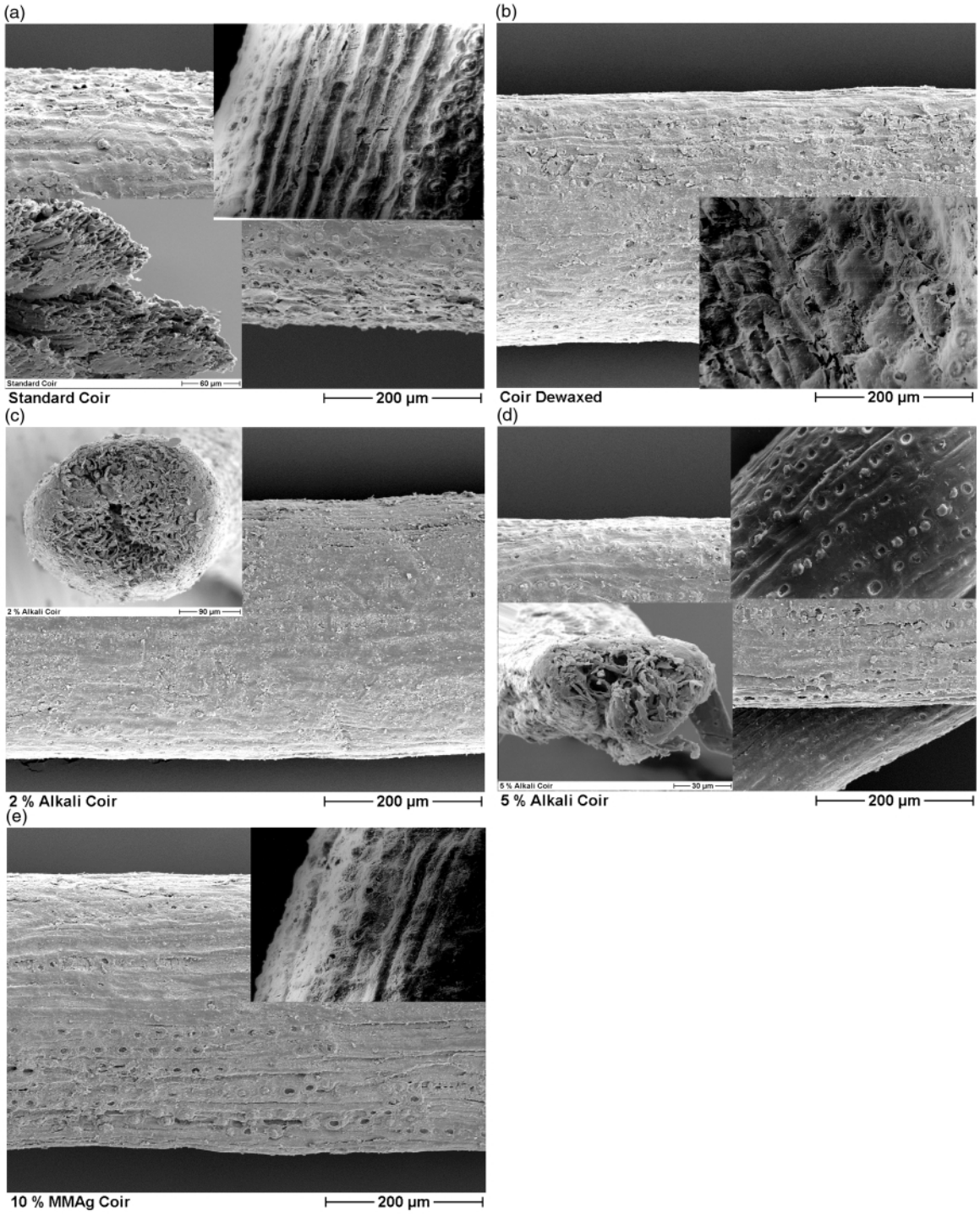

Fig. 1 (a) Original, untreated (standard) coir fiber, plane view (×250) and cross section, and magnified plane view (×500). (b) Dewaxed coir fiber, plane view, and magnified plane view (×1000). (c) Coir fiber treated with 2% NaOH, plane view and cross section. (d) Coir fiber treated with 5% NaOH, plane view and cross section, and magnified plane view (×1000). (e) Coir fiber grafted with 10% polymethyl methacrylate, plane view and magnified plane view (×1000).

like saturated hydrocarbons long-chain alcohols and acids, which cannot be saponified and (ii) components, esters of higher acids, which can be saponified)[32] during treatment with the dewaxing solvent mixture.[33] Fig. 1(a)–(e) also shows some higher magnification SEM images (to clearly visualize differences in the fiber surface morphology caused by modifications; magnification factor ×1000) of untreated and differently surface modified coir fibers. The SEM micrograph of untreated (standard) coir [Fig.1(a)] clearly demonstrates the presence of longitudinally orientated unit cells with more or less parallel orientations. The intercellular space is filled up by the binder lignin and fatty substances, which hold the unit cells firmly in a fiber. Particularly on the right side of Fig. 1(a) a large number of globular protrusions or patches embedded in the fiber surface at regular intervals are observed. Fig. 1(d) shows micrographs of 5% alkali treated coir fibers. A large number of regularly placed holes or pits on the surface can be observed. Such observations are most likely due to the removal of fatty deposits, so called 'tyloses', from the fiber. A large number of globular fatty deposits lie hidden below the surfaces of the untreated fiber. Therefore, these are not revealed by the SEM pictures of untreated fibers and are only partially revealed in dewaxed fiber and to a larger extent revealed in the alkali treated fibers. Similar results have also been reported by Prasad *et al.*[34] Comparison of Fig. 1(e) with Fig. 1(d) shows that in the intercellular gaps as well as on the surface of the unit cells, grafted polymethylmethacrylate (PMMA) has been deposited. Again, the surface of PMMA grafted coir seems to be uniform and smooth in comparison with alkali treated coir. PMMA grafting on to coir is targeted with a view to improve surface as well as the bulk mechanical properties for its potential use as a reinforcing fiber for polymer composites. As reported earlier,[35] PMMA grafting on to coir up to an optimum 'graft-on'-percentage enhances the strength of the coir fiber. Such low or optimum PMMA grafted coir fibers show better compatibility with polyester amide resin, thus better fiber-matrix adhesion and thereby display superior physico-mechanical properties of the resulting composites.[36]

Comparing the coir fibers with sisal fibers [Fig. 2(a)–(d), magnification factor ×400) it is seen that coir fibers are much larger in diameter and they look smoother. Again only the unmodified sisal fiber [Fig. 2(a)] seems to be a little bit rougher compared to the surface modified sisal fibers [Fig. 2(b)–(d)] containing small particles (possibly waxes and fats) attached to the fiber surface. These particles thus appear to be removed by the applied modification procedures (dewaxing, treatment with NaOH). All sisal fibers display a grain-like surface structure.

Thermal behavior of sisal and coir fibers

The thermal stability of the fibers was measured by means of TG. All investigated fibers showed a two-step decomposition curve and an onset of degradation between 190 and 230 °C.

Fig. 3 shows DSC and TG traces for the investigated coir and sisal fibers while Table 2 lists the main results. A broad endotherm peak was observed at temperatures between 60 and 160 °C. This peak is connected to a weight loss of 7–9% as observed by TG. Since all natural fibers are quite hydrophilic, they are subject to a dehydration process in which absorbed or crystal water is released. However, the amount of adsorbed

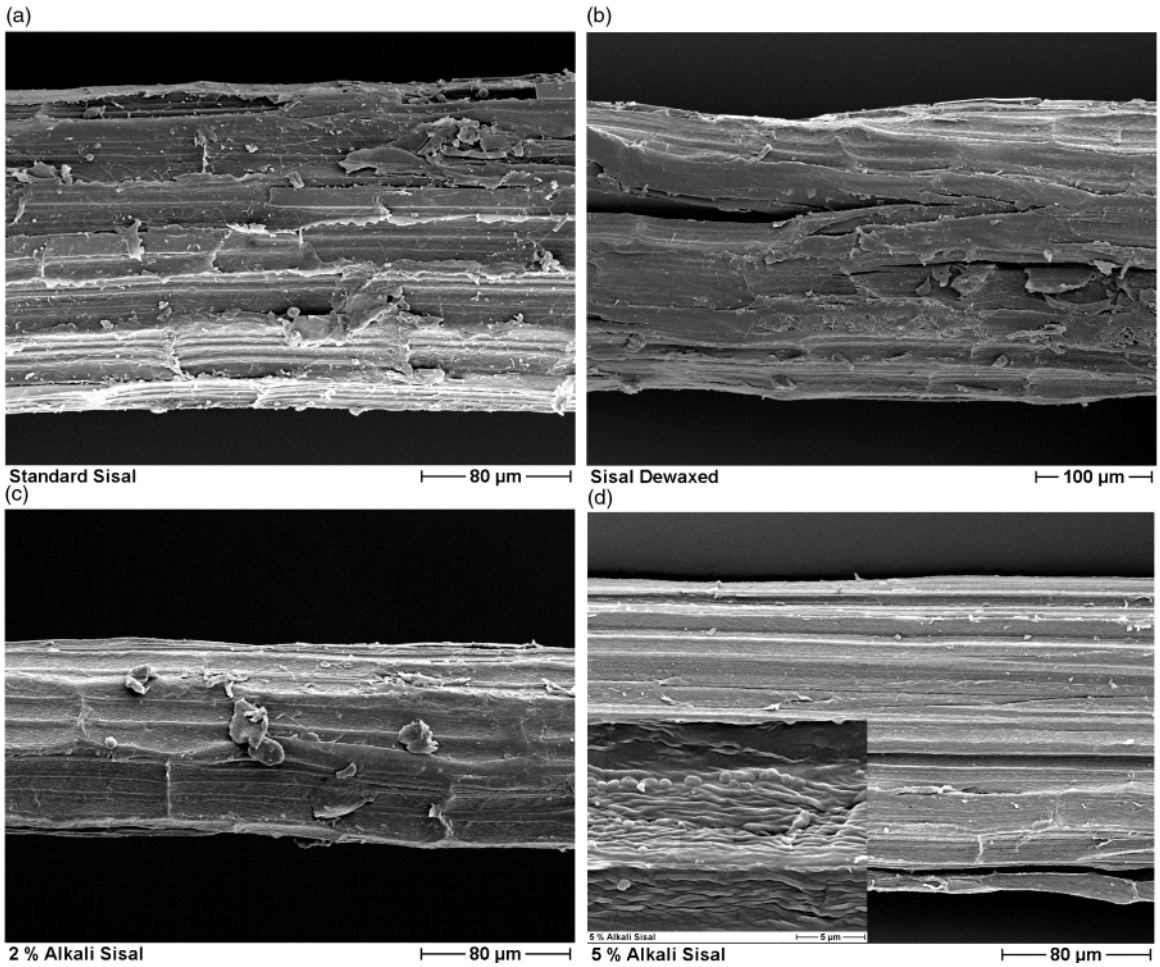

Fig. 2 (a) Original, untreated (standard) sisal fiber, plane view. (b) Dewaxed sisal fiber, plane view. (c) Sisal fiber treated with 2% NaOH, plane view. (d) Sisal fiber treated with 5% NaOH, plane view and magnified section of the outer fiber surface.

water is dependent on the ambient humidity. Other thermal processes (like phase transition or melting) could not be detected. As reported in the literature[38] no polymer degradation process takes place until 160 °C, however at temperatures above 200 °C polymer degradation leads to a considerable weight loss of 30%.

The maximum decomposition temperature (T_D), the temperature at which significant weight loss starts, of each investigated fiber is taken as a basis to compare their thermal stability. The maximum decomposition temperature was determined form the point were the slopes of the DSC and TG courses begin to change drastically. T_D values of the untreated (standard), dewaxed, alkali treated and PMMA-grafted coir fibers are found to be 255, 255, 265 and 268 °C, respectively. Similarly untreated, dewaxed and alkali treated sisal fibers showed T_D values at 270, 271 and 280 °C, respectively. Thus sisal is thermally more stable than coir. Again certain specific surface modifications like alkali treatment, increase the thermal stability of both coir and sisal fibers by *ca.* 10 °C (for coir from 255 to 265 °C, for sisal from 270 to 280 °C) because the applied surface treatments lead to a reduced amount of fiber companions, which decompose earlier than the major component cellulose. For PMMA-grafted coir, we also observe an *ca.* 10 °C enhancement in the T_D value. The increase of thermal stability with increasing graft yield has also been reported earlier.[22]

In order to obtain optimum mechanical properties, as far as composite fabrication of the modified natural fiber is concerned, we require fibers grafted with a low percentage of polymer.[35] Dewaxing of both coir and sisal does not change their thermal behavior.

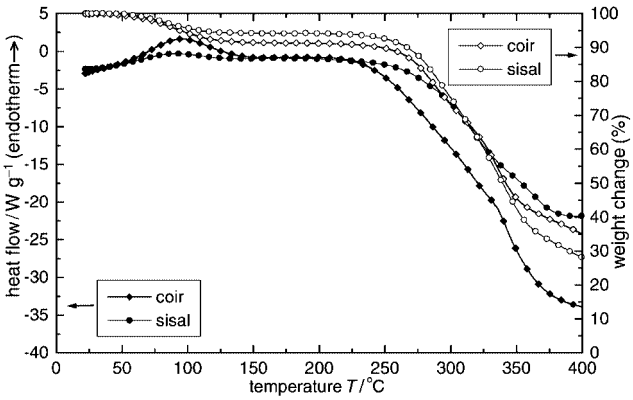

Fig. 3 DSC/TG traces (heat flow and weight change) measured in oxygen atmosphere of sisal and coir fibers as a function of temperature.

Table 2 The maximum decomposition temperature, the water content for fibers stored in a 'normal' environment ($T \approx 20$ °C, RH ≈ 65%), and weight loss due to polymer degradation in oxygen of coir and sisal fibers

Natural fiber	T_D/°C	Water content (wt%)	Polymer degradation to 410 °C (wt%)
Sisal (standard)	270	5.8	72.7
Dewaxed	271	6.5	71.0
AT 2%	280	6.5	70.0
AT 5%	280	7.5	67.5
Coir (standard)	255	8.6	62.5
Dewaxed	255	6.5	61.1
AT 2%	265	9.1	62.8
AT 5%	265	9.2	60.7
Coir 10% MMA grafted[a]	268	8.1	64.7

[a] Dewaxed coir fibers were used as starting material for the MMA grafting reactions.

ζ-Potential measurements: ζ-potential time dependence

As already shown,[31] time-dependent ζ-potential measurements can be used to estimate the water up-take behavior of solid (polymeric) materials (synthetic[37] as well as natural[19]), which is in good agreement with conventional water absorption measurements performed for differently modified flax fibers.¶ In the present case one can see that all investigated natural fibers display a different ζ-potential decay with time. This ζ-potential decay depends on the degree of hydrophilicity of the investigated fibers. This is due to the swelling of the solid that causes a transfer of the shear plane into the liquid, which excludes the diffuse part of the electric double layer from mechanical or electrical interaction. Other factors include the slow dissolution of water-soluble (ionic) components (*e.g.* for sisal 1.2%[38]) from the fibers into the electrolyte solution,[39] which might also cause a decrease of the ζ-potential. This behavior correlates with a different water up-take behavior (swelling in water). One can ascertain (Table 3, summarizing the main results) that sisal (Fig. 4) and coir fibers (Fig. 5) show different degrees of hydrophilicities. Although both types of natural fibers are hydrophilic, the sisal fibers are much more hydrophilic than coir. This can be quantified (more or less since the 'real' initial value of the 'dry' fibers is hard to measure and has to be therefore fitted[31]) by the quotient $(\zeta_0 - \zeta_\infty)/\zeta_0$, which correlates with the water up-take at 100% relative humidity (RH).

As can be seen from the results (Table 3) applied fiber modifications, like dewaxing, alkali treatment and even grafting

Table 3 Main results of the time dependence of the ζ-potential measured in 1 mM KCl electrolyte solution: ζ_0 = ζ-potential value measured immediately after starting the measurement, ζ_∞ = ζ-potential value after established equilibrium, $(\zeta_0 - \zeta_\infty)/\zeta_0$-value which should correspond to the water up-take at 100% RH

Natural fiber	ζ_0/mV	ζ_∞/mV	$(\zeta_0 - \zeta_\infty)/\zeta_0$
Sisal (standard)	−3.4	−2.6	0.76
Dewaxed	−2.4	−1.5	0.38
FAT 2%	−0.2	—	—
AT 5%	+3.5	+0.7	0.80
Coir (standard)	−6.9	−5.4	0.22
Dewaxed	−7.0	−5.0	0.28
AT 2%	−5.1	−2.5	0.51
AT 5%	−1.1	—	—
Coir 10% MMA grafted[a]	−5.9	−4.0	0.32

[a] Dewaxed coir fibers were used as starting material for the MMA grafting reactions.

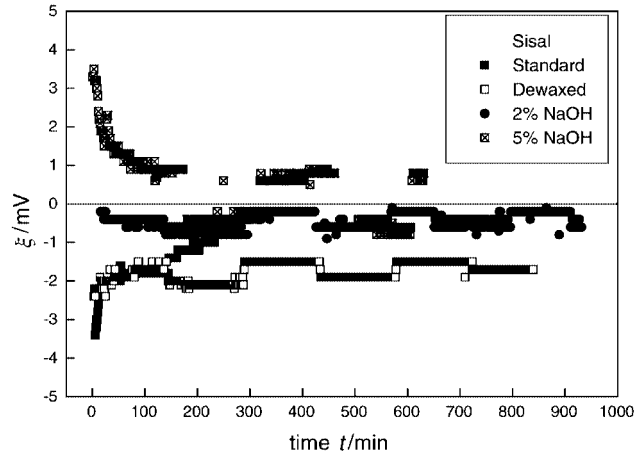

Fig. 4 ζ-Potential–time dependence of unmodified and modified sisal fibers measured in 1 mM KCl.

¶ A manuscript dealing with surface characterization of pure cellulose, hemp and differently separated and modified flax fibers is in preparation.

of methylmethacrylate (MMA) 'onto' coir fibers increase the amount of absorbed water. The reason for this behavior is that all studied fiber surface modifications affect the natural protecting wax-layers at the fiber surface. For MMA-grafted coir fibers, it seems that the surface coverage by PMMA is not sufficiently high (since polymerization takes place in the fiber as well, as seen by SEM) to give the same 'protection' against water as the natural waxes.

ζ-Potential pH-dependence

The measured pH-dependent ζ-potentials of different sisal fibers also reflects the above-discussed high hydrophilic character (Fig. 6 and Table 4). The swelling of the hydrophilic fibers results in a reduction of the ζ-potential, because of the shift of the shear plane into the liquid phase,[39] which causes these small $\zeta_{plateau}$-values. For sisal fibers the isoelectric point (i.e.p.), where ζ = 0, cannot be measured, since the ζ-potential decreases drastically at low pH.‖ This rapid change in the ζ-potential course at low pH for the sisal fibers might be caused by a protonation process of the acetal- or ether-linkages that exist in cellulose (for sisal, *ca.* 65.8%[38]) or are present also in the lignin component (*ca.* 9.9%[38]) of natural fibers. Such a protonation process would create a higher positive charge in the electrical double layer, which could induce excess absorption of anions (Cl^-) and might cause the rapid increase of the negative ζ-potential at low pH. Dewaxing (the waxes which are present at a level of *ca.* 0.3% in sisal consist of different types of alcohols, which cannot be dissolved in water or several acids[38]) of the original (standard) sisal fibers leads to a slight increase of the negative ζ-potential plateau value ($\zeta_{plateau}$), which is caused by an increased accessibility of dissociable surface functional groups like carbonyl, which are present in the pectin component[38] and hydroxy groups.[17,40] One has to bear in mind, that water up-take and therefore, swelling reduce the ζ-potential, whereas a greater accessibility of dissociated surface functional groups increases the ζ-potential. On the other hand alkali treatment of the fibers using 2 and 5% NaOH solutions, causes a ζ-potential reversal of the modified fibers. These treated fibers now display a positive $\zeta_{plateau}$-value. As a result of alkali treatment, some of the wax-components at the fiber surfaces are saponified[38] and, thereby removed from the fiber surface.[17] Such alkali treatment increases the active fiber surface and simultaneously the accessibility of the dissociable surface groups. The positive ζ-potential measured after NaOH treatment might be caused by alkali metal ions, 'strongly adsorbed' on the fiber surface after the alkali treatment process[41] (possibly $-CO_2^-\cdots Na^+$). Even after prolonged time measurements and, therefore, thorough rinsing the fiber samples in the measuring cell, the ζ-potentials remain positive (see also Fig. 4). The effectiveness of such an alkali treatment process in order to increase the accessibility of surface groups can clearly be seen from the drastic change of the ζ-potential at low pH values as compared that of the original and dewaxed fibers. This increase of the negative ζ-potential is more pronounced after NaOH treatment. An increasing NaOH concentration from 2 to 5% for the alkalization process results also in increased ζ-potential values. The higher accessibility of the surface groups is also accompanied by a shift of pH at which the ζ-potential changes rapidly to higher pH (Table 4), which indicates that the 'protonation process' becomes less hindered. The results described above for sisal fibers are similar to data obtained for jute fibers.[19]

Looking at the ζ-potential pH-dependences measured for coir fibers (Fig. 7) it becomes obvious that these fibers behave completely differently when compared to all other investigated natural fibers (such as jute,[19] flax, hemp, cellulose and sisal). The overall function ζ = f(pH) looks much more complicated; two more or less pronounced local minima appear, one at low and the other at high pH. The first minimum may be caused by a protonation process of surface functionalities inducing an excess adsorption of counter ions (Cl^-) followed by the 'normal' adsorption process of potential determining protons. This causes the decrease of the negative ζ-potential. Such a proton adsorption results in some cases (except for the original, untreated (standard) and MMA-grafted coir fibers) in a reversal of the measured ζ-potentials in the low pH range, an i.e.p. of *ca.* pH = 3.1 ± 0.1 was measured. The second minimum might be

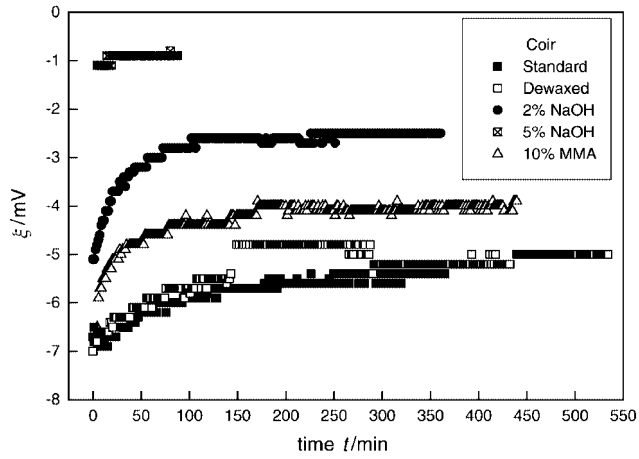

Fig. 5 ζ-Potential–time dependence of unmodified and modified coir fibers measured in 1 mM KCl.

Table 4 Results of the ζ-potential pH-dependence: ζ_{pateau} = ζ-potential plateau value at pH ⩾ 7; $pH_{\zeta,changes}$ the pH at which the ζ-potential changes drastically

Natural fiber	$\zeta_{plateau}$/mV	$pH_{\zeta,changes}$
Sisal (standard)	−1.7	4.1
Dewaxed	−2.1	4.2
AT 2%	+1.8	4.3
AT 5%	+1.5	5.2
Coir (standard)	−3.8	
Coir dewaxed	−4.6	
Coir AT 2%	−1.1	
Coir AT 5%	−0.4	
Coir 10% MMA grafted	−3.1	

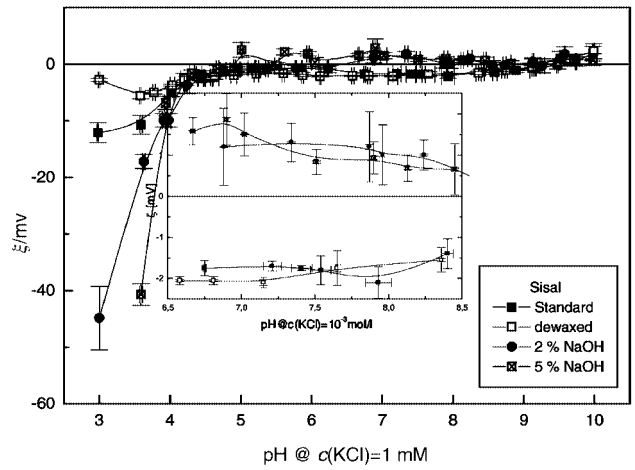

Fig. 6 ζ-Potential pH-dependence of unmodified and modified sisal fibers.

‖ The same analogous behavior for measured ζ = f(pH), the increase of the negative ζ-potential at low pH either in peak form or just a steep increase, was also found for other natural fibers including jute,[19] flax and cellulose. It turns out that this process is reproducible for natural fibers, even over a period of nearly two years and many repeated measurements.

due to the adsorption of hydroxyl ions on the surface, which leads to an increase of the negative surface charge. Despite this unusual ζ–pH course, the '$\zeta_{plateau}$-values' (at $5.5 \leqslant pH \leqslant 7.5$) follow the expected observed trend for other natural fibers. Compared to the untreated, original coir fibers the negative $\zeta_{plateau}$-value increases after dewaxing (removing of the waxes by suitable solvents, see Experimental section) due to increased accessibility (uncovering from wax) of the present dissociable surface groups. In contrast to that behavior PMMA-grafting leads to a decrease of the actual number of surface groups by partially covering the fiber surface with grafted polymer. Alkali treatment, using 2 and 5% NaOH, however results in a decrease of the negative $\zeta_{plateau}$-values. The alkalization leads to a partial removal of waxes[32,42] and therefore an increased accessibility of the protonable surface functions. An increased number of 'polar' surface functionalities will increase the amount of water adsorbed on the fibers. However, the adsorption of ions determining the ζ-potential occurs in competition with water adsorption[43] and, therefore, a decrease of the negative $\zeta_{plateau}$-values can be observed. For alkali treated coir fibers a point of ζ-potential reversal (p.ζ.r.) at high pH (for the fibers treated in 2% NaOH at pH = 9.3 and for the fibers treated in 5% NaOH at pH = 8.9) was found. This behavior indicates that the alkalized coir fiber surfaces become positively charged in the 1mM KCl measuring solution due to the specific interactions between the charged surface and the dissolved ions.[44] This behavior corresponds to the classical charge reversal brought by the adsorption of ions of opposite charge on the surface.[27] This also explains the occurrence of the local ζ-potential minima at higher pH obtained for all investigated coir fibers. For the other fibers (standard and dewaxed coir) the adsorption of the counter charges is not that distinct, whereas for MMA-grafted fibers the point of ζ-potential reversal can not be reached, because of the higher negative surface charge.

Influence of natural fiber surface modifications on the mechanical performance of biodegradable coir- and sisal-polyester amide composites[36,45]

The influence of the above discussed surface modifications applied to the studied natural fibers on the mechanical performance of coir and sisal (fiber content: 50 wt%) reinforced biodegradable polyester amide has been studied separately (the experimental details are described in refs. 36 and 45). Polyester amide (in film form), a biodegradable thermoplastic polymer (Bayer AG, Germany, trade name: BAK® 1095)[46] is used as the matrix polymer for making the composites. The coir/sisal–polyester amide composites are prepared by sandwiching layers of non-woven fiber mats between the layers of pre-weighted polyester amide films in a close mold heated at 135 °C for 15–20 min followed by applying a pressure of 20 MPa for 5 min and finally cooled to room temperature obtaining the final composite. The tensile and flexural strength of polyester amide composites reinforced with 5% alkali treated sisal fibers were measured (Table 5). The same properties of the composite containing the standard sisal fibers were measured for comparison purposes. The composite made of 5% alkali treated sisal fibers had a higher tensile strength compared to composites made from the standard sisal fibers. The tensile strength resulting from the use of 5% alkali treated sisal fibers as reinforcement was enhanced by *ca.* 20% as compared to standard fibers. This can be attributed to the fact that alkali treatment leads to fiber fibrillation, *i.e.* breaking down of fiber bundles into smaller fibers and thereby increasing the effective surface area but also the accessibility of polar surface functional groups (*cf.* ζ-potential measurements) that may lead to improved attractive interactions to the polyester amide matrix. As shown above alkali treatment causes the removal of natural (wax and fat) and artificial impurities and hence a considerable increase in mechanical properties can be observed.

Even though coir fibers have lower tensile strength than sisal (see also Table 1), improved composite properties, like tensile and flexural strength (Table 5), can be achieved after suitable optimized surface treatments. Thus optimized surface treatments can result in composites exhibiting quite promising levels of mechanical properties even for the low strength coir fibers.

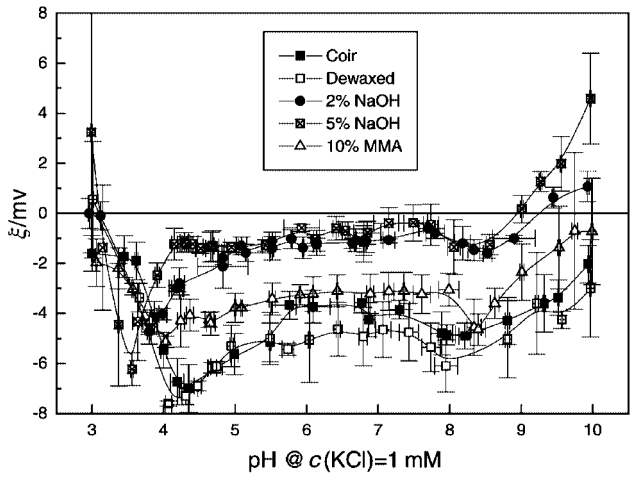

Fig. 7 ζ-Potential pH-dpendence of unmodified and modified coir fibers.

Table 5 Effect of different surface modifications applied to sisal and coir fibers on the tensile and flexural strength of natural fiber reinforced polyester amide composites

Natural fiber	Tensile strength/ MPa	Flexural strength/MPa
Sisal (standard)	60.0 ± 6.1	78.2 ± 5.6
AT 5%	72.3 ± 4.3	81.2 ± 7.2
Coir (standard)	28.9 ± 1.0	53.9 ± 3.3
AT 5%	32.2 ± 2.8	56.6 ± 7.1
Coir 10% MMA grafted[a]	30.1 ± 2.1	78.2 ± 3.6

[a] Dewaxed coir fibers were used as starting material for the MMA grafting reactions.

Conclusions

We have studied the influence of several surface modifications, like dewaxing, alkali treatment and methylmethacrylate grafting, on the thermal and electrokinetic properties of coir and sisal fibers. SEM micrographs show coir fibers are much larger in diameter than sisal fibers. The surfaces of coir fibers display many pinholes. High magnification resolves changes in surface morphology between unmodified and modified fibers. After dewaxing and alkali treatment the surfaces of the natural fibers are rougher, mainly because of the partial removal of waxes and fatty substances. After polymethylmethacrylate (PMMA) grafting on coir fibers the surface becomes more uniform and smooth as compared to alkali treated coir. PMMA is deposited in the intercellular gaps as well as on the surfaces of the unit cells.

Alkali treatment as well as MMA-grafting of coir fibers, increases the maximum decomposition temperature by *ca.* 10 °C as compared to untreated fibers. However, dewaxing of both coir- and sisal fibers seems to have no influence on the thermal stability.

Sisal is much more hydrophilic than coir. However, the water up-take or swelling behavior is influenced by surface modifications. All fiber modifications, like dewaxing, alkalization and even grafting of polymethylmethacrylate 'onto' coir fibers

increase the amount of absorbed water, since all modifications affect the natural protecting wax layer at the fiber surface. All studied natural fibers contain dissociable acidic surface functional groups as revealed by ζ-potential measurements. Comparing the ζ-potential results with measured mechanical composite properties it becomes obvious that the performance of such materials, *i.e.* higher tensile and flexural strength, is improved by the applied surface modifications in the same way as the measured ζ-potentials are effected: a higher accessibility of the surface functional groups results in lower ζ-potentials due to the increased hydrophilicity but on the other hand leads to improved interactions between the fibers and the polar polyester amide matrix and therefore to better mechanical composite properties.

It can be seen that ζ-potential measurements are a very useful tool to follow changes effected by modifications necessary to improve the compatibility of such natural fibers and polymers for composite applications in the surface properties of natural fibers.

Acknowledgements

We thank David Richter (ITC of the TU-Berlin) for very fruitful discussions. The financial support of the Berliner Verband für Polymerforschung e.V. (B.V.P.) and the Fonds der Chemischen Industrie is gratefully acknowledged. One of us (A. K. M) is grateful to the Alexander von Humboldt Foundation, Germany for an AvH-fellowship. We are grateful to Dr Adam F. Lee (Dept. Chemistry, The University of Hull) for proof reading the manuscript.

References

1 E. T. N. Bisanda and M. P. Ansell, *J. Mater. Sci.*, 1994, **27**, 1690.
2 N. Chand, R. K. Tiwary and P. K. Rohatgi, *J. Mater. Sci.*, 1998, **23**, 381.
3 Y. Li, Y.-W. Mai and L. Ye, *Composites Sci. Technol.*, 2000, **60**, 2037.
4 P. S. Mukherjee and K. G. Satyanarayan, *J. Mater. Sci.*, 1984, **19**, 3925.
5 N. Chand, S. Sood, P. K. Rohatgi and K. G. Satyanarayan, *J. Sci. Ind. Res.*, 1984, **43**, 489.
6 E. T. N. Bisanda, *J. Mater. Process Technol.*, 1992, **38**, 369.
7 K. Bledzki, S. Reihmane and J. Gassan, *J. Appl. Polym. Sci.*, 1996, **59**, 1329.
8 K. Bledzki, S. Reihmane and J. Gassan, *Polym-Plast. Technol Eng.*, 1998, **37**, 451.
9 D. N. S. Hon, *Polym. News*, 1992, **17**, 102.
10 A. K. Mohanty, M. Misra and G. Hinrichsen, *Macromol. Mater. Eng.*, 2000, **276**, 1.
11 D. S. Varma, M. Varma and I. K. Varma, *Thermochim. Acta*, 1986, **108**, 199.
12 K. G. Satyanarayana, A. G. Kulkarni and P. K. Rohatgi, *J. Sci. Ind. Res.*, 1981, **40**, 222.
13 V. G. Geethamma, K. T. Mathew, R. Lakshminarayanan and S. Thomas, *Polymer*, 1998, **39**, 1483.
14 J. Rout, M. Misra and A. K. Mohanty, *Polym. Adv. Technol.*, 1999, **10**, 1.
15 H.-J. Jacobasch, K. Grundke and C. Werner, *Papier (Paris)*, 1995, **12**, 740.
16 M. Espinosa-Jiménez and F. González-Caballero, *Cellulose Chem. Technol.*, 1991, **52**, 65.
17 V. Ribitsch, K. Stana-Kleinschek and S. Jeler, *Colloid Polym. Sci.*, 1996, **274**, 388.
18 A. Ontiveros-Ortega, M. Espinosa-Jiménez, E. Chibowski and F. González-Caballero, *J. Colloid Interface Sci.*, 1998, **202**, 189.
19 A. Bismarck, J. Springer, A. K. Mohanty, G. Hinrichsen and M. A. Khan, *Colloid Polym. Sci.*, 2000, **278**, 229.
20 M. Münker, *Werkstoffe Fertigung*, 1998, **3**, 15.
21 B. Wielage, Th. Lampke, G. Marx, K. Nestler and D. Starke, *Thermochim. Acta*, 1999, **337**, 169.
22 A. K. Mohanty and B. C. Singh, *J. Appl. Polym. Sci.*, 1989, **37**, 1423.
23 A. K. Mohanty, S. Pattnaik, B. C. Singh and M. Misra, *J. Appl. Polym. Sci.*, 1989, **37**, 1171.
24 J. M. Felix and P. Gatenholm, *Polym. Composites*, 1993, **14**, 449.
25 J. M. van Hazendonk, J. C. van der Putten, J. T. F. Keurentjes and A. Prins, *Colloids Surf. A*, 1993, **91**, 251.
26 A. K. Mohanty, M. Misra, D. Pattanaik and P. C. Tripathy, *Polym.-Plast. Technol. Eng.*, 1996, **35**, 403.
27 R. J. Hunter, *Zeta-potentials in Colloid Science, Principles and Applications*, Academic Press, New York, 1981.
28 H.-J. Jacobasch, *Oberflächenchemie faserbildender Polymerer*, Akademie-Verlag, Berlin, 1984.
29 H.-J. Jacobasch, F. Simon, C. Werner and C. Bellmann, *Tech. Mot.*, 1996, **63**, 447.
30 R. Tahhan, *Elektrokinetische und Oberflächenenergetische Untersuchungen an Silizium und Kohlenstoff*, Doctoral-Thesis, TU-Berlin, D83, Wissenschaft und Technik Verlag, Berlin, 1997.
31 K. Kanamaru, *Kolloid-Z*, 1960, **168**, 115.
32 W. I. Chodyrew, *Melliand Textilberichte*, 1990, **11**, 825.
33 J. Rout, S. S. Tripathy, S. K. Nayak, M. Misra and A. K. Mohanty, *J. Appl. Polym. Sci.*, 2001, **79**, 1169.
34 S. V. Prasad, C. Pavithran and P. K. Rohatgi, *J. Mater. Sci.*, 1983, **18**, 1443.
35 J. Rout, M. Misra and A. K. Mohanty, *Polym. Adv. Technol.*, 1999, **10**, 336.
36 J. Rout, M. Misra, S. S. Tripathy, S. K. Nayak and A. K. Mohanty, *Polym. Composites*, 2001, in press.
37 C. Wuertz, A. Bismarck, J. Springer and R. Königer, *Prog. Org. Coat.*, 1999, **37**, 113.
38 A. K. Bledzki and J. Gassan, Natural Fiber Reinforced Plastics, in *Handbook of Engineering Polymeric Materials*, ed. N. P. Cheremisinoff, Marcel Dekker, New York, 1998, pp. 787–810.
39 V. Ribitsch and K. Stana-Kleinschek, *Textile Res. J.*, 1998, **68**, 701.
40 G. L. Madan and S. K. Shrivastava, *Colloid Polym. Sci.*, 1977, **255**, 269.
41 K. J. Saunders, *Organic Polymer Chemistry*, Chapman and Hall, London, 1973.
42 K. K. Stana, C. Polar and V. Ribitsch, *Colloid Polym. Sci.*, 1995, **173**, 1174.
43 N. Kuehn, H.-J. Jacobasch and K. Lunkenheimer, *Acta Polym.*, 1986, **37**, 394.
44 L. L. Schramm, K. Mannhardt and J. J. Novosad, *Colloids Surf.*, 1991, **55**, 309.
45 S. Mishra, M. Misra, S. S. Tripathy, S. K. Nayak and A. K. Mohanty, *J. Reinf. Plast. Compos.*, 2001, in press.
46 Some more information about the used compostable biodegradable thermoplastic resin BAK 1095 are available from: http://www.bayer-us.com/new/1997/9.25.97.html